



## CATALYTIC AZO DYE REDUCTION IN ADVANCED ANAEROBIC BIOREACTORS Gergö Mezöhegyi

ISBN: 978-693-7672-0  
Dipòsit Legal: T-1751-2010

**ADVERTIMENT.** La consulta d'aquesta tesi queda condicionada a l'acceptació de les següents condicions d'ús: La difusió d'aquesta tesi per mitjà del servei TDX ([www.tesisenxarxa.net](http://www.tesisenxarxa.net)) ha estat autoritzada pels titulars dels drets de propietat intel·lectual únicament per a usos privats emmarcats en activitats d'investigació i docència. No s'autoritza la seva reproducció amb finalitats de lucre ni la seva difusió i posada a disposició des d'un lloc aliè al servei TDX. No s'autoritza la presentació del seu contingut en una finestra o marc aliè a TDX (framing). Aquesta reserva de drets afecta tant al resum de presentació de la tesi com als seus continguts. En la utilització o cita de parts de la tesi és obligat indicar el nom de la persona autora.

**ADVERTENCIA.** La consulta de esta tesis queda condicionada a la aceptación de las siguientes condiciones de uso: La difusión de esta tesis por medio del servicio TDR ([www.tesisenred.net](http://www.tesisenred.net)) ha sido autorizada por los titulares de los derechos de propiedad intelectual únicamente para usos privados enmarcados en actividades de investigación y docencia. No se autoriza su reproducción con finalidades de lucro ni su difusión y puesta a disposición desde un sitio ajeno al servicio TDR. No se autoriza la presentación de su contenido en una ventana o marco ajeno a TDR (framing). Esta reserva de derechos afecta tanto al resumen de presentación de la tesis como a sus contenidos. En la utilización o cita de partes de la tesis es obligado indicar el nombre de la persona autora.

**WARNING.** On having consulted this thesis you're accepting the following use conditions: Spreading this thesis by the TDX ([www.tesisenxarxa.net](http://www.tesisenxarxa.net)) service has been authorized by the titular of the intellectual property rights only for private uses placed in investigation and teaching activities. Reproduction with lucrative aims is not authorized neither its spreading and availability from a site foreign to the TDX service. Introducing its content in a window or frame foreign to the TDX service is not authorized (framing). This rights affect to the presentation summary of the thesis as well as to its contents. In the using or citation of parts of the thesis it's obliged to indicate the name of the author.

Gergő Mezőhegyi

# **Catalytic azo dye reduction in advanced anaerobic bioreactors**

DOCTORAL THESIS

UNIVERSITAT  
ROVIRA I VIRGILI

2010

UNIVERSITAT ROVIRA I VIRGILI  
CATALYTIC AZO DYE REDUCTION IN ADVANCED ANAEROBIC BIOREACTORS  
Gergö Mezöhegyi  
ISBN:978-693-7672-0/DL:T-1751-2010

Gergő Mezőhegyi

**CATALYTIC AZO DYE REDUCTION IN ADVANCED  
ANAEROBIC BIOREACTORS**

DOCTORAL THESIS

supervised by Dr. Azael Fabregat Llangostera and Dr. Agustí Fortuny Sanroma  
Departament d'Enginyeria Química



UNIVERSITAT ROVIRA I VIRGILI

Tarragona  
June 2010

UNIVERSITAT ROVIRA I VIRGILI  
CATALYTIC AZO DYE REDUCTION IN ADVANCED ANAEROBIC BIOREACTORS  
Gergö Mezöhegyi  
ISBN:978-693-7672-0/DL:T-1751-2010



UNIVERSITAT  
ROVIRA I VIRGILI

**Escola Tècnica Superior d'Enginyeria Química**  
**Departament d'Enginyeria Química**

Avinguda dels Països Catalans, 26  
43007 Tarragona (Spain)  
Tel.: 977 559700  
Fax: 977 559699

I, Dr. Azael Fabregat Llangostera, Professor in the Department of Chemical Engineering of the Rovira i Virgili University,

CERTIFY:

That the present study, entitled "Catalytic azo dye reduction in advanced anaerobic bioreactors", presented by Gergő Mezőhegyi for the award of the degree of Doctor, has been carried out under my supervision at the Department of Chemical Engineering of this university, and that it fulfils all the requirements to be eligible for the European Doctorate Label.

Tarragona, 1st April 2010

UNIVERSITAT ROVIRA I VIRGILI  
CATALYTIC AZO DYE REDUCTION IN ADVANCED ANAEROBIC BIOREACTORS  
Gergö Mezöhegyi  
ISBN:978-693-7672-0/DL:T-1751-2010



UNIVERSITAT  
ROVIRA I VIRGILI

**Escola Tècnica Superior d'Enginyeria Química**  
**Departament d'Enginyeria Química**

Avinguda dels Països Catalans, 26  
43007 Tarragona (Spain)  
Tel.: 977 559700  
Fax: 977 559699

I, Dr. Agustí Fortuny Sanroma, Professor in the Department of Chemical Engineering of the Polytechnic University of Catalonia,

CERTIFY:

That the present study, entitled "Catalytic azo dye reduction in advanced anaerobic bioreactors", presented by Gergő Mezőhegyi for the award of the degree of Doctor, has been carried out under my supervision at the Department of Chemical Engineering of this university, and that it fulfils all the requirements to be eligible for the European Doctorate Label.

Tarragona, 1st April 2010



UNIVERSITAT ROVIRA I VIRGILI  
CATALYTIC AZO DYE REDUCTION IN ADVANCED ANAEROBIC BIOREACTORS  
Gergö Mezöhegyi  
ISBN:978-693-7672-0/DL:T-1751-2010

*To the Memory of My Beloved Father, István  
(1947 – 2009)*

## Acknowledgements

First of all, I would like to give thanks to my parents for encouraging and supporting me to come to sunny Tarragona and complete this PhD. Also, to my wife Oana whom I met here and who always stood by me.

My infinite gratefulness to my supervisors Dr. Azael Fabregat and Dr. Agustí Fortuny, who admitted me doing research with them, who tried to be as good bosses as they could, who trusted me and helped me to become a researcher.

I am grateful to all the members of Chemical Reaction Engineering & Process Intensification Group who made me feel to be a part of a great team.

My life, both in and out of the laboratory, would have been incomparably more difficult without my friends. Thank all of you for the numberless inforgettable moments.

My special thanks to Dr. Alex Fragoso for his help with the voltammetric experiments; to both Dr. José Órfão and Dr. Filomena Gonçalves for both the useful experiences and beautiful 3 months at Porto University; to Dr. Ignacio Lombraña for accepting me to fulfil a fruitful 1-month research stage at University of the Basque Country; and, to Dr. Frank van der Zee for his helpful advices on writing the review article.

I am furthermore grateful to Dr. Josep Font (Rovira i Virgili University), Dr. Alex Fragoso (Rovira i Virgili University), Dr. Maria Teresa Coll (Polytechnic University of Catalonia), Dr. Ignacio Lombraña (University of the Basque Country) and Dr. Gyula Vatai (Corvinus University of Budapest) for their acceptance of the membership in the doctoral committee.

The financial support for the PhD project was provided by the Rovira i Virgili University (fellowship), by the Spanish Ministry of Science and Education (CTM2005-01873; CTM2008-03338) and by the Catalan Government (2007ITT-00008).

## Summary

During the last decade, several methods of colour removal from wastewaters containing dyestuffs have been found effective and potentially applicable for scaling up. A particular approach to reduce operation expenses and/or enhance dye removal rates is the inclusion of activated carbon (AC) and its beneficial features in the decolourisation process. The review on the role of AC in aqueous dye removal processes demonstrates that most physico-chemical and biological dye removal techniques could be successfully improved by the involvement of AC in the operation, showing a big versatility of its main role in dye degradation. Although it generally has a high affinity to adsorb dyes, AC adsorption is by far not the only mechanism that contributes to higher colour removal rates. The role of AC in dye wastewater treatments varies with the applied method: it acts as a simple dye adsorber in AC-amended coagulation, membrane filtration and single adsorption processes; it can catalyse the generation of strong oxidant hydroxyl radicals in electrochemical and advanced oxidation processes; moreover, AC enhances biomass activity in biological decolourisation and acts as a redox mediator during anaerobic azo dye reduction. As the experimental results show, the reductive azo bond cleavage and dye removal can be significantly accelerated by involving AC in the bioreactor. The continuous experiments were run in packed-bed-type reactors containing the AC with an immobilised anaerobic mixed culture. In an upflow packed-bed reactor (UPBR), high azo dye Acid Orange 7 conversion rates were achieved during very short space times ( $\tau$ ) up to 99% in 2.0 min, that corresponds to extremely short hydraulic residence time (HRT) of about 5.4 min. By testing other support materials –graphite and alumina– in UPBRs, it was cleared that both electron conductivity and specific surface area of AC with functional groups contribute to higher reduction rates. Although UPBR with the biological activated carbon (BAC) seemed to be very effective for azo reduction, development of the reactor system became necessary in order to both avoid microbial clogging in the reactor and provide more reproducible data to make kinetic modeling of azo dye decolourisation possible. The application of special stirring in the carbon bed resulted in both more representative results and an increase of Acid Orange 7 bioconversion up to 96% in a  $\tau$  of 0.5 min (HRT of 1.4 min), compared to the unstirred reactor system. First-order, autocatalytic and Michaelis–Menten models were all found to give good fittings to experimental points of dye conversion at lower inlet dye concentration. Expanding the Michaelis–Menten kinetics by a substrate inhibition factor resulted in a model giving good fitting to experimental points, independently on the initial colourant concentration. After the establishment of upflow stirred packed-bed reactor (USPBR) system together with a decolourisation kinetic model involving both heterogeneous catalysis and biological

degradation, the anaerobic biodegradability of several commercially important colourants was investigated. Decolourisation with very high reduction rates took place in the case of azo dyes tested: at least 80% of conversion was achieved for these pollutants at a  $\tau$  of 2.0 min or higher (HRT  $\geq$  1.8 min). The reaction products of the more biodegradable dyes possessed autocatalytic properties. AC high capacity for these dyes was found not to be the crucial promoter of reduction. On the other hand, results from voltammetric experiments showed that anaerobic biodegradability of an azo dye can be predicted by its reduction potential value in the continuous USPBR system, independently from the azo colourant type and complexity. The biomass was found to be sensitive to some operating factors that require appropriate control and limitation in order to ensure an efficient bioreduction process. Although the USPBR system provided a powerful biological removal of azo dyes compared with the results of the literature, further increase in decolourisation rates might be expected by tailoring the AC catalyst. Several bioreactors were prepared with ACs having different textural properties and various surface chemistries. The kinetic model proposed previously described well the anaerobic and catalytic azo reduction for all the ACs tested. Best dye removals were ensured by the AC having the highest surface area: conversion values above 88% were achieved in the case of both azo dyes Orange II and Reactive Black 5 at a  $\tau$  of 0.23 min or higher (HRT  $\geq$  0.30 min). The decolourisation rates were found to be significantly influenced by the textural properties of AC and moderately affected by its surface chemistry. The results confirmed the catalytic effects of carbonyl/quinone sites on the AC and, in addition, delocalised  $\pi$ -electrons seemed to play a role in the catalytic reduction in the absence of surface oxygen groups. On the whole, the innovative USPBR-BAC system seems to be an attractive alternative for economically improving textile/dye wastewater technologies.

## Resumen

En la última década se han presentado varios métodos nuevos para la eliminación del color de las aguas residuales conteniendo colorantes, que se han mostrado efectivos y potencialmente escalables. Un enfoque novedoso para reducir gastos de operación y/o incrementar las velocidades de eliminación de colorante consiste en la inclusión de carbón activo (AC) en el proceso de decoloración. La revisión del rol del AC en los procesos de eliminación de colorante en medio acuoso muestra que la mayoría de las técnicas existentes de eliminación de colorantes, físico-químicas y biológicas, pueden ser muy mejoradas por la inclusión del AC en la operación, mostrando el AC, además, roles diferentes y una gran versatilidad en la degradación de colorantes. Aunque los ACs tienen generalmente una alta afinidad para adsorber colorantes, la adsorción no es, ni mucho menos, el único mecanismo que contribuye a las altas velocidades de eliminación de color observadas. El rol del AC en los tratamientos de aguas residuales con colorantes varía con el método aplicado: actúa como un simple adsorbedor de colorantes en los procesos de coagulación elevada, filtración con membranas y procesos de adsorción simple; puede catalizar la generación de radicales hidroxilo, oxidantes fuertes, en procesos electroquímicos y de oxidación avanzada; y además, el AC mejora la actividad de la biomasa en la decoloración biológica y actúa como un mediador redox en la reducción anaeróbica de colorantes azoicos. Como muestran los resultados experimentales, la ruptura reductiva del enlace azoico y la consecuente remoción del colorante puede ser significativamente acelerada incorporando AC en el reactor. Se realizaron experimentos en reactores continuos de lecho empacado conteniendo el AC con un cultivo anaeróbico inmovilizado. En un reactor de lecho empacado de flujo ascendente (UPBR) se obtuvieron altas velocidades de conversión del colorante azoico Acid Orange 7 a tiempos espaciales ( $\tau$ ) muy cortos (más del 99% en 2.0 min) que corresponde a tiempos de residencia hidráulicos (HRT) extremadamente cortos de 5.4 min. La prueba de otros materiales de soporte diferentes del AC, como el grafito y la alúmina, evidenció que tanto la conductividad electrónica como el área superficial específica del AC con grupos funcionales contribuyen a las mayores velocidades de reducción. Aunque el sistema de reacción UPBR con carbón activo soportando un sistema biológico anaeróbico (BAC) pareció ser muy efectivo para la reducción de colorantes azoicos, fue necesario proceder al desarrollo de este sistema reactivo con el fin de mejorar su funcionamiento y, así, evitar la obstrucción microbiana del reactor y, también, proveer datos reproducibles con los que hacer posible el modelado cinético de la decoloración de colorantes azoicos. La aplicación de agitación especial en el lecho de carbón produjo resultados más representativos y un incremento de la bioconversión de

Acid Orange 7 hasta el 96% en un  $\tau$  de 0.5 min (HRT de 1.4 min), comparado con el sistema reactivo no agitado. Los resultados experimentales de la conversión de colorante a bajas concentraciones de entrada de colorante se ajustaron a modelos de primer orden, autocatalítico y Michaelis–Menten. La expansión de las cinéticas de Michaelis–Menten con un factor de inhibición de sustrato produjo un modelo que se ajusta bien a los resultados experimentales, independientemente de la concentración inicial del colorante. Una vez establecido el sistema reactivo agitado de lecho empacado y flujo ascendente (USPBR) junto con el modelo cinético de decoloración que implica catálisis heterogénea y degradación biológica, se investigó la biodegradabilidad anaeróbica de varios colorantes comercialmente importantes. Se obtuvieron muy altas velocidades de reducción con todos los colorantes azoicos ensayados: un mínimo de 80% de conversión se obtuvo con estos contaminantes a  $\tau$  de 2.0 min o mayores (HRT  $\geq$  1.8 min). Los productos de reacción de los colorantes más biodegradables mostraron propiedades autocatalíticas. La alta capacidad adsorbente del AC para estos colorantes no resultó ser el promotor crucial para la reducción. Por otra parte, los resultados de experimentos voltamétricos mostraron que la biodegradabilidad anaeróbica de un colorante azoico en un sistema continuo USPBR puede ser predecida por su potencial de reducción, independientemente del tipo de colorante azoico y de su complejidad. Se encontró que la biomasa es sensible a algunos factores de operación que requieren un control y limitación apropiados para asegurar un eficiente proceso de bio-reducción. Aunque el sistema USPBR proveyó un poderoso instrumento para la eliminación biológica de colorantes azoicos en comparación con los resultados de la literatura, pudieron aún esperarse mayores incrementos en las velocidades de decoloración por nuevos ACs, preparados para esta aplicación. Se operaron varios bioreactores con ACs que tenían diferentes propiedades texturales y varias superficies químicas. El modelo cinético propuesto previamente describió bien la reducción azoica catalítica y anaeróbica para todos los ACs probados. La mayor eliminación de colorantes se obtuvo con los ACs con la mayor área superficial: valores de conversión superiores al 88% se obtuvieron con los colorantes Orange II y Reactive Black 5 a un  $\tau$  de 0.23 min o mayores (HRT  $\geq$  0.30 min). Las velocidades de decoloración fueron significativamente influenciadas por las propiedades texturales del AC y moderadamente afectadas por su química superficial. Los resultados confirmaron los efectos catalíticos de los sitios activos carbonil/quinona sobre el AC y, además, los  $\pi$ -electrones deslocalizados parecieron representar un rol en la reducción catalítica en ausencia de grupos oxígeno en la superficie. Finalmente, en conjunto, el sistema innovativo USPBR-BAC parece ser una alternativa atractiva para la mejora económica de las tecnologías de tratamiento de aguas residuales textiles y de colorantes.

## Összefoglalás

Az elmúlt évtizedben számos hatékony és ipari alkalmazásra bevezethető módszert dolgoztak ki festékanyagok szennyvizekből való eltávolítására. Egy különleges megoldás a műveleti költségek csökkentésére és/vagy a színtelenítési hatásfok növelésére a szennyvíztisztító folyamat aktív szénrel és annak előnyös tulajdonságaival történő elősegítése. Az irodalmi áttekintés az aktív szén festékszennyvizek tisztításában való szerepéről rámutat, hogy a legtöbb fizikai-kémiai és biológiai színtelenítési technika aktív szén segítségével javítható, amely a festékeltávolításban való funkcióját illetően igen nagy változatosságot mutat. Bár az aktív szén affinitása festékanyagok adszorpciójára többnyire nagy, ez közel sem az egyetlen mechanizmus, ami a hatékonyabb festékeltávolítást eredményezi. Az aktív szén szerepe festékszennyvizek kezelésében az alkalmazott tisztítási módszertől függ: egyszerű adszorberként működik koagulációs, membránszűrési és hagyományos adszorpciós folyamatokban; katalizálhatja az erősen oxidáns hidroxil-gyökök generálását elektrokémiai és az ún. nagyhatékonyságú oxidációs folyamatokban; ezenkívül, biológiai színtelenítésben növeli a biomassza aktivitását és redox közvetítőként funkcionál azofestékek anaerob redukciójában. A kísérleti eredmények megmutatták, hogy az azo-kötés redukív hasadása és a biológiai festékeltávolítás jelentősen felgyorsíthatóak az aktív szenet is tartalmazó bioreaktorokban. A kísérletek folytonos, az aktív szenet és a rajta rögzített vegyes anaerob kultúrát tartalmazó töltött ágyas reaktorokban valósultak meg. Függőleges átfolyású töltött ágyas reaktorban (UPBR) jelentős Acid Orange 7 azofesték-konverziót (99%) sikerült elérni nagyon rövid, katalizátorra vonatkoztatott tartózkodási idő ( $\tau$ ) alatt (2.0 perc), ami rendkívül rövid hidraulikus tartózkodási időnek (HRT) felelt meg (5.4 perc). Az aktív szén mellett egyéb töltetek (grafit és alumínium-oxid) is tesztelésre kerültek, s az eredmények azt mutatták, hogy mind az aktív szén elektromos vezetőképessége, mind a fajlagos felülete a funkciócsoportokkal hozzájárultak a hatékonyabb redukcióhoz. Bár az UPBR az aktív szénrel és biomasszával együtt rendkívül eredményesnek bizonyult az azo-kötés redukcióját illetően, a reaktor további fejlesztése vált szükségessé mind a mikrobiológiai eltömődés elkerülése végett, mind –a kinetikai modellezéshez elengedhetetlen– reprodukálhatóbb mérések céljából. A speciális keverés alkalmazása a széntöltetben a reprezentatívabb mérési eredmények mellett jelentős Acid Orange 7 biokonverzió-növekedéshez vezetett (96% festékredukció  $\tau = 0.5$  perc és HRT = 1.4 perc alatt) a keverésmentes reaktorhoz képest. Az elsőrendű, autokatalitikus és Michaelis–Menten modellek egyaránt jól illeszkedtek a festékkonverzió mért pontjaihoz kisebb kiindulási festékkoncentráció esetén. A szubsztrát-gátlási tényezővel kibővített Michaelis–Menten kinetika a kiindulási koncentrációtól függetlenül a mérési pontokhoz jól illeszthető



modellt eredményezett. A függőleges átfolyású kevert töltött ágyas reaktor (USPBR), valamint a színtelenítési folyamatot leíró, heterogén katalízist és biológiai lebontást egyszerre magában foglaló kinetikai modell létesítése után számos, a különböző iparágakban gyakran előforduló festékanyag anaerob (biológiai) lebonthatósága került vizsgálatra. Az összes azofesték esetében a színtelenítés nagy redukciós hatásokkal ment végbe:  $\tau \geq 2.0$  perc alatt (HRT  $\geq 1.8$  perc) a festékek legalább 80%-a lebomlott. A biológiailag könnyebben lebontható festékek redukív bomlástermékei autokatalitikus tulajdonságokkal rendelkeztek. Az aktív szén festékekre vonatkozó nagy (adszorpció) felvevőképessége nem a döntően befolyásoló tényező volt a redukcióban. Ezzel szemben a voltametriás mérések kimutatták, hogy az azofestékek anaerob lebonthatósága, a redukciós potenciáljuk ismeretében, az azofesték típusától és összetettségétől függetlenül előre meghatározhatóak a folytonos USPBR rendszerben. A biomassza komoly érzékenységet mutatott néhány műveleti paraméterre, melyek a hatékony redukciós folyamat érdekében megfelelő szabályozást és korlátozást kívánnak. Bár az USPBR –az irodalom eredményeivel összevetve– egy erőteljes biológiai azofesték-eltávolítási megoldást nyújtott, a színtelenítési hatások további növelésére lehetett számítani az aktív szén katalizátor megfelelő módosításával. Számos bioreaktor került tesztelésre a struktúrájában és kémiájában eltérő aktív szén töltettel. A korábban javasolt kinetikai modell az összes szén töltet esetében jól illeszkedett a katalitikus azo-redukció mért pontjaihoz. A leghatékonyabb festékeltávolítás a legnagyobb felszínű aktív szén esetében ment végbe: mindkét azofesték (Orange II és Reactive Black 5) legalább 88%-ban redukálódott nem egészen  $\tau \geq 0.23$  perc alatt (HRT  $\geq 0.30$  perc). A színtelenítési hatásfokot lényegesen meghatározták az aktív szén szerkezeti tulajdonságai és mérsékelten befolyásolta annak felszíni kémiája. Az eredmények igazolták az aktív szénen található karbonil- és kinoncsoportok katalitikus hatását, valamint a delokalizált  $\pi$ -elektronok katalitikus redukcióban való szerepét a felszíni oxigén-csoportok hiányában. Összességében elmondható, hogy az innovatív USPBR a 'biológiai' aktív szénrel vonzó alternatívának tűnik a textilipari/festékes szennyvizek kezelésének költséghatékony fejlesztésére.

# Table of contents

|  |           |
|--|-----------|
| <b>List of Figures and Tables</b>  | <b>13</b> |
| <b>Chapter 1. Introduction</b>   | <b>15</b> |
| <b>Chapter 2. Role of activated carbon in catalytic and non-catalytic aqueous dye removal processes: a review</b>  | <b>17</b> |
| 1. Introduction  | 18        |
| 2. AC adsorption of dyes   | 19        |
| 2.1. Dye adsorption isotherms  | 19        |
| 2.2. Dye adsorption kinetics   | 20        |
| 2.3. Effect of pH  | 21        |
| 2.4. Effect of AC surface chemical characteristics   | 24        |
| 2.5. Effect of AC textural characteristics   | 24        |
| 2.6. Regeneration of AC  | 25        |
| 3. AC-amended physico-chemical dye removal processes   | 26        |
| 3.1. AC-amended coagulation of dyes  | 26        |
| 3.2. AC-amended membrane filtration of dyes  | 27        |
| 3.3. AC-amended electrochemical treatment of dyes  | 28        |
| 3.4. AC-amended advanced oxidation processes for dye removal   | 29        |
| 3.4.1. <i>Wet oxidation of dyes</i>  | 30        |
| 3.4.2. <i>Wet peroxide oxidation of dyes</i>   | 31        |
| 3.4.3. <i>Ozonation of dyes</i>  | 38        |
| 3.4.4. <i>Photochemical and photocatalytic removal of dyes</i>   | 39        |
| 3.4.5. <i>Miscellaneous dye removal processes</i>  | 41        |
| 4. AC-amended biological dye removal processes   | 42        |
| 4.1. AC-supported microbial degradation of dyes  | 43        |
| 4.2. AC-catalysed bioreduction of azo dyes   | 46        |
| 5. Conclusions   | 47        |
| <b>Chapter 3. Effective anaerobic decolorization of azo dye Acid Orange 7 in continuous upflow packed-bed reactor using biological activated carbon system</b> | <b>49</b> |
| 1. Introduction  | 50        |
| 2. Materials and methods   | 51        |
| 2.1. Chemicals   | 51        |
| 2.2. Batch experiment  | 52        |
| 2.3. Continuous experiments  | 53        |
| 2.4. Adsorption experiments  | 54        |
| 2.5. Analytical methods  | 54        |

|   |           |
|---|-----------|
| 3. Results and discussion   | 54        |
| 3.1. Adsorption kinetics  | 54        |
| 3.2. Equilibrium adsorption isotherm  | 55        |
| 3.3. Batch experiment   | 55        |
| 3.4. Continuous experiments   | 57        |
| 3.5. AO7–SA ratio   | 60        |
| 4. Conclusions  | 61        |
| <b>Chapter 4. Novel bioreactor design for decolourisation of azo dye effluents</b>  | <b>63</b> |
| 1. Introduction   | 64        |
| 2. Materials and methods  | 65        |
| 2.1. Chemicals  | 65        |
| 2.2. Upflow stirred packed-bed reactor setup  | 66        |
| 2.3. Biological activated carbon system   | 66        |
| 2.4. Analytical methods   | 67        |
| 3. Results and discussion   | 67        |
| 3.1. Stirring of BAC in packed-bed reactor  | 67        |
| 3.1.1. <i>Agitation effects on biomass</i>  | 67        |
| 3.1.2. <i>Periodical stirring</i>   | 68        |
| 3.1.3. <i>Continuous stirring</i>   | 69        |
| 3.2. Modeling AO7 anaerobic biodegradation in USPBR   | 69        |
| 3.2.1. <i>Determination of reaction rate</i>  | 69        |
| 3.2.2. <i>Kinetic models</i>  | 70        |
| 3.3. Substrate inhibition and toxicity effects  | 72        |
| 3.4. Acetate consumption  | 74        |
| 4. Conclusions  | 75        |
| <b>Chapter 5. Advanced bioreduction of commercially important azo dyes:<br/>Modeling and correlation with electrochemical characteristics</b> | <b>77</b> |
| 1. Introduction   | 78        |
| 2. Materials and methods  | 80        |
| 2.1. Chemicals  | 80        |
| 2.2. Feed and bioreactor system   | 81        |
| 2.3. Adsorption experiments   | 81        |
| 2.4. Voltammetric experiments   | 82        |
| 2.5. Analytical methods   | 82        |
| 3. Results and discussion   | 82        |
| 3.1. Adsorption kinetics of dyes  | 82        |
| 3.2. Reduction of (azo) dyes  | 83        |
| 3.3. Role of redox characteristics in bioreduction  | 87        |
| 3.4. Biomass sensitivity  | 87        |
| 4. Conclusions  | 90        |

|   |            |
|---|------------|
| <b>Chapter 6. Tailored activated carbons as catalysts in biodecolourisation of textile azo dyes</b> | <b>91</b>  |
| 1. Introduction   | 92         |
| 2. Experimental   | 93         |
| 2.1. Preparation of activated carbons   | 93         |
| 2.1.1. <i>Activated carbons with different textural properties</i>                                  | 93         |
| 2.1.2. <i>Activated carbons with different surface chemistries</i>                                  | 94         |
| 2.2. Characterization of activated carbons  | 94         |
| 2.2.1. <i>Textural characterization</i>   | 94         |
| 2.2.2. <i>Surface chemistry characterization</i>  | 95         |
| 2.3. Chemicals  | 95         |
| 2.4. Feed and bioreactor system   | 95         |
| 2.5. Analytical methods   | 96         |
| 3. Results and discussion   | 96         |
| 3.1. Characterization of activated carbons  | 96         |
| 3.1.1. <i>Textural characterization</i>   | 96         |
| 3.1.2. <i>Surface chemistry characterization</i>  | 97         |
| 3.2. Reduction of azo dyes  | 103        |
| 3.2.1. <i>Modeling</i>  | 103        |
| 3.2.2. <i>Catalytic reduction by ACs with different textural properties</i>                         | 103        |
| 3.2.3. <i>Catalytic reduction by ACs with different surface chemistries</i>                         | 105        |
| 4. Conclusions  | 107        |
| <b>Chapter 7. General conclusions and future works</b>  | <b>109</b> |
| <b>References</b>   | <b>111</b> |
| <b>About the author</b>   | <b>125</b> |



## List of Figures and Tables

|   |    |
|---|----|
| <b>Figure 1.1.</b> Upflow stirred packed-bed reactor (USPBR).   | 16 |
| <b>Figure 3.1.</b> Role of activated carbon in anaerobic azo dye degradation.   | 51 |
| <b>Figure 3.2.</b> Anaerobic degradation of Acid Orange 7.  | 52 |
| <b>Figure 3.3.</b> Continuous and anaerobic upflow packed-bed reactor setup.  | 53 |
| <b>Figure 3.4.</b> Acid Orange 7 adsorption on activated carbon predicted by a second-order kinetic model.  | 56 |
| <b>Figure 3.5.</b> Acid Orange 7 equilibrium adsorption on activated carbon predicted by Langmuir isotherm.   | 56 |
| <b>Figure 3.6.</b> Acid Orange 7 conversion in batch reactor using graphite as solid electron-mediator catalyst.  | 57 |
| <b>Figure 3.7.</b> Acid Orange 7 conversion in continuous UPBR using different support materials.   | 60 |
| <b>Figure 3.8.</b> Ratio between destroyed Acid Orange 7 and produced sulfanilic acid in different reactor systems.   | 60 |
| <b>Figure 4.1.</b> Anaerobic upflow stirred packed-bed reactor setup.   | 68 |
| <b>Figure 4.2.</b> Effect of stirring in BAC in the packed-bed reactors.  | 69 |
| <b>Figure 4.3.</b> Effect of continuous stirring in BAC in <i>USPBR-3</i> .   | 70 |
| <b>Figure 4.4.</b> Kinetic modeling of Acid Orange 7 anaerobic biodegradation in <i>USPBR-4</i> : (a) first-order kinetic model, (b) autocatalytic model and (c) Michaelis–Menten model.  | 72 |
| <b>Figure 4.5.</b> Substrate inhibition and toxicity effects during Acid Orange 7 decolourisation in <i>USPBR-4</i> .   | 73 |
| <b>Figure 4.6.</b> Theoretical consumption of acetate for Acid Orange 7 reduction.  | 74 |
| <b>Figure 4.7.</b> The change of pH of the outlet solution at different acetate consumptions in <i>USPBR-3</i> and <i>USPBR-4</i> .   | 74 |
| <b>Figure 5.1.</b> Chemical structures of the dyes investigated.  | 80 |
| <b>Figure 5.2.</b> Kinetic modeling of azo dye anaerobic biodecolorization in USPBR: (a) Orange II, (b) Orange G, (c) Sunset Yellow FCF, (d) Tartrazine, (e) Acid Red 88, and (f) hydrolyzed Reactive Black 5.                              | 86 |
| <b>Figure 5.3.</b> Disappearance of Rhodamine in the anaerobic USPBR.   | 87 |
| <b>Figure 5.4.</b> Cyclic voltammograms of azo dyes in 80 mM H <sub>2</sub> SO <sub>4</sub> at 0.1 V/s scan rate: (a) Orange II, (b) Orange G, (c) Sunset Yellow FCF, (d) Tartrazine, (e) Acid Red 88, and (f) hydrolyzed Reactive Black 5. | 89 |
| <b>Figure 5.5.</b> Correlation between kinetic constants ( $k_1$ ) and the reduction potentials of azo dyes.  | 90 |

|  |       |
|--|-------|
| <b>Figure 6.1.</b> Activated carbon surface without (a) and with (b) biofilm (ESEM).   | 97    |
| <b>Figure 6.2.</b> N <sub>2</sub> adsorption isotherms at 77 K for activated carbons with different textural properties (a) and surface chemistries (b). | 97    |
| <b>Figure 6.3.</b> TPD spectra of activated carbons with different textural properties: (a) CO <sub>2</sub> and (b) CO evolution.                        | 98    |
| <b>Figure 6.4.</b> TPD spectra of activated carbons with different surface chemistries: (a) CO <sub>2</sub> and (b) CO evolution.                        | 100   |
| <b>Figure 6.5.</b> Deconvolution of TPD spectra: example for (a) CO <sub>2</sub> and (b) CO evolution (AC <sub>0</sub> ).                                | 101   |
| <b>Figure 6.6.</b> Example of kinetic modeling of azo anaerobic biodecolourisation in USPBR (AC <sub>0</sub> ).  | 104   |
| <b>Figure 6.7.</b> Correlation between catalytic azo reduction and surface quinonic densities of activated carbons with different textural properties.   | 105   |
| <b>Figure 6.8.</b> Correlation between catalytic azo reduction and surface quinonic densities of activated carbons with different surface chemistries.   | 106   |
| <hr/>  |       |
| <b>Table 2.1.</b> Selected results of dye adsorption studies with different ACs.   | 22–23 |
| <b>Table 2.2.</b> Selected results of physico-chemical dye oxidation studies with AC-catalysed decolourisation.  | 32–37 |
| <b>Table 2.3.</b> Selected results of AC-amended biological dye removal studies.   | 44–45 |
| <b>Table 3.1.</b> Anaerobic degradation of Acid Orange 7: selected results of studies reported in the literature.  | 59    |
| <b>Table 4.1.</b> Kinetic data of models used for anaerobic AO7 degradation in <i>USPBR-4</i> .  | 71    |
| <b>Table 5.1.</b> Adsorption, biodecolorization kinetic, and electrochemical data of dyes used in this study.  | 83    |
| <b>Table 5.2.</b> Microbial sensitivity for temperature, inlet pH, acetate concentration, and dye concentration at a $\tau$ of $0.50 \pm 0.02$ min.      | 88    |
| <b>Table 6.1.</b> Textural data of selected activated carbons used in this study.  | 99    |
| <b>Table 6.2.</b> Surface chemistry data of activated carbon samples.  | 99    |
| <b>Table 6.3.</b> Results of the deconvolution of TPD spectra.   | 102   |

# 1

## Introduction

Dyes make the world more beautiful through coloured substances. Nowadays, as reported in the so-called Colour Index (C.I.) managed by the Society of Dyers and Colourists and the American Association of Textile Chemists and Colourists, about 10,000 different dyes are produced. Textile industry is one of those industries that intensively use colourants. Unfortunately, it simultaneously consumes large amounts of water in the manufacturing process and discharge great amounts of effluents with synthetic dyes to the environment causing public concern and legislation problems. Azo dyes, being the largest and most versatile class of dyes, are considered to be serious health-risk factors. Apart from the aesthetic deterioration of water bodies, many azo colourants and their breakdown products are toxic or even mutagenic. So far, the efficient and low-cost treatment of these hazardous effluents at industrial sites has remained unsolved.

The most physicochemical dye removal techniques appear to face the facts of technical and economical limitations. However, microbial decolourisation of dyes is one of the most attractive technologies considering its economic, environmentally suitable and methodologically relatively simple features. One possible strategy for efficient biomineralisation of azo compounds is a sequential anaerobic–aerobic process that can provide complex removal of azo colourants by reduction together with their degradation products, aromatic amines by oxidation. The bottleneck of this combined method is the anaerobic azo bond cleavage, so by having an efficient first step in azo dye decolourisation, the more complete sequential treatment can be carried out. The most serious drawback of azo dye reduction by bacteria is the slowness of the process. To overcome this problem, by using redox mediators during the reduction, anaerobic biodecolourisation can be enhanced resulting in much higher dye removal rates. Certain electron mediators, such as quinone-like compounds, can greatly accelerate azo dye reduction in homogeneous reactions. However, immobilisation of the redox mediator in the bioreactor is indispensable to ensure lower process costs. Promising results have been obtained to enhance anaerobic azo dye removal by the use of activated carbon –containing surface quinonic structures– as a solid electron mediator in the bioreactor (Van der Zee et al., 2003).



In different catalytic reactions, activated carbons (ACs) have been mainly used as supports, but their use as catalysts on their own is growing quickly, even in dye removal processes. According to the literature, the addition of AC into a biological system treating dye or textile wastewaters presents a positive contribution to pollutant removal. A rather new approach for AC-amended microbial decolourisation is to consider AC as a catalyst. Since AC furthermore plays a role in obtaining high concentrations of active microorganisms in the bioreactor, the logical way is to operate with high GAC apparent volume/reactor volume ratios. To our knowledge, packed-bed-type reactors using biological activated carbon system (Figure 1.1) have never been applied for anaerobic and catalytic azo dye decolourisation by other authors.

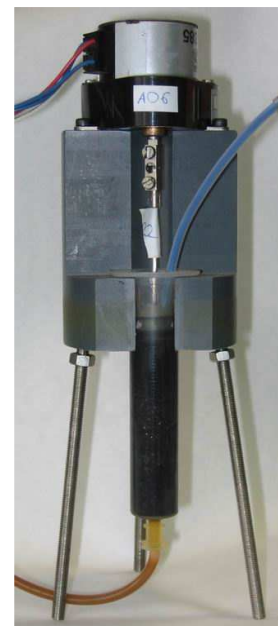


**Figure 1.1.** USPBR.

#### AIMS OF THE THESIS

Considering the amount of azo dye wastewaters mainly originated from the textile industry, it is clear that continuous systems have to be designed for treating these effluents. The main objective of this Ph.D. work was to develop a novel and efficient biological treatment for the decolourisation of azo dyes in a continuous reactor system, both at soft conditions and at extremely short hydraulic residence times (minutes) that are indispensable for ensuring an effective and economic process on industrial scale. The specific aims were related to different chapters of the thesis: to review the current developments in textile/dye wastewater treatments, focusing on activated carbon-enhanced decolourisation techniques (**Chapter 2**); to evaluate the significant role of AC in the anaerobic bioreduction of an azo dye in upflow packed-bed reactor system using different support materials (**Chapter 3**); to investigate the effects of appropriate stirring of biological activated carbon in the upflow stirred packed-bed reactor (USPBR) on azo dye decolourisation rate and to propose a model for anaerobic azo dye reduction (**Chapter 4**); to test different azo dyes with different molecular structures and chemical properties, to compare their decolourisation rates and determine the crucial factors of their biodegradability in USPBR; to examine the influence of different operation/feed parameters (e.g., temperature, pH, dye concentration) on biological dye removal rates (**Chapter 5**); to determine the crucial factors of AC textural and chemical properties in the catalytic azo dye reduction by using modified ACs with diverse pore structures and surface chemistries in USPBR (**Chapter 6**); and, to conclude the general findings of the thesis and to make suggestions for further investigations (**Chapter 7**).

## **Role of activated carbon in catalytic and non-catalytic aqueous dye removal processes: a review**

### **Abstract**

During the last decade, several methods of colour removal from textile wastewaters have been found effective and potentially applicable for scaling up. However, most of them still face cost problems, demanding their further developments. The widespread applicability of activated carbon (AC) in water and wastewater treatment, both as adsorbent and catalyst support, or even as a catalyst itself, predicted its contribution to enhanced dye removal rates in AC-amended decolourisation strategies. Certain features of AC always play a part in the combined treatment, irrespectively of the applied method, such as its strong propensity to adsorb dyes and its (normally) high surface area; others contribute to colour removal specifically, depending on the treatment method, such as AC's ability to conduct electrons, to support impregnated elements/bacteria on its surface or to catalyse dye degradation on its own. By tailoring the textural and surface chemical properties of AC, dye wastewater remediation can be optimised for the applied treatment method. The review demonstrates that most physico-chemical and biological dye removal techniques can be successfully improved by the involvement of AC in the operation, showing a big versatility of its main role in dye degradation.

<Submitted as: Mezohegyi G, van der Zee FP, Font J, Bengoa C, Stuber F, Fortuny A, Fabregat A. (2010). *Carbon*.>

## 1. Introduction

Textile industry is one of those industries that consume large amounts of water in the manufacturing process and, at the same time, release great amounts of effluents with synthetic dyes into the environment causing public concern and legislation problems. It is estimated that about 40–65 L of textile effluent is generated per kg of cloth produced (Manu and Chaudhari, 2002). These dyes may cause serious problems of environmental pollution due to both their visibility –even at very low concentration– and recalcitrance, giving undesirable colour to the water, reducing sunlight penetration, resisting photochemical and biological attack. Moreover, many dyes and their degradation products have been associated with toxicity and/or mutagenicity (Weisburger, 2002). Hitherto, relevant factories have shown deficiencies of efficiently treating these effluents on industrial scale, particularly at higher dye concentrations and at lower energy consumptions.

Up to date, several physico-chemical and biological methods have been found and compared to treat dye/textile wastewaters (Slokar and Le Marechal, 1998; Robinson et al., 2001; Forgacs et al., 2004; Dos Santos et al., 2007; Hai et al., 2007), each having its own advantages and drawbacks. The literature indicates that nowadays, those dye removal techniques and investigations are dominant which can meet the requirements of stricter and stricter environmental regulations, i.e., the green(er) and clean(er) technologies, offering minimal (or no) secondary waste streams, less (or no) use of chemicals, less hazardous effluents and both higher dye decolourisation and mineralisation efficiencies. However, in general, cleaner dye wastewater treatment methods imply higher energy/operation costs. Significant reduction of expenses and/or enhancement of dye removal can be achieved e.g., by the use of hybrid treatments (Hai et al., 2007).

A particular approach for hybrid decolourisation methods is the inclusion of activated carbon (AC) and its beneficial features in the physical, chemical or biological process. In textile and dye wastewater treatment, the role of AC used to be limited to dye adsorption (Choy et al., 1999; Kannan and Sundaram, 2001; Namasivayam and Kavitha, 2002; Malik, 2003). AC is probably the most versatile adsorbent because of its large surface area, polymodal porous structure, high adsorption capacity and variable surface chemical composition (Bansal and Goyal, 2005). Although the cost of AC is still considerable, it can be significantly reduced by using different solid wastes for AC preparation, e.g., agricultural residues (Kannan and Sundaram, 2001; Namasivayam and Kavitha, 2002; Kavitha and Namasivayam, 2007; Demirbas, 2009) or waste tyres (Mui et al., 2004). AC adsorption of dyes can be discussed as individual treatment but it takes place as an accompanying mechanism in all the developed dye/textile wastewater treatments involving AC either as a porous high-surface support material or a catalyst. In different

catalytic reactions, ACs have been mainly used as supports, but their use as catalysts on their own –especially due to their surface oxygen groups– is growing quickly (Radovic and Rodríguez-Reinoso, 1997; Rodríguez-Reinoso, 1998; Figueiredo and Pereira, 2009), even in dye removal processes. What furthermore makes ACs attractive to facilitate (textile) wastewater treatment is the possibility of tailoring their physical and/or chemical properties in order to optimise their performance.

The aim of this review is to summarise the results of AC-amended textile/dye wastewater treatment processes, highlighting the diverse roles of AC in decolourisation techniques. The article includes three main sections, i.e., dye removal by single AC adsorption (Section 2), by AC-enhanced physico-chemical processes (Section 3) and by AC-amended biological degradation (Section 4).

## **2. AC adsorption of dyes**

Activated carbons (ACs) are excellent adsorbents of countless pollutants. Their industrial applications in liquid phase involve the adsorptive removal of colour, odour, taste and other undesirable organic and inorganic material from drinking water and the treatment of industrial wastewaters. Due to its unique molecular structure, AC has an extremely high affinity for many classes of dyes (Table 2.1). Numerous physico-chemical factors affect dye adsorption, including the interaction between the adsorbate and adsorbent, AC surface area and pore structure, AC surface chemistry, effect of other components, characteristics of the dye molecule, AC particle size, pH, temperature, contact time etc. This section does not make an attempt to summarise the hundreds of studies on dye adsorption by AC but instead tries to give a general insight into most of the key issues.

### **2.1. Dye adsorption isotherms**

The adsorption isotherms are the basic requirements in the design of adsorption processes. The isotherm indicates how the adsorbate molecules distribute between the liquid and solid phase when the adsorption reaches the equilibrium state. In most studies related to dye adsorption by AC, two well-known isotherms predominate. The Langmuir isotherm assumes monolayer sorption at homogeneous sites of the AC surface without any interaction among the adsorbed molecules which possess equal sorption activation energies. The Langmuir equation can be given as (Eq. 1):

$$Q_E = \frac{Q_M K_L C_E}{1 + K_L C_E} \quad (1)$$

where  $Q_E$  is the dye equilibrium concentration on the AC phase ( $\text{mg g}_{\text{AC}}^{-1}$ ),  $Q_M$  is the maximum amount of dye corresponding to complete monolayer coverage on the carbon surface ( $\text{mg g}_{\text{AC}}^{-1}$ ),  $C_E$  is the equilibrium concentration in the liquid phase ( $\text{mg L}^{-1}$ ) and  $K_L$  is the Langmuir constant ( $\text{L mg}^{-1}$ ). The Freundlich isotherm, on the other hand, presumes heterogeneous surface energies in which the energy term varies as a function of the surface coverage, and can be used for nonideal sorption processes. It is expressed by the following equation (Eq. 2):

$$Q_E = K_F C_E^{1/n} \quad (2)$$

where  $Q_E$  is the amount of dye adsorbed onto the AC ( $\text{mg g}_{\text{AC}}^{-1}$ ),  $C_E$  is the equilibrium concentration in the liquid phase ( $\text{mg L}^{-1}$ ),  $K_F$  is the Freundlich constant indicating the dye adsorption capacity and  $n$  index shows the adsorption intensity. For example, Acid Yellow 36 adsorption onto ACs prepared from sawdust and rice husk (Malik, 2003) and Methylene Blue adsorption onto various –commercial and indigenously prepared– activated carbons (Kannan and Sundaram, 2001) fitted well with both isotherms. Some less common isotherms have been also discussed to describe the AC adsorption of dyes, such as the Redlich-Peterson isotherm (incorporating the features of the Langmuir and Freundlich isotherms), providing the best correlation for the sorption of acid (Choy et al., 1999) and basic dyes (El Qada et al., 2008).

## 2.2. Dye adsorption kinetics

In general, the mechanism of dye adsorption onto AC involves the following steps: (1) migration of dye from the bulk solution to the AC surface; (2) diffusion of dye through the boundary layer to the AC surface; (3) adsorption of dye at an active site on the AC surface; and (4) intra-particle diffusion of dye into the interior pores of the AC particle (Kannan and Sundaram, 2001). The rate of dye adsorption can be determined by the use of adsorption kinetic models. Among several kinetic approaches (Kavitha and Namasivayam, 2007; Mall et al., 2005), the second-order model was generally found to give very good correlations with the experimental data of dye adsorption onto AC. The model corresponds to the equation (Eq. 3):

$$Q = \frac{kQ_E^2 t}{1 + kQ_E t} \quad (3)$$

where  $Q$  represents the dye concentration in the solid phase ( $\text{mg g}_{\text{AC}}^{-1}$ ),  $Q_E$  is the corresponding value at equilibrium ( $\text{mg g}_{\text{AC}}^{-1}$ ),  $t$  is the contact time and  $k$  is the adsorption

rate constant. For instance, Kavitha and Namasivayam (2007) tested an activated coir pith carbon prepared from coconut husk to remove Methylene Blue and used different kinetic models such as Lagergren first-order, second-order, intra-particle diffusion and Bangham models to fit the experimental data. The calculated correlations were the closest to unity in case of the second-order model, confirming the chemisorption of the colourant onto the AC particles. The same kinetic model was proposed for the AC adsorption of numerous colourants, such as Congo Red (Namasivayam and Kavitha, 2002), Reactive Red 241 (Órfão et al., 2006), Acid Red 97, Acid Orange 61, Acid Brown 425 (Gómez et al., 2007) or Acid Orange 7 (Mezohegyi et al., 2007). The fast adsorption mechanism by mesoporous AC prepared from coconut coir dust followed a pseudo-second-order kinetics with a significant contribution of intra-particle diffusion in case of Methylene Blue and Remazol Yellow dyes (Macedo et al., 2006). Apart from second-order kinetics, other models for AC adsorption of dyes have been occasionally reported such as the simple first-order model (Kannan and Sundaram, 2001; Malik, 2003) or the dual resistance modified Matthews-Weber model (Walker and Weatherley, 1999a).

### 2.3. Effect of pH

The solution pH plays a major role in the dye adsorption process. Its effect can be described on the basis of the influence of pH on the point of zero charge ( $\text{pH}_{\text{PZC}}$ ): AC acts as a positively charged surface in the dye solution for  $\text{pH} < \text{pH}_{\text{PZC}}$  and as a negatively charged surface for  $\text{pH} > \text{pH}_{\text{PZC}}$ . Consequently, a colourant with cationic characteristics has higher affinity for AC adsorption when  $\text{pH} > \text{pH}_{\text{PZC}}$  and, on the contrary, anionic dyes rather tend to be adsorbed onto AC when  $\text{pH} < \text{pH}_{\text{PZC}}$  (Órfão et al., 2006). E.g., El Qada et al. (2008) showed that the maximum adsorption capacity of AC ( $\text{pH}_{\text{PZC}}$ : 6.3) for the basic dye Methylene Blue was nearly doubled by increasing the pH from 4 to 11. The lower adsorption of this dye at acidic pH ( $< \text{pH}_{\text{PZC}}$ ) was not solely due to the presence of excess  $\text{H}^+$  ions competing with the dye cation for the adsorption sites, but also to the electrostatic repulsion between the cationic dye and protonated AC surface. On the other hand, anionic Congo Red was preferably adsorbed onto activated coir pith carbon at acidic pH while its removal efficiency was slightly decreased when the pH was changed from 2 to 4 (Namasivayam and Kavitha, 2002). However, significant dye adsorption still occurred at higher pH, suggesting the operative presence of chemisorption. Similar behaviour was observed during the adsorption of anionic Acid Yellow 36 when increasing the pH from 3 to 9 resulted in a ca. 40% drop of the AC adsorption capacity on average (Malik, 2003). Calorimetric studies confirmed that the dye-AC interaction forces are correlated with the pH of the solution and the increase of pH promoted an endothermic process for the anionic Remazol Yellow and an exothermic process for the cationic Methylene Blue (Macedo et al., 2006).

**Table 2.1.** Selected results of dye adsorption studies with different ACs.

| dye                              | AC characteristics <sup>a</sup>  | dye adsorption capacity <sup>b</sup><br>(mg g <sup>-1</sup> ) | reference                  |
|----------------------------------|--|---|----------------------------|
| Acid Red 114                     | com.: d: 500–710   | 101   | Choy et al. (1999)         |
| Polar Blue RAWL                  |  | 101   |                            |
| Polar Yellow                     |  | 129   |                            |
| Methylene Blue                   | com. (Merck); d: 90  | 980   | Kannan and Sundaram (2001) |
|                                  | o: bamboo dust; d: 90  | 143   |                            |
|                                  | o: coconut shell; d: 90  | 278   |                            |
|                                  | o: groundnut shell; d: 90  | 165   |                            |
|                                  | o: rice husk; d: 90  | 343   |                            |
|                                  | o: straw; d: 90  | 472   |                            |
| Acid Yellow 36                   | o: mahogany sawdust; d: 74–250; S <sub>BET</sub> : 516   | 184   | Malik (2003)               |
|                                  | o: rice husk; d: 74–1190; S <sub>BET</sub> : 272   | 87  |                            |
| Methylene Blue                   | com. (Filtrisorb 400); d < 106; S <sub>BET</sub> : 1216; pH <sub>PZC</sub> : 7.8                                 | 455 (pH 7)  | El Qada et al. (2008)      |
|                                  | o: BC; d < 106; S <sub>BET</sub> : 857; pH <sub>PZC</sub> : 6.3  | 345 (pH 7)  |                            |
|                                  | o: BC; d < 106; S <sub>BET</sub> : 863; pH <sub>PZC</sub> : 8.3  | 307 (pH 7)  |                            |
| Basic Red                        | com. (Filtrisorb 400); d < 106; S <sub>BET</sub> : 1216; pH <sub>PZC</sub> : 7.8                                 | 556 (pH 7)  |                            |
|                                  | o: BC; d < 106; S <sub>BET</sub> : 857; pH <sub>PZC</sub> : 6.3  | 588 (pH 7)  |                            |
| Basic Yellow                     | com. (Filtrisorb 400); d < 106; S <sub>BET</sub> : 1216; pH <sub>PZC</sub> : 7.8                                 | 833 (pH 7)  |                            |
|                                  | o: BC; d < 106; S <sub>BET</sub> : 857; pH <sub>PZC</sub> : 6.3  | 625 (pH 7)  |                            |
| Reactive Red 241<br>(hydrolysed) | com. (Norit ROX 0.8); d < 50; S <sub>BET</sub> : 1032; pH <sub>PZC</sub> : 8.4                                   | 186 (pH 7)  | Órfão et al. (2006)        |
|                                  | com. mod: HNO <sub>3</sub> ; d < 50; S <sub>BET</sub> : 893; pH <sub>PZC</sub> : 2.0                             | 130 (pH 7)  |                            |
|                                  | com. mod: HNO <sub>3</sub> /heat under H <sub>2</sub> ; d < 50; S <sub>BET</sub> : 987; pH <sub>PZC</sub> : 10.0 | 242 (pH 7)  |                            |
| Acid Red 97                      | com. (J.T. Baker)  | 52  | Gómez et al. (2007)        |
| Acid Orange 61                   |  | 169   |                            |
| Acid Brown 425                   |  | 222   |                            |
| Remazol Yellow                   | com. (Filtrisorb 400); d: 300–500; S <sub>BET</sub> : 1100; pH <sub>PZC</sub> : 7.2                              | 1111  | Al-Degs et al. (2000)      |
| Remazol Red                      |  | 400   |                            |
| Remazol Black                    |  | 434   |                            |

**Table 2.1.** Selected results of dye adsorption studies with different ACs. (cont.)

| dye                              | AC characteristics <sup>a</sup>  | dye adsorption capacity <sup>b</sup><br>(mg g <sup>-1</sup> ) | reference                              |
|----------------------------------|--|---|--|
| Basic Red 14                     | com. (Norit GAC 1240 PLUS); d < 50; S <sub>BET</sub> : 972; pH <sub>PZC</sub> : 9.7                              | 546   | Faria et al. (2004)                    |
|                                  | com. mod: HNO <sub>3</sub> ; d < 50; S <sub>BET</sub> : 909; pH <sub>PZC</sub> : 2.7                             | 633   |  |
|                                  | com. mod: H <sub>2</sub> O <sub>2</sub> ; d < 50; S <sub>BET</sub> : 949; pH <sub>PZC</sub> : 5.4                | 568   |  |
|                                  | com. mod: HNO <sub>3</sub> /heat under H <sub>2</sub> ; d < 50; S <sub>BET</sub> : 972; pH <sub>PZC</sub> : 10.8 | 714   |  |
|                                  | com. mod: HNO <sub>3</sub> /heat under N <sub>2</sub> ; d < 50; S <sub>BET</sub> : 946; pH <sub>PZC</sub> : 9.9  | 680   |  |
|                                  | com. (Norit GAC 1240 PLUS); d < 50; S <sub>BET</sub> : 972; pH <sub>PZC</sub> : 9.7                              | 190   |  |
| Reactive Red 241<br>(hydrolysed) | com. mod: HNO <sub>3</sub> ; d < 50; S <sub>BET</sub> : 909; pH <sub>PZC</sub> : 2.7                             | 157   | Wang et al. (2005)                     |
|                                  | com. mod: H <sub>2</sub> O <sub>2</sub> ; d < 50; S <sub>BET</sub> : 949; pH <sub>PZC</sub> : 5.4                | 201   |  |
|                                  | com. mod: HNO <sub>3</sub> /heat under H <sub>2</sub> ; d < 50; S <sub>BET</sub> : 972; pH <sub>PZC</sub> : 10.8 | 246   |  |
|                                  | com. mod: HNO <sub>3</sub> /heat under N <sub>2</sub> ; d < 50; S <sub>BET</sub> : 946; pH <sub>PZC</sub> : 9.9  | 223   |  |
|                                  | com. (Norit GAC 1240 PLUS); d < 50; S <sub>BET</sub> : 972; pH <sub>PZC</sub> : 9.7                              | 310   |  |
|                                  | com. mod: HNO <sub>3</sub> ; d < 50; S <sub>BET</sub> : 909; pH <sub>PZC</sub> : 2.7                             | 197   |  |
| Acid Blue 113                    | com. mod: H <sub>2</sub> O <sub>2</sub> ; d < 50; S <sub>BET</sub> : 949; pH <sub>PZC</sub> : 5.4                | 244   | Wang et al. (2005)                     |
|                                  | com. mod: HNO <sub>3</sub> /heat under H <sub>2</sub> ; d < 50; S <sub>BET</sub> : 972; pH <sub>PZC</sub> : 10.8 | 345   |  |
|                                  | com. mod: HNO <sub>3</sub> /heat under N <sub>2</sub> ; d < 50; S <sub>BET</sub> : 946; pH <sub>PZC</sub> : 9.9  | 262   |  |
|                                  | com. (BDH, Merck); S <sub>BET</sub> : 1118; pH <sub>PZC</sub> : 10.2   | 289 <sup>c</sup> (pH 5)                                       |  |
|                                  | com. (F100, Calgon); S <sub>BET</sub> : 957; pH <sub>PZC</sub> : 7.8   | 219 <sup>c</sup> (pH 5)                                       |  |
|                                  | com. (BPL, Calgon); S <sub>BET</sub> : 972; pH <sub>PZC</sub> : 8.6  | 309 <sup>c</sup> (pH 5)                                       |  |
| Methylene Blue                   | com. (BPL) mod: HCl; S <sub>BET</sub> : 1015; pH <sub>PZC</sub> : 6.7  | 282 <sup>c</sup> (pH 5)                                       | Lorenc-Grabowska and Gryglewicz (2007) |
|                                  | com. (BPL) mod: HNO <sub>3</sub> ; S <sub>BET</sub> : 987; pH <sub>PZC</sub> : 3.0                               | 272 <sup>c</sup> (pH 5)                                       |  |
|                                  | o: BC; d: 200–500; S <sub>BET</sub> : 679; V <sub>M</sub> /V <sub>T</sub> : 53.4; pH <sub>PZC</sub> : 10.2       | 52  |  |
|                                  | o: BC; d: 200–500; S <sub>BET</sub> : 475; V <sub>M</sub> /V <sub>T</sub> : 76.8; pH <sub>PZC</sub> : 11.3       | 159   |  |
|                                  | o: BC; d: 200–500; S <sub>BET</sub> : 331; V <sub>M</sub> /V <sub>T</sub> : 82.1; pH <sub>PZC</sub> : 12.0       | 161   |  |
|                                  | o: BC; d: 200–500; S <sub>BET</sub> : 370; V <sub>M</sub> /V <sub>T</sub> : 80.9; pH <sub>PZC</sub> : 12.2       | 189   |  |

<sup>a</sup> Abbreviations: com., commercial; d, AC particle size,  $\mu\text{m}$ ; o, origin; S<sub>BET</sub>, BET surface area, m<sup>2</sup> g<sup>-1</sup>; pH<sub>PZC</sub>, point of zero charge; BC, bituminous coal; mod, modified; V<sub>M</sub>/V<sub>T</sub>, mesopore/total pore volume ratio, %. <sup>b</sup> Unless not indicated differently, refers to Langmuir monolayer capacity at natural pH of dye solution. <sup>c</sup> Adsorption capacities determined by second-order kinetic model.



## 2.4. Effect of AC surface chemical characteristics

Certain physical and chemical properties of the AC may strongly influence dye adsorption, and one of the most determining factors among them is the surface chemistry of the carbon. E.g., Al-Degs et al. (2000) evaluated the adsorption of some anionic reactive dyes on a commercial AC and attributed its high adsorption capacity to its net positive surface charge. By modifying the specific properties of AC, it is possible to enhance its effectiveness for contaminant uptakes from aqueous solutions (Yin et al., 2007). Some researches have focused on this issue and one of the key target has become the modification of the surface chemistry of ACs (Figueiredo et al., 1999; Berenguer et al., 2009). Tailoring the carbon surface chemical groups can lead to significant changes in dye adsorption performance. In the works of Pereira et al. (2003), Faria et al. (2004) and Órfão et al. (2006), several ACs were modified by different acid and thermal treatments for the adsorption of different classes of dyes, without inducing any major changes in the AC textural properties. In case of all anionic (reactive, direct and acid) dyes tested, a similar behaviour was observed, following an improvement of the adsorption capacity by increasing the basicity of the AC sample. On the other hand, for cationic (basic) dyes (Pereira et al., 2003; Faria et al., 2004), the acid oxygen-containing surface groups originating from  $\text{HNO}_3$ -treatment had a positive effect on adsorption, but the thermally treated samples still presented good performances, indicating the existence of two parallel adsorption mechanisms. The first involves electrostatic interactions between the basic dye and the negatively charged carbon surface groups, while the second suggests dispersive interactions between the dye molecule and the graphene layers. Otherwise, the basic AC sample obtained by thermal treatment under  $\text{H}_2$  flow at  $700^\circ\text{C}$  was found to be the best material for adsorption of most of the dyes tested. Some other studies, however, reported dissimilar results referred to basic dye adsorption. For example, a moderate decrease in Methylene Blue (Wang et al., 2005; Wang and Zhu, 2007) and Crystal Violet (Wang and Zhu, 2007) uptake was observed after treating the AC with  $\text{HNO}_3$ .

## 2.5. Effect of AC textural characteristics

Aside from the surface chemistry, textural properties of AC play an important role. Most commercially available ACs are predominantly microporous, making them especially suitable for the adsorption of smaller pollutants. As the fraction of mesopores is increased, the obtained ACs are expected to be more efficient adsorbents of larger molecules (Macedo et al., 2006). One possible method to enlarge the porosity of ACs is  $\text{CO}_2$  gasification, e.g., with the help of previously impregnated cobalt, catalysing the formation of mesopores (Pereira et al., 2004). It is evident that if the AC pore size is crucial in dye adsorption, then the molecular size of the colourant is likewise decisive. Tamai et al.

(1999) investigated the adsorption of several acid, direct and basic dyes onto both mesoporous and microporous AC fibers in terms of the size of dye molecules and AC pore size. High amounts of sterically small-sized acid and basic dyes were adsorbed on both carbons. Among acid dyes, Acid Blue 74 and Acid Orange 10 with smaller molecular weights did not only perform better adsorption than Acid Blue 9 and Acid Orange 51 with relatively large molecular structures but were also adsorbed in higher amounts on the microporous fiber than on the mesoporous one, indicating the additional importance of specific surface area of AC in dye adsorption. On the other hand, large direct dyes were not only adsorbed to a much higher extent on the mesoporous AC than on the microporous AC but also the amounts of direct dyes adsorbed on mesoporous carbon decreased in the order of Direct Yellow 50, Direct Black 19, Direct Yellow 11, being the same order as of the one large dimension of these dyes. Lorenc-Grabowksa and Gryglewicz (2007) showed that the adsorption capacity of the diazo dye Congo Red increased with both the mesopore volume and the share of mesopores to the total pore volume. The so-called ordered mesoporous carbons (OMCs) may also be ideal model materials for studying dye adsorption on mesopores due to their periodic pore symmetry, large pore volume, high specific surface area, centralised mesopore distribution and tuneable pore diameter. When a microporous carbon and OMCs with varying pore size were simultaneously tested to remove Methylene Blue and Neutral Red from solution, the OMCs showed at least doubled dye adsorption affinities compared to the microporous carbon (Yuan et al., 2007).

## 2.6. Regeneration of AC

Although AC is an excellent material to adsorb higher amounts of dye pollutants, using it for adsorption as an individual treatment is not cost-effective and the exhausted carbon needs to be either disposed or regenerated, generating extra expenses. AC regeneration, normally, is not only cheaper than replacement but, in addition, a more environmentally friendly solution in general. Conventional methods for AC recovery have included thermal, biological and solvent regeneration (Cooney et al., 1983; Aktaş and Çeçen, 2007). In latter case, the choice of appropriate solvent is essential, that may depend on both the AC and colourant characteristics. E.g., desorption of the basic dye Malachite Green from an AC packed column was nearly complete using acetone (Gupta et al., 1997) and commercial ACs with the adsorbed azo dye Direct Red 79 were effectively regenerated by liquid water at high pressure and temperature (Salvador and Jiménez, 1999). Certain surfactants have the advantages of being both efficient under mild operation conditions and relatively innocuous from environmental point of view. The so-called surfactant enhanced carbon regeneration showed that anionic surfactants performed significantly better than a cationic one during the desorption of anionic dyes Eosin (Purkait et al., 2005) and Congo Red (Purkait et al., 2007). Also some advanced regeneration techniques removing colourants

from AC have been reported, such as wet oxidative regeneration (Shende and Mahajani, 2002), microwave irradiation (Quan et al., 2004), electrochemical regeneration (Han et al., 2008) or regeneration with dielectric barrier discharge plasma (Qu et al., 2009). In general, however, these techniques are costly, can result in significant changes in the textural/chemical characteristics of the AC, may cause considerable carbon loss and are probably much more efficient when using them as complex AC-enhanced dye wastewater treatments involving *in situ* regeneration of the carbon, instead of being separated and subsequently treated.

### **3. AC-amended physico-chemical dye removal processes**

Besides adsorption, physico-chemical dye removal techniques include coagulation, membrane filtration, electrochemical degradation and advanced oxidation processes (AOPs). Despite that most of these methods have been shown promising and highly efficient, these technologies generally appear to face several limitations since they are financially and often also methodologically demanding. To make them undoubtedly attractive, their further improvement is required. As it is presented in the following, physical and chemical dye wastewater treatments can be successfully enhanced by incorporating AC.

#### **3.1. AC-amended coagulation of dyes**

Chemical coagulation by the use of inorganic coagulants such as aluminium sulphate, ferrous sulphate or ferric chloride, used to be a feasible way of removing colour from dye wastewater (Chu, 2001; Kim et al., 2004; Golob et al., 2005). Its main advantage is the removal of dye molecules themselves without their decomposition leading to even more potentially harmful and toxic aromatic compounds (Golob et al., 2005). However, the drawback of producing a huge amount of chemical sludge has pushed this method into the background and improvements of dye coagulation processes have become necessary. Better strategies have been reported for dye removal, such as the reuse of the produced sludge (Chu et al., 2001), combined electrocoagulation process (Daneshvar et al., 2006) or AC-amended coagulation (Sanghi and Bhattacharya, 2003). In the latter study, polyaluminium chloride as coagulant was added to different dye solutions (Direct Orange, Eriochrome Black T and Malachite Green) previously treated with powdered activated carbon (PAC). The role of coagulant was dual; not only to remove the colour but also to flocculate the suspended PAC remaining in the solution after adsorption. Although significant enhancement of dye removal after the addition of a very small dose of coagulant was observed only in case of Eriochrome Black T, the formed sludge settled

much faster than PAC alone and could be effectively reused. It is possible to use AC adsorption indirectly, as a post-treatment of coagulation to ensure better process performance. The azo dyes Reactive Red 45 and Reactive Green 8 were treated by the two-step, aluminium chloride coagulation/PAC adsorption method resulting in less coagulant consumption and lower sludge volume compared to dye removal by coagulation only (Papić et al., 2004). During the treatment of Reactive Orange 16 and Reactive Black 5, coagulation by aluminium chloride followed by PAC adsorption was found to be more efficient than the reverse adsorption/coagulation method in terms of overall dye removal and chemical requirement (Lee et al., 2006a).

### 3.2. AC-amended membrane filtration of dyes

Pressure-driven membrane processes have been found suitable for the treatment of dye wastewaters from the textile industry (Xu et al., 1999; Marcucci et al., 2001; Chakraborty et al., 2003). Among microfiltration (MF), ultrafiltration (UF), nanofiltration (NF) and reverse osmosis (RO), NF was considered as probably the most adequate membrane process to separate dyes from textile effluents effectively (Xu et al., 1999; Chakraborty et al., 2003). Although NF does not reach the retention behaviour of RO, it works under less demanding conditions implying cost reduction (Marcucci et al., 2001). Lately, the use of low-pressure membrane processes (MF, UF) have received greater attention in dye removal processes which demand considerably lower operational costs than NF (Lee et al., 2006b) but, on the other hand, require intensification or combination with another process in order to ensure an appropriate permeate quality. One possibility to enhance the MF/UF process for dye removal is their integration with the dye adsorption ability of ACs. Banat and Al-Bastaki (2004) studied the separation of Methylene Blue from aqueous solutions where the dye feed containing either GAC or PAC was introduced to the UF membrane module. The UF process alone was not able to reject the colourant but, on the contrary, 85% of dye removal was achieved in the combined process with the PAC performing better than GAC. Microfiltration of the reactive dye Ostazin Red HB by a submerged membrane was not effective on its own but the addition of very low dose of PAC to dye wastewater resulted in a nearly complete colour removal, although retention of the pollutant decreased with 50% after a few hours of operation (Jirankova et al., 2007). In a hybrid coagulation–adsorption–membrane process, the submerged microfiltration membrane alone was not sufficient to reject Reactive Black 5 and Reactive Orange 16, and significant membrane fouling occurred (Lee et al., 2006b). However, the filtration performance after alum coagulation and PAC adsorption pre-treatments was very high, both concerning dye retention and micro-flocks/carbon particles separation, while only a little decline in the permeate flux was observed for the entire hours of experimental run. An efficacious development among combined membrane processes is the membrane bioreactor, nowadays widely used for municipal and industrial wastewater treatment,

which can be enhanced by the addition of AC (Park et al., 1999; Hai et al., 2008). During the removal of azo dye Acid Orange II by a submerged MF membrane fungi reactor, PAC addition resulted not only in the improvement of permeate quality but also in stable decolourisation and enzymatic activity for a period of 1 month, confirming the occurrence of simultaneous adsorption and biodegradation of the dye (Hai et al., 2008).

### 3.3. AC-amended electrochemical treatment of dyes

Electrochemical oxidation uses electrons as the main reagent, requires a little or even no chemical reagent and is a clean and effective wastewater treatment method (Yi et al., 2008) that has been successfully applied for dyeing wastewater treatment as well, with a wide variety of electrodes (anodes) tested, e.g., iron (Ling and Peng, 1994), conductive diamond (Cañizares et al., 2006) or Pt/Ti (Vlyssides et al., 1999). Although the method is quite environmentally friendly, its drawback –apart from electricity cost– is that side-reactions (e.g., electrolysis of water) may compete with the destruction of contaminant (Wang et al., 2005). Improvement of electrochemical dye degradation can be reached by the use of porous electrodes such as ACs, reducing both the energy requirement of electrolysis and side-effects, enhancing the surface area of electrode and regulating the electric current density. For example, Jia et al. (1999) reported the efficient treatment of several simulated wastewaters with dyes of reactive, acid, direct, cationic and vat groups, and real wastewaters containing vat, reactive or direct dyes or their mixtures using activated carbon fiber (ACF) electrodes; nearly all the wastewaters were decolourised for more than 90% with COD removals within about 40-80%. Similarly, Shen et al. (2001) tested the mineralisation of 29 colourants of different classes and confirmed the feasibility of ACF electrolytic process, with colour removals above 85% and TOC removals ranged between 30 and 70%.

Depending on the method and the electrode configuration, AC may be used both as a cathode or anode in the electrochemical treatment. E.g., the anthraquinone dye Alizarin Red S was successfully oxidised using an AC fiber felt as anode with considerable colour (> 95%) and COD (> 76%) removals within 60 min of electrolysis (Yi et al., 2008; Yi and Chen, 2008). The ACF anode compared with a simple carbon fiber anode worked much better in terms of colour removal, probably due to both the high specific surface area of ACF and its capability of promoting the electro-generation of the strong oxidising agent hydroxyl radical ( $\cdot\text{OH}$ ) from the oxidation of  $\text{H}_2\text{O}$  on the anode surface (Yi and Chen, 2008). The results confirmed the three-step mechanism of the electrochemical treatment, i.e., (1) dye adsorption onto the ACF surface, (2) electrolytic degradation of the adsorbed colourant and (3) *in situ* regeneration of the ACF. Larger specific surface area and higher mesopore percentage of the ACF anode lead to more effective electrochemical dye removal (Yi et al., 2008).

The electrooxidation of dyes can also be indirect based on the electrogeneration of  $H_2O_2$  from the two-electron reduction of  $O_2$  on the cathode, that is especially advantageous in the case of combined methods. Wang et al. (2005) studied the mineralisation of the azo dye Acid Red 14 by an electro-Fenton reaction based on the  $H_2O_2$  production on ACF felt cathode. During the Fenton reaction,  $\cdot OH$  radicals are generated from  $H_2O_2$  in the presence of catalytic amounts of ferrous ions (section 3.4.2). For comparative purposes, both ACF cathode and graphite cathode were tested in the absence of  $Fe^{2+}$ . Although similar decolourisation rates were achieved by these two cathode materials, the mineralisation ability of ACF felt was much higher than of graphite, due to both the large surface area of ACF and the different ability of peroxide electrogeneration of these two cathodes. On the other hand, the electro-Fenton process resulted in better TOC reduction than the single  $H_2O_2$  electrogeneration or the simple anodic oxidation that could be ascribed to the existence of fast homogeneous reaction of organics with the great amounts of  $\cdot OH$  generated. Same azo dye degradation was investigated in the so-called photoelectro-Fenton process, i.e. the UV-enhanced variant of electro-Fenton treatment, that yielded significantly more TOC removal than the UV-free electro-Fenton oxidation (Wang et al., 2008).

Apart from using ACs as electrodes, electrochemical dye removal can be improved by using the so-called three-dimensional electrode system, involving AC granules as particle electrodes between the cathode and anode. Koparal et al. (2002) used an activated carbon-perlite mixture placed inside a bipolar trickle reactor for the 'electroadsorption' of textile dye Acilan Blau, considering AC rather as dye adsorbent than particle electrode. The removal of Acid Orange 7 using the three-dimensional electrode reactor was found to be mainly dependent on the oxidation by the active substances (e.g.,  $\cdot OH$ ) produced both on ACF electrodes and GAC microelectrodes (Xu et al., 2008; Zhao et al., 2010). This method has been reported effective, both as posttreatment for colour and COD removal in a combined ferrous coagulation-electrooxidation process (Xiong et al., 2001) and as pretreatment prior to the biological process (Zhao et al., 2010). It has to be noticed that the surface chemistry of the AC can be altered by the electrochemical treatment, depending on the applied electrochemical variables (Berenguer et al., 2009). Apart from electrochemical oxidation, GAC as particle cathode can enhance the current efficiency of internal electrolysis during azo dye reduction by zero-valent iron treatment (Liu et al., 2007).

### 3.4. AC-amended advanced oxidation processes for dye removal

Advanced oxidation processes (AOPs) are characterised by a common feature: the capability of exploiting high reactive oxidising agents such as  $\cdot OH$  radicals to completely destroy the majority of organic pollutants present in wastewaters (Andreozzi et al., 1999;

Gogate and Pandit, 2004). Hydroxyl radicals with their high oxidation potential ( $E^0 = 2.33$  V) can be produced by numerous different methods and most of these have been found applicable for dye wastewater treatments. Moreover, enhanced dye removal has been reported using AC as catalyst in various processes involving oxidation by  $\cdot\text{OH}$  (Table 2.2). Techniques such as electrochemical treatments, generating  $\cdot\text{OH}$  radicals contingently and secondarily, are discussed elsewhere (section 3.3).

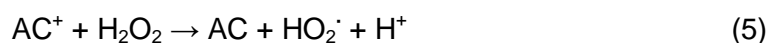
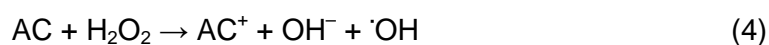
### 3.4.1. *Wet oxidation of dyes*

Catalytic wet oxidation (CWO) is a known process for oxidative treatment of industrial wastewaters. It proceeds under relatively mild conditions (125–220 °C, 5–50 bar) in the presence of an adequate catalyst (Garcia et al., 2005). The enhanced solubility of oxygen in aqueous solutions at elevated temperatures and pressures provides a strong driving force to oxidation of contaminants by active oxygen species such as hydroxyl radicals (Levec and Pintar, 2007). Wet oxidation of different toxic contaminants can be catalysed by AC (Santiago et al., 2005; Stüber et al., 2005; Suarez-Ojeda et al., 2005) and CWO of textile dyes using AC as catalyst is considered a promising technology as well. E.g., Santos et al. (2007) studied the abatement of synthetic dyes Orange G, Brilliant Green and Methylene Blue by means of the CWO method in a fixed-bed reactor with AC as catalyst. All colourants with high initial concentrations were almost completely decolourised, and TOCs were moderately removed at a hydraulic residence time (HRT) of 15 min. Although the strong oxidation conditions promote certain changes in AC textural and surface chemical properties, the catalyst kept its activity and stability for at least 200 h of continuous operation at a weight lost of less than 5%. CWO with AC-supported copper catalyst promoted significantly better TOC removal from real dyeing and printing wastewater than the identical treatment without a catalyst, and moderately better oxidation than the treatment with either homogeneous (copper nitrate solution) catalyst or aluminium-supported copper catalyst, although Cu itself (immobilised on AC) seemed to have a little effect on the catalytic activity (Hu et al., 1999). A newer class of advanced materials for catalytic applications is the nanostructured carbon (Serp et al., 2003) with a broad range of potential applications, e.g., as support for preparing heterogeneous catalysts for liquid-phase reactions. Garcia et al. (2005) tested a platinum catalyst with a multi-walled carbon nanotube (MWNT) support activated by nitric acid oxidation for the catalytic oxidation of textile azo dyes and a real textile effluent. While decolourisation of the dyes by wet oxidation at a temperature of 150 °C and 6.9 bar of oxygen partial pressure was very poor in the absence of catalyst, each azo dye was almost completely decolourised in the CWO process catalysed by Pt/MWNT. The treatment of real wastewater under the same conditions showed that the same catalyst could significantly improve both colour and TOC removal efficiencies. Other nanocarbons such as carbon nanofibers (CNFs), impregnated with copper after their acidic activation, have been

furthermore reported to improve both TOC and colour removal from washing textile industrial wastewater (Rodríguez et al., 2008) and from mono-, di- and triazo dye solutions (Rodríguez et al., 2009) in the CWO process.

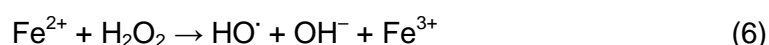
### 3.4.2. Wet peroxide oxidation of dyes

A couple of studies have shown that oxidation of different organic compounds by the environmentally friendly  $\text{H}_2\text{O}_2$  can be enhanced by AC (Lücking et al., 1998; Huang et al., 2003; Georgi and Kopinke, 2005). The peroxide ( $E^0 = 1.78 \text{ V}$ ) can be activated on the AC surface involving the formation of free oxidising species such as the hydroxyl radical (Eqs. (4) and (5)):



where AC functions as an electron transfer catalyst and AC and  $\text{AC}^+$  symbolizes the oxidised and reduced catalyst states, respectively (Georgi and Kopinke, 2005; Kimura and Miyamoto, 1994). High colour removal efficiencies were reported in a combined catalytic peroxide oxidation/catalytic wet air oxidation system treating the dyes Direct Blue 71 and Direct Black 19 (Lin and Lai, 1999). Parameters such as the amount of GAC or the concentration of  $\text{V}_2\text{O}_5$  catalyst showed significant effects on the decolourisation while the presence of peroxide as additional oxidant was found unnecessary at an air supply of  $3 \text{ L min}^{-1}$ , possibly due to either the high dye removal rates even without peroxide or the (partial)  $\text{H}_2\text{O}_2$  decomposition under the applied conditions. A recent study proved that decolourisation of dye solutions by oxidation with  $\text{H}_2\text{O}_2$  in the presence of AC is strongly influenced by the carbon surface chemistry (Santos et al., 2009). While non-catalytic reaction without AC was inefficient in case of most dyes from several groups, the combination of AC with  $\text{H}_2\text{O}_2$  could significantly enhance the oxidation process due to the catalytic decomposition of  $\text{H}_2\text{O}_2$  into free radicals. Latter findings were explained by the involvement of the free electrons on the graphene basal planes of AC as active centres for the catalytic reaction.

Another method for peroxide activation is the Fenton reaction in which ferrous ions as catalysts react with hydrogen peroxide in acidic medium, producing hydroxyl radicals (Eq. 6):



Although the Fenton process has been demonstrated effective in decolourising dye wastewaters (Kuo, 1992; Solozhenko, 1995; Shueh et al., 2005), it has the disadvantage of producing effluents with generally higher Fe ion concentrations than the European Union directives allow to release into the environment ( $2 \text{ mg L}^{-1}$ ). By immobilising Fe ions



**Table 2.2 (I).** Selected results of physico-chemical dye oxidation studies with AC-catalysed decolourisation.

| oxidation process  | system characteristics <sup>a</sup>  | AC catalytic role   | AC characteristics <sup>b</sup>   |
|--------------------|--|---|---|
| electrochemical    | cont.; A: ACF felt; C: stainless steel sheet; V: 110; HRT: ~46.8             | $\cdot$ OH generation by H <sub>2</sub> O oxidation                                       | S <sub>BET</sub> : 893.7; S <sub>MIC</sub> /S <sub>BET</sub> : 0.749<br>S <sub>BET</sub> : 1053; S <sub>MIC</sub> /S <sub>BET</sub> : 0.720<br>S <sub>BET</sub> : 1374; S <sub>MIC</sub> /S <sub>BET</sub> : 0.572<br>S <sub>BET</sub> : 1682; S <sub>MIC</sub> /S <sub>BET</sub> : 0.200   |
| electrochemical    | batch; A: RuO <sub>2</sub> /Ti; C: ACF felt; V: 500                          | $\cdot$ OH generation from H <sub>2</sub> O <sub>2</sub> produced on the cathode          | S <sub>BET</sub> : 1237   |
| electro-Fenton     | batch; A: RuO <sub>2</sub> /Ti; C: ACF felt; Fe <sup>2+</sup> (c: 1); V: 500 |   |   |
| electrochemical    | batch; A: viscose-based ACF felt; C: stainless steel sheet; V: 50            | $\cdot$ OH generation by H <sub>2</sub> O oxidation                                       | S <sub>BET</sub> : ~1000  |
| electrochemical    | batch; A: stainless steel plate; C: ACF                                      | $\cdot$ OH generation from H <sub>2</sub> O <sub>2</sub> produced on the cathode          | S <sub>BET</sub> : 764.1  |
|                    | batch; A: stainless steel plate; C: ACF; PE: GAC; V: 500                     |   | ACF (S <sub>BET</sub> : 764.1) + GAC (cc: 100; S <sub>BET</sub> : 910.7)  |
| wet oxidation      | batch; p: 6.9; T: 150; V: 75   | $\cdot$ OH generation from O <sub>2</sub> -saturated H <sub>2</sub> O at elevated p and T | Pt-imp. MWNT; cc: ~10.7; S <sub>BET</sub> : ~175  |
| wet oxidation      | cont. fixed-bed reactor; p: 16; T: 160; HRT: 15                              | $\cdot$ OH generation from O <sub>2</sub> -saturated H <sub>2</sub> O at elevated p and T | GAC (Ind. React FE0160A); d: 800–1000; ccv: ~0.32; S <sub>BET</sub> : 745   |
| wet oxidation      | batch; p: 8.7; T: 140; V: 75   | $\cdot$ OH generation from O <sub>2</sub> -saturated H <sub>2</sub> O at elevated p and T | Cu-imp. CNF; dxl: 20–50 × 50–100; S <sub>BET</sub> : 188  |
| peroxide oxidation | batch; H <sub>2</sub> O <sub>2</sub> (c: 1500); V: 600                       | $\cdot$ OH generation from peroxide   | GAC (Norit GAC 1240 PLUS); d: 100–300; cc: ~2.2; S <sub>BET</sub> : 972; pH <sub>PZC</sub> : 7.9; CO: 995<br>GAC mod: HNO <sub>3</sub> ; d: 100–300; cc: ~2.2; S <sub>BET</sub> : 909; pH <sub>PZC</sub> : 3.0; CO: 2920<br>GAC mod: HNO <sub>3</sub> /heat under H <sub>2</sub> ; d: 100–300; cc: ~2.2; S <sub>BET</sub> : 946; pH <sub>PZC</sub> : 9.8; CO: 575 |

**Table 2.2 (II).** Selected results of physico-chemical dye oxidation studies with AC-catalysed decolourisation.

| wastewater characteristics <sup>c</sup> | results <sup>d</sup>   |   | reference               |
|---|--|---|-------------------------|
|   | with AC  | without AC  |                         |
| SW: Alizarin Red S (c: 200); pH: ~6.5   | X <sub>COL</sub> : ~0.63 (λ: 507)<br>X <sub>COL</sub> : ~0.70 (λ: 507)<br>X <sub>COL</sub> : ~0.75 (λ: 507)<br>X <sub>COL</sub> : ~0.82 (λ: 507) | –   | Yi et al. (2008)        |
| SW: Acid Red 14 (c: 200); pH: 3.0       | X <sub>TOC</sub> : 0.50 (6 h)<br><br>X <sub>COL</sub> : ~1.00 (1.5 h);<br>X <sub>TOC</sub> : 0.70 (6 h)  | –<br><br>X <sub>COL</sub> : ~1.00 (1.5 h)<br>X <sub>TOC</sub> : 0.40 (6 h)<br>[C: graphite]                     | Wang et al. (2005)      |
| SW: Alizarin Red S (c: 700); pH: 7.0    | X <sub>COL</sub> : ~0.98 (1 h)<br>X <sub>COD</sub> : 0.765 (1 h)   | X <sub>COL</sub> : ~0.50 (1 h)<br>[A: carbon fiber]   | Yi and Chen (2008)      |
| SW: Acid Orange 7 (c: 300); pH: 3.0     | X <sub>COL</sub> > 0.96 (10×1 h)<br>X <sub>TOC</sub> : 0.574 (10×1 h)  | X <sub>TOC</sub> : 0.460 (10×1 h)<br>[C: graphite]<br>X <sub>TOC</sub> : 0.413 (10×1 h)<br>[C: stainless steel] | Xu et al. (2008)        |
| SW: Acid Orange 7 (c: 300); pH: 3.0     | X <sub>COL</sub> > 0.99 (3 h)<br>X <sub>TOC</sub> : 0.719 (3 h)  | –   |                         |
| SW: Solophenyl Green BLE (c: 2000)      | X <sub>COL</sub> : 0.995 (2 h)<br>X <sub>TOC</sub> : 0.212 (2 h)   | X <sub>COL</sub> : 0.0 (2 h)  | Garcia et al. (2005)    |
| SW: Chromotop 2R (c: 2000)              | X <sub>COL</sub> : 1.00 (2 h)<br>X <sub>TOC</sub> : 0.635 (2 h)  | X <sub>COL</sub> : 0.0 (2 h)  |                         |
| SW: Erionyl Red B (c: 2000)             | X <sub>COL</sub> : 0.995 (2 h)<br>X <sub>TOC</sub> : 0.781 (2 h)   | X <sub>COL</sub> : 0.280 (2 h)  |                         |
| SW: Orange G (c: 1000)                  | X <sub>COL</sub> : ~1.00<br>X <sub>TOC</sub> : ~0.40   | X <sub>COL</sub> , X <sub>TOC</sub> : ~0.0<br>[glass spheres]   | Santos et al. (2007)    |
| SW: Brilliant Green (c: 1000)           | X <sub>COL</sub> : ~1.00<br>X <sub>TOC</sub> : ~0.55   |   |                         |
| SW: Methylene Blue (c: 1000)            | X <sub>COL</sub> : ~1.00<br>X <sub>TOC</sub> : ~0.55   |   |                         |
| SW: Acid Orange 7 (c: 1000)             | X <sub>COL</sub> : 0.996 (3 h)<br>X <sub>TOC</sub> : 0.241 (3 h)   | X <sub>COL</sub> : 0.241 (3 h)<br>X <sub>TOC</sub> : 0.120 (3 h)  | Rodríguez et al. (2008) |
| SW: Eriochrome Blue Black (c: 1000)     | X <sub>COL</sub> : 1.00 (3 h)<br>X <sub>TOC</sub> : 0.500 (3 h)  | X <sub>COL</sub> : 0.973 (3 h)<br>X <sub>TOC</sub> : 0.041 (3 h)  |                         |
| SW: Direct Blue 71 (c: 1000)            | X <sub>COL</sub> : 1.00 (3 h)<br>X <sub>TOC</sub> : 0.068 (3 h)  | X <sub>COL</sub> : 0.582 (3 h)<br>X <sub>TOC</sub> : 0.010 (3 h)  |                         |
| SW: Reactive Black 5 (c: 1000)          | X <sub>COL</sub> : 1.00 (3 h)<br>X <sub>TOC</sub> : 0.250 (3 h)  | X <sub>COL</sub> : 0.340 (3 h)<br>X <sub>TOC</sub> : 0.186 (3 h)  |                         |
| SW: Reactive Red 241 (c: 50); pH: 3.0   | k: 6.2×10 <sup>-3</sup><br><br>k: 5.4×10 <sup>-3</sup><br><br>k: 8.7×10 <sup>-3</sup>  | k: 4.2×10 <sup>-4</sup>   | Santos et al. (2009)    |

**Table 2.2 (I).** Selected results of physico-chemical dye oxidation studies with AC-catalysed decolourisation. (cont.)

| oxidation process  | system characteristics <sup>a</sup>                         | AC catalytic role                  | AC characteristics <sup>b</sup>  |
|--------------------|---|------------------------------------|--|
| peroxide oxidation | batch; H <sub>2</sub> O <sub>2</sub> (c: ~1.14); V: ~1000   | ·OH generation from peroxide       | GAC (F400, Calgon); d: 425–600; cc: 2; S <sub>BET</sub> : 800–900  |
| Fenton             | batch; H <sub>2</sub> O <sub>2</sub> (c: ~1.14); V: ~1000   |                                    | GAC (F400, Calgon); d: 425–600; cc: 4; S <sub>BET</sub> : 800–900  |
|                    | batch; H <sub>2</sub> O <sub>2</sub> (c: ~1.14); V: ~1000   |                                    | Fe-imp. GAC (~3.7%); d: 425–600; cc: 2   |
|                    | batch; H <sub>2</sub> O <sub>2</sub> (c: ~1.14); V: ~1000   |                                    | Fe-imp. GAC (~3.7%); d: 425–600; cc: 4   |
| peroxide oxidation | batch; H <sub>2</sub> O <sub>2</sub> (c: 6); V: 200         | ·OH generation from peroxide       | o: olive stone; d < 200; cc: 0.2; S <sub>BET</sub> : 691   |
| Fenton             |   |                                    | Fe-imp. GAC (~7.0%); d < 200; cc: 0.2  |
| ozonation          | batch; q <sub>G</sub> : 285; q <sub>O</sub> : 2.15; V: 600  | ·OH generation from O <sub>3</sub> | GAC (Norit GAC 1240 PLUS); d: 100–300; cc: 0.5; S <sub>BET</sub> : 972; pH <sub>PZC</sub> : 9.7                              |
|                    |   |                                    | GAC mod: HNO <sub>3</sub> ; d: 100–300; cc: 0.5; S <sub>BET</sub> : 909; pH <sub>PZC</sub> : 2.7                             |
|                    |   |                                    | GAC mod: HNO <sub>3</sub> /heat under H <sub>2</sub> ; d: 100–300; cc: 0.5; S <sub>BET</sub> : 972; pH <sub>PZC</sub> : 10.8 |
| ozonation          | batch; q <sub>G</sub> : 4000; q <sub>O</sub> : 0.5; V: 2000 | ·OH generation from O <sub>3</sub> | GAC; d: ~5000; cc: 5; S <sub>BET</sub> : 893   |
|                    |   |                                    | GAC; d: ~5000; cc: 50; S <sub>BET</sub> : 893  |
| ozonation          | batch; q <sub>G</sub> : 150; q <sub>O</sub> : 7.5; V: 700   | ·OH generation from O <sub>3</sub> | GAC (Norit GAC 1240 PLUS); d: 100–300; cc: 0.5; S <sub>BET</sub> : 909   |
|                    |   |                                    | GAC/cerium oxide composite (Ce-O: ~45%); d: 100–300; cc: 0.5; S <sub>BET</sub> : 583   |

**Table 2.2 (II).** Selected results of physico-chemical dye oxidation studies with AC-catalysed decolourisation. (cont.)

| wastewater characteristics <sup>c</sup>  | results <sup>d</sup>   |  | reference             |
|--|--|--|-----------------------|
|  | with AC  | without AC   |                       |
| SW: Acid Black 24<br>(c: 120); pH: 2.0<br>TW; pH: 1.9  | X <sub>COL</sub> : 0.74 (3 h)<br>X <sub>COL</sub> : 0.60 (3 h)   | X <sub>COL</sub> : 0.59 (3 h)<br>X <sub>COL</sub> : 0.12 (3 h)   | Fan et al. (2006)     |
| SW: Acid Black 24<br>(c: 120); pH: 2.0<br>TW; pH: 1.9  | X <sub>COL</sub> : 0.78 (3 h)<br>X <sub>COL</sub> : 0.62 (3 h)   | X <sub>COL</sub> : 0.59 (3 h)<br>X <sub>COL</sub> : 0.12 (3 h)   |                       |
| SW: Orange II<br>(c: 35); pH: 3.0  | X <sub>COL</sub> : 0.98 (20 h)<br>X <sub>COL</sub> : 0.98 (4 h)  | X <sub>COL</sub> : 0.036 (20 h)  | Ramirez et al. (2007) |
| SW: Acid Blue 113<br>(c: 100)<br>SW: H. Reactive Red 241 (c: 100)<br>SW: Basic Red 14 (c: 100)<br>SW: Acid Blue 113 (c: 100)<br>SW: H. Reactive Red 241 (c: 100)<br>SW: Basic Red 14 (c: 100)<br>SW: Acid Blue 113 (c: 100)<br>SW: H. Reactive Red 241 (c: 100)<br>SW: Basic Red 14 (c: 100)   | k: 0.470<br>X <sub>TOC</sub> : ~0.59 (1.5 h)<br>k: 0.330<br>X <sub>TOC</sub> : ~0.63 (1.5 h)<br>k: 0.532<br>X <sub>TOC</sub> : ~0.54 (1.5 h)<br>k: 0.462<br>k: 0.325<br>k: 0.456<br>k: 0.413<br>k: 0.337<br>k: 0.520   | k: 0.412<br>X <sub>TOC</sub> : ~0.35 (1.5 h)<br>k: 0.326<br>X <sub>TOC</sub> : ~0.50 (1.5 h)<br>k: 0.470<br>X <sub>TOC</sub> : ~0.15 (1.5 h)<br>k: 0.412<br>k: 0.326<br>k: 0.470<br>k: 0.412<br>k: 0.326<br>k: 0.470   | Faria et al. (2005)   |
| TW; COD: 484   | X <sub>COL</sub> : ~0.95 (1 h)<br>X <sub>COD</sub> : ~0.40 (1 h)<br>X <sub>COL</sub> : ~0.98 (1 h)<br>X <sub>COD</sub> : ~0.77 (1 h)   | X <sub>COL</sub> : ~0.94 (1 h)<br>X <sub>COD</sub> : ~0.29 (1 h)   | Lin and Lai (2000)    |
| SW: Acid Blue 113<br>(c: 50); pH: 5.8<br>SW: Reactive Yellow 3<br>(c: 50); pH: 5.8<br>SW: Reactive Blue 5<br>(c: 50); pH: 5.6<br>TW (bio-treated);<br>TOC: 150; pH: 9.3<br>SW: Acid Blue 113<br>(c: 50); pH: 5.8<br>SW: Reactive Yellow 3<br>(c: 50); pH: 5.8<br>SW: Reactive Blue 5<br>(c: 50); pH: 5.6<br>TW (bio-treated);<br>TOC: 150; pH: 9.3 | X <sub>TOC</sub> : ~0.87 (2 h)<br>X <sub>TOC</sub> : ~0.81 (2 h)<br>X <sub>TOC</sub> : ~0.79 (2 h)<br>X <sub>TOC</sub> : ~0.40 (2 h)<br>X <sub>TOC</sub> : ~0.98 (2 h)<br>X <sub>TOC</sub> : ~0.97 (2 h)<br>X <sub>TOC</sub> : ~1.00 (2 h)<br>X <sub>TOC</sub> : ~0.35 (2 h) | X <sub>COL</sub> : ~0.97 (5 min)<br>X <sub>TOC</sub> : ~0.87 (2 h)<br>X <sub>COL</sub> : ~0.88 (5 min)<br>X <sub>TOC</sub> : ~0.73 (2 h)<br>X <sub>COL</sub> : ~0.98 (5 min)<br>X <sub>TOC</sub> : ~0.64 (2 h)<br>X <sub>TOC</sub> : ~0.27 (2 h)<br>X <sub>COL</sub> : ~0.97 (5 min)<br>X <sub>TOC</sub> : ~0.87 (2 h)<br>X <sub>COL</sub> : ~0.88 (5 min)<br>X <sub>TOC</sub> : ~0.73 (2 h)<br>X <sub>COL</sub> : ~0.98 (5 min)<br>X <sub>TOC</sub> : ~0.64 (2 h)<br>X <sub>TOC</sub> : ~0.27 (2 h) | Faria et al. (2009a)  |

**Table 2.2 (I).** Selected results of physico-chemical dye oxidation studies with AC-catalysed decolourisation. (cont.)

| oxidation process | system characteristics <sup>a</sup>   | AC catalytic role                              | AC characteristics <sup>b</sup>   |
|-------------------|---|--|---|
| photochemical     | batch; UV, H <sub>2</sub> O <sub>2</sub> (c: 12, without GAC; c: 9, with GAC); V: ~5000 | ·OH generation from peroxide                   | GAC (Prolab); d: 840–1680; cc: 8  |
| photocatalytic    | batch; UV, TiO <sub>2</sub> (C <sub>PC</sub> : 1); V: 800                               | sensitization of photocatalytic ·OH generation | PAC (Norit C GRAN); cc: 0.2; S <sub>BET</sub> : 1400<br>PAC (Norit GAC 1240 PLUS); cc: 0.2; S <sub>BET</sub> : 1000<br>PAC (Norit ROX 0.8); cc: 0.2; S <sub>BET</sub> : 1100<br>PAC (ROX 0.8) mod: H <sub>2</sub> O <sub>2</sub> ; cc: 0.2; S <sub>BET</sub> : 908<br>PAC (ROX 0.8) mod: HNO <sub>3</sub> ; cc: 0.2; S <sub>BET</sub> : 893<br>PAC (ROX 0.8) mod: HNO <sub>3</sub> /heat under H <sub>2</sub> ; cc: 0.2; S <sub>BET</sub> : 987 |
| photocatalytic    | batch; UV, TiO <sub>2</sub> (C <sub>PC</sub> : 1); V: 800                               | sensitization of photocatalytic ·OH generation | GAC (Norit C GRAN); d: 100–300; cc: 0.2; S <sub>BET</sub> : 1400  |
| photocatalytic    | batch; UV, TiO <sub>2</sub> (C <sub>PC</sub> : 2); V: ~250                              | sensitization of photocatalytic ·OH generation | TiO <sub>2</sub> -imp. ACF; S <sub>BET</sub> : 434.9; T <sub>C</sub> : 600<br><br>TiO <sub>2</sub> -imp. ACF; S <sub>BET</sub> : 555.1; T <sub>C</sub> : 800  |

<sup>a</sup>Abbreviations: cont., continuous; A, anode; C, cathode; V, volume of wastewater treated, mL; HRT, hydraulic residence time, min; c, concentration, mM; PE, particle electrode; p: oxygen partial pressure, bar; T, temperature, °C; q<sub>G</sub>, ozone–gas mixture flow rate, cm<sup>3</sup> min<sup>-1</sup>; q<sub>O</sub>, ozone mass flow rate, mg min<sup>-1</sup>; UV, ultraviolet irradiation; C<sub>PC</sub>, photocatalyst concentration, g L<sup>-1</sup>. <sup>b</sup>Abbreviations: S<sub>BET</sub>, BET surface area, m<sup>2</sup> g<sup>-1</sup>; S<sub>MIC</sub>/S<sub>BET</sub>, microporous surface area/BET surface area ratio; cc, carbon concentration in the liquid phase, g L<sup>-1</sup>; imp., impregnated; MWNT, multi-walled carbon nanotube; d, AC particle size, μm; ccv, carbon concentration in the fixed-bed volume, g mL<sup>-1</sup>; CNF, carbon nanofiber; dxl, diameter×length, nm×nm; pH<sub>PZC</sub>, point of zero charge; CO, amount of CO-emitting groups on AC surface, μmol g<sup>-1</sup>; mod, modified; o, origin; T<sub>C</sub>, calcination temperature, °C.

(or Fe oxides) on an appropriate support, the problem noted may be overcome. E.g., Fan et al. (2006) compared removal efficiencies of the azo dye Acid Black 24 in several treatment processes such as GAC (only adsorption), H<sub>2</sub>O<sub>2</sub> (noncatalytic oxidation), GAC/H<sub>2</sub>O<sub>2</sub> (catalytic oxidation with GAC) and FeGAC/H<sub>2</sub>O<sub>2</sub> (catalytic oxidation with iron oxide-coated GAC). Among all, FeGAC/H<sub>2</sub>O<sub>2</sub> provided the best dye removals, suggesting a synergic effect between AC and iron catalysis. The solution pH strongly affected the removal efficiency sequence of the processes tested and treatments with H<sub>2</sub>O<sub>2</sub> were more

**Table 2.2 (II).** Selected results of physico-chemical dye oxidation studies with AC-catalysed decolourisation. (cont.)

| wastewater characteristics <sup>c</sup>    | results <sup>d</sup>   |  | reference              |
|--|--|--|------------------------|
|  | with AC  | without AC   |                        |
| SW: H. Everzol Black<br>GSP (c: 36); pH: 7 | k: 0.29 (20 min, $\lambda$ : 596)<br>$k_{\text{TOC}}$ : 0.019 (45 min)                         | k: 0.20 (20 min, $\lambda$ : 596)<br>$k_{\text{TOC}}$ : 0.011 (45 min) | Ince et al. (2002)     |
| SW: Solophenyl Green<br>BLE (c: 40–50 ADA) | k: 0.0475<br><br>k: 0.0382<br><br>k: 0.0457<br><br>k: 0.0435<br><br>k: 0.0245<br><br>k: 0.0389 | k: 0.0243  | Silva and Faria (2003) |
| SW: Solophenyl Green<br>BLE (c: 41–50 ADA) | k: 0.048   | k: 0.042 (9 min) [UV]<br>k: 0.024 (9 min) [UV/TiO <sub>2</sub> ]       | Silva et al. (2006)    |
| SW: Erionyl Red B<br>(c: 41–50 ADA)        | k: 0.063   | k: 0.030 (9 min) [UV]<br>k: 0.059 (9 min) [UV/TiO <sub>2</sub> ]       |                        |
| SW: Chromotrope 2R<br>(c: 41–50 ADA)       | k: 0.034   | k: 0.024 (9 min) [UV]<br>k: 0.023 (9 min) [UV/TiO <sub>2</sub> ]       |                        |
| SW: Methyl Orange<br>(c: 120)              | k: 0.379   | k: 0.253 (1st cycle, 30 min)<br>[UV/TiO <sub>2</sub> ]                 | Shi et al. (2008)      |
| SW: Acid Fuchsine<br>(c: 120)              | k: 0.251   | k: 0.164 (1st cycle, 30 min)<br>[UV/TiO <sub>2</sub> ]                 |                        |
| SW: Methyl Orange<br>(c: 120)              | k: 0.355   | k: 0.253 (1st cycle, 30 min)<br>[UV/TiO <sub>2</sub> ]                 |                        |
| SW: Acid Fuchsine<br>(c: 120)              | k: 0.143   | k: 0.164 (1st cycle, 30 min)<br>[UV/TiO <sub>2</sub> ]                 |                        |

<sup>c</sup>Abbreviations: SW, simulated wastewater; c, inlet concentration, mg L<sup>-1</sup>; TW, textile wastewater; H, hydrolysed; COD, chemical oxygen demand, mg L<sup>-1</sup>; TOC, total organic carbon, mg L<sup>-1</sup>; ADA, after dark adsorption. <sup>d</sup>Abbreviations:  $X_{\text{COL}}$ , colour removal;  $\lambda$ , wavelength of colour analysis, nm;  $X_{\text{TOC}}$ , total organic carbon removal;  $X_{\text{COD}}$ , chemical oxygen demand removal; k, first-order decolourisation rate constant, min<sup>-1</sup>;  $k_{\text{TOC}}$ , first-order TOC removal rate constant, min<sup>-1</sup>.

effective under acidic conditions. In case of a real dye wastewater, the decolourisation by GAC/H<sub>2</sub>O<sub>2</sub> and FeGAC/H<sub>2</sub>O<sub>2</sub> methods was about six times higher than by single H<sub>2</sub>O<sub>2</sub> oxidation. In a heterogeneous Fenton-like reaction for azo dye Orange II decolourisation using iron-impregnated AC catalyst as peroxide activator, the catalytic activity of Fe/AC surpassed the activity of AC support itself (Ramirez et al., 2007). However, an important limitation of this catalyst was the iron loss from the support. This problem can be avoided either by preparing other types of carbon supports such as carbon aerogels in which iron is within the aerogel structure (Ramirez et al., 2007) or, alternatively, by tailoring the AC to

meet the demands of the catalytic reaction considered and using it as a catalyst on its own (Santos et al., 2009).

### 3.4.3. Ozonation of dyes

Ozone is a more powerful oxidising agent ( $E^0 = 2.07$  V) than other well-known oxidants such as  $H_2O_2$ . It is capable of oxidising a vast range of organic pollutants in industrial wastewaters, such as wastewaters from the textile industry (Lin and Lin, 1993). Single ozonation, however, rarely leads to total mineralisation. The oxidation can be strongly enhanced in terms of ozone consumption efficiency, operation time and mineralisation rate by homogeneous or heterogeneous catalysis (Legube and Leitner, 1999). Apart from the most common catalysts such as metal oxides or supported metal oxides (Legube and Leitner, 1999; Kasprzyk-Hordern et al., 2003), AC was suggested as an attractive alternative, accelerating the transformation of  $O_3$  into  $\cdot OH$  radicals in aqueous phase (Jans and Hoigné, 1998). In general, catalytic ozonation with AC is strongly influenced by its textural and surface chemical features and favoured by ACs with large surface areas and high basicity (Faria et al., 2005; Sánchez-Polo et al., 2005; Faria et al., 2006). It has to be noted that even in liquid phase, ozone may oxidise the AC surface to a certain extent, resulting in both the introduction of oxygenated electron-withdrawing groups and the decrease of catalytic activity (Faria et al., 2006).

Most of the studies suggesting AC catalysis during the ozonation of a dye wastewater showed that ozone alone is strong enough to decolourise the colourants and that AC plays merely a role in COD/TOC removal enhancement. E.g., Lin and Lai (2000) investigated the ozone oxidation of a textile wastewater in a fluidised or fixed GAC bed reactor. While the amount of GAC had a relatively little effect on wastewater colour removal, COD reduction was considerably enhanced by adding more GAC into the reactor up to a maximum amount. The non-catalytic ozonation of Acid Blue 113, Reactive Red 241 and Basic Red 14 quickly decolourised all the dye solutions but no satisfactory TOC removals were achieved (Faria et al., 2005). However, AC-amended ozonation not only increased decolourisation but also mineralisation of the organic matter, the latter showing a close relationship with the basicity of the AC sample. Gül et al. (2007) ozonised the azo dyes Reactive Red 194 and reactive Yellow 145 in aqueous solutions and reached double TOC removal efficiencies in the presence of GAC. The authors showed that although the formation of hydroxyl radicals took place on the GAC surface, the main oxidative reactions proceeded in the bulk of the solution. The positive contribution of AC to dye removal efficiencies during ozonation was furthermore evidenced by an optimisation study for the removal of Bomaplex Red CR-L textile dye, by using the so-called Taguchi method. The study investigated the effects of  $HCO_3^-$  ions, temperature, ozone–air flow rate, dye concentration, AC amount,  $H_2O_2$  concentration, pH and treatment time on decolourisation

(Oguz et al., 2006). The most important parameter affecting the dye removal was the amount of AC (with maximum value as optimal). The  $\text{HCO}_3^-$  ions have a negative effect on decolourisation in the catalytic ozonation process, probably due to their scavenging effect on the  $\cdot\text{OH}$  radicals (Kasprzyk-Hordern et al., 2003; Oguz et al., 2006; Oguz and Keskinler, 2008). Under continuous operation of AC-enhanced ozonation, the reactor configuration (e.g., distribution of the gas bubbles) can affect not only the colour and TOC removal rates from dye solutions/textile wastewaters but other cost-sensitive parameters such as the ozone requirement (Soares et al., 2007).

Further improvements in dye mineralisation can be achieved when the catalytic ozonation runs with the use of an advanced catalyst, e.g. when AC is combined with a metal (or metal oxide) catalyst. Faria et al. (2009a) studied the catalytic ozonation of dyes Acid Blue 113, Reactive Yellow 3, Reactive Blue 5 and textile effluents by AC, cerium oxide and ceria-AC composite as catalyst materials. Compared to single ozonation, no major improvements were observed in colour removal rates by the catalysed processes. On the other hand, mineralisation of the dye solutions was enhanced by using the catalysts. The metal oxide performed better than AC alone, while the composite showed a synergic effect between them, leading to the best catalyst performance among all. However, during real textile wastewater treatment,  $\text{O}_3/\text{AC}$  provided better TOC reduction than ozonation with either cerium oxide or composite catalyst. This behaviour was attributed to the scavenging effect of bicarbonate and carbonate ions in the effluent (Kasprzyk-Hordern et al., 2003; Oguz et al., 2006; Oguz and Keskinler, 2008) that somehow was less significant in case of single AC catalysis. Another study of these authors (Faria et al., 2009b) examined the effect of AC impregnation by manganese, cobalt or cerium on the removal of diazo dye Acid Blue 113 by catalytic ozonation. As it could be expected, the catalytic treatments resulted in an increase, particularly of dye mineralisation, compared to single ozonation. Although the best results were obtained by the catalyst containing cerium, the major part of the catalytic effect observed with the supported metal oxides must have been attributed to the AC support. From the studies above it can be concluded that AC can be an effective choice as catalyst on its own for the catalytic ozonation of real (textile) wastewaters.

#### 3.4.4. Photochemical and photocatalytic removal of dyes

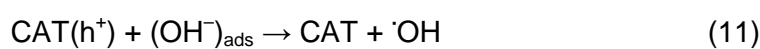
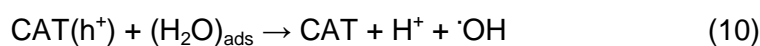
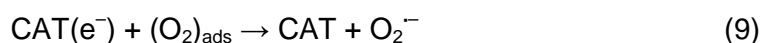
In recent years, photochemical processes based on ultraviolet (UV) radiation have been progressively developed for the removal of hazardous organic compounds due to their efficient, environmentally- and relatively cost-friendly nature. The role of UV in advanced oxidation processes is the formation of hydroxyl radicals when used in combination with a strong oxidising agent such as hydrogen peroxide (Eq. 7):





The UV/H<sub>2</sub>O<sub>2</sub> treatment was suitable for dye removal from wastewater (Shu et al., 1994; Ince and Gönenç, 1997). During the UV/H<sub>2</sub>O<sub>2</sub> photochemical treatment of the textile reactive dye Eversol Black-GSP, both decolourisation and TOC reduction was enhanced by GAC addition (Ince et al., 2002). Although this increment was ascribed solely to GAC adsorption, it is probably also due to the AC-catalysed peroxide decomposition producing additional ·OH radicals (section 3.4.2).

Heterogeneous photocatalysis has received an increasing attention as it is carried out under ambient conditions, does not require expensive oxidants or additives and the catalysts are generally inexpensive, chemically stable and non-toxic (Herrmann, 2005). The process is initiated upon UV irradiation of the photocatalyst with the formation of electron/hole pairs (e<sup>-</sup>/h<sup>+</sup>), which can migrate rapidly to the surface and initiate redox reactions with suitable substrates. Oxygen over the catalyst acts as electron acceptor to form superoxide radicals while adsorbed OH<sup>-</sup> groups and H<sub>2</sub>O molecules are available as electron donors to yield the hydroxyl radical (Silva and Faria, 2003):



The degradation of colourants by semiconductor-assisted photocatalytic processes has been thoroughly investigated (Tanaka et al., 2000; Lachheb et al., 2002; Konstantinou and Albanis, 2004; Behnajady et al., 2006; Bizani et al., 2006). Most of these studies demonstrate efficient colour and TOC removal. Nevertheless, the addition of AC into the catalyst-suspended aqueous dye solution can have remarkable effect on pollutant removal. For instance, Silva and Faria (2003) conducted a study with photochemical and photocatalytic degradation of the triazo dye Solophenyl Green BLE in aqueous solution by UV irradiation. The photocatalysis was carried out by using both commercial titanium dioxide and mixtures of TiO<sub>2</sub> with different ACs suspended in the solution. Although single UV treatment performed the best at lower dye concentrations, photocatalytic decolourisation was more efficient for solutions with higher dye content. The presence of AC enhanced the photoefficiency of TiO<sub>2</sub> catalyst over the entire range of dye concentrations studied, and best performances took place in case of ACs with some electron availability (ACs with basic or slightly acid surfaces). This supports the hypothesis that AC acts as a photosensitiser, injecting an electron in the conduction band of TiO<sub>2</sub> and triggering the photocatalytic formation of ·OH radical. During the photooxidation of azo dyes Solophenyl Green BLE, Erionyl Red B and Chromotrope 2R, the powerful decolourisation efficiency of AC-amended photocatalytic treatment by suspended TiO<sub>2</sub> (and GAC) was furthermore confirmed by the evaluation of both mineralisation degrees

and initial quantum yields (Silva et al., 2006). Although a direct relationship between the structure characteristics of azo dyes and their photodegradation could not be established, it might be interesting to check a possible correlation between the electrochemical characteristics of dyes and their decolourisation rates.

The problem of possible catalyst leaching and their recovery from the suspended solutions urged researchers to investigate photocatalyst immobilisation. Wang et al. (2007) prepared nanocrystalline  $\text{TiO}_2/\text{AC}$  composite catalysts by a modified sol-gel method for the photocatalytic degradation of monoazo Chromotrope 2R dye. The composite exhibited higher activities than  $\text{TiO}_2$  alone and photocatalytic decolourisation was more efficient than photolytic degradation. Enhanced dye removals by photocatalysis were also reported with  $\text{TiO}_2$ -impregnated AC (Subramani et al., 2007),  $\text{TiO}_2$  immobilised on ACF (Shi et al., 2008) and even with both  $\text{TiO}_2$  and AC being immobilised on a support material such as silicone rubber film (Gao and Liu, 2005) or silica beads (Follansbee et al., 2008). Apart from the popular titanium dioxide, zinc oxide has been found a suitable alternative for photocatalytic decolourisation processes, indicating the synergism with AC e.g. in the form of  $\text{ZnO}/\text{AC}$  composites (Byrappa et al., 2006; Sobana and Swaminathan, 2007). By doping another semiconductor on the surface of the photocatalyst, it is possible to further improve its photocatalytic efficiency due to the increased charge separation and extended photo-responding range. Sun et al. (2009) showed that the photocatalytic decolourisation rate of the azo dye Congo Red was higher with  $(\text{WO}_3\text{-TiO}_2)/\text{AC}$  catalyst than with  $\text{TiO}_2/\text{AC}$ . On the other hand, AC-amended photocatalysis can be enhanced by developing the carbon material itself. Both (activated) carbon nanotubes with unique electronic properties (Yu et al., 2005) and ordered mesoporous carbon with periodic pore structure (Park et al., 2008) have been reported to facilitate the photocatalytic activity of  $\text{TiO}_2$  in dye degradation more efficiently than AC. Recently, some combined photocatalytic dye treatment systems presented powerful decolourisation potentials such as the microwave-enhanced photodegradation using  $\text{TiO}_2/\text{AC}$  composite catalyst (He et al., 2009) or the electro-photocatalytic oxidation using  $\text{TiO}_2$  immobilised on ACF anode (Hou et al., 2009). However, the possibly significant additional costs of operation were not evaluated.

#### 3.4.5. Miscellaneous dye removal processes

Lately, some individual AC-enhanced oxidation treatments for dye degradation have been published which could not be clearly classified into any of the previously discussed advanced oxidation techniques. This section includes these methods such as oxidation by non-thermal plasma or by irradiation.

In a study by Zhang et al. (2007a), a gas-liquid series electrical discharge reactor was applied for the degradation of Methyl Orange in the presence of different GACs. The pulse discharge alone ensured fast decolourisation with the non-thermal plasma produced that could generate various reactive agents such as radicals ( $\cdot\text{O}$ ,  $\cdot\text{OH}$ ) or molecular species ( $\text{H}_2\text{O}_2$ ,  $\text{O}_3$ ). However, dye degradation could be further increased and COD could be removed effectively by the combination of pulse discharge and GAC, the latter promoting the decomposition of molecular oxidising agents into hydroxyl radicals. The study of Zhang et al. (2007b) was based on the fact that AC, aside from being an excellent adsorbent, can strongly absorb microwave energy, resulting in the fast chemical oxidation of pollutants on the AC surface. The results indicated that decolourisation of the Congo Red dye solution proceeded much faster by PAC-enhanced microwave irradiation than by single AC adsorption or microwave treatment and, in addition, the combined system provided very efficient TOC removals, probably due to the only minor formation of intermediate products. However, catalytic activity of PAC simultaneously decreased with its cyclic reuse because of its synchronous oxidation with the colourant. Microwave irradiation, on the other hand, may also be applied for dye degradation indirectly. Yang et al. (2009) investigated the azo dye Acid Orange 7 degradation in an oxidation process using sulphate free radical ( $\text{SO}_4^{\cdot-}$ ) ( $E^0 = 2.6 \text{ V}$ ), produced from the decomposition of persulphate anion ( $\text{S}_2\text{O}_8^{2-}$ ) by microwave activation, in the absence or presence of AC. Although persulphate anion is a strong oxidising agent itself ( $E^0 = 2.01 \text{ V}$ ), it reacts only very slowly at ambient temperatures. In the control experiments, no colour removal was observed when only microwave irradiation or persulphate were applied. In contrast, their simultaneous application led to rapid and complete decolourisation. The oxidation could be enhanced by the addition of AC, mainly due to its catalytic role under microwave treatment (Zhang et al., 2007b).

#### **4. AC-amended biological dye removal processes**

Microbial decolourisation and degradation of dyes is one of the oldest but probably the most cost-effective among all methods for colour removal from wastewaters. Moreover, it is an environmentally friendly process that does not require hazardous or aggressive chemicals. Some excellent reviews have been published reporting the variety of aspects in microbial dye degradation (Banat et al., 1996; Stolz, 2001; Pearce et al., 2003; Fu and Viraraghavan, 2001). As it is well-documented in the literature, the addition of AC into a biological system treating dye or textile wastewaters presents a positive contribution to pollutant removal (Table 2.3). These studies may be grouped according to the main role of AC considered: whether the process enhancement is rather due to higher biomass activity (biofilm on AC surface) and dye adsorption or to AC catalysis.

#### 4.1. AC-supported microbial degradation of dyes

Several studies have examined the enhancement of biological dye wastewater treatment by AC. The predominant conclusion was that the synergy is due to the simultaneous occurrence of well-developed biomass on the AC support, carbon adsorption and biodegradation. Most traditional biological systems decolourising dyes with the assistance of AC operated with an aerobic activated sludge (Shaul et al., 1983; Specchia and Gianetto, 1984). Dye degradation is strongly dependent on the biomass concentration and its overload in the biological activated carbon (BAC) can inhibit the biological activity near to the AC surface, resulting in colour removal decrease (Márquez and Costa, 1996; Mezohegyi et al., 2008). From a technological point of view, GAC is a better choice than PAC considering its stability and retention in the bioreactor. Some sequential batch reactor (SBR) treatments showed that the removal efficiencies of colourants having minimal adsorption affinity for the carbon used such as disperse (Sirianuntapiboon and Srisornsak, 2007) or direct dyes (Sirianuntapiboon et al., 2007; Sirianuntapiboon and Sansak, 2008) increased through the addition of GAC into the SBR system, hence GAC acted mainly as a media for biofilm. Although it is not practical to work with pure cultures since mixed ones are effective for dye biodegradation and mineralisation as well (Pearce et al., 2003), a couple of studies evidenced that the use of AC in combination with a specific microorganism in the BAC system outperformed the conventional biotreatment of dyes (Walker and Weatherley, 1999b; Zhang and Yu, 2000). The biological dye degradation in BAC systems has often been described with models based on Monod kinetics (Mezohegyi et al., 2008; Walker and Weatherley, 1997; Costa and Márquez, 1998; Lin and Leu, 2008).

Commercial dyes are not uniformly susceptible to microbial attack in aerobic treatment because of their unique and stable chemical structures. Nevertheless, azo dyes –representing the largest class of dyes– can be decolourised by the reduction of the azo bond(s) in anaerobic bioreactors (Delée et al., 1998) and can be mineralised completely by a sequential anaerobic–aerobic treatment (Van der Zee and Villaverde, 2005). So far, using BAC for azo dye removal under anaerobic conditions has not been so widespread. E.g., Kuai et al. (1998) carried out a sequential anaerobic/aerobic process of a textile wastewater containing soluble acid and metal-complex azo colourants and used GAC in the UASB (upflow anaerobic sludge blanket) reactor in order to protect the top-layer granular sludge from toxicants. The combined GAC-amended UASB/aerobic activated sludge treatment showed a stable performance with a COD and colour removal of 98 and 95%, respectively. Since AC plays a role in obtaining high concentrations of active microorganisms in the bioreactor, the logical way is to operate with high GAC apparent volume/reactor volume ratios. Effective biodecolourisation of the azo dye Acid Orange 7 has been reported under reductive environment in some packed-bed-like reactor configurations with immobilised mixed cultures on GAC such as packed-bed with BAC

**Table 2.3.** Selected results of AC-amended biological dye removal studies.

| reactor system <sup>a</sup>                                 | organisms used             | AC characteristics <sup>b</sup>                                 | wastewater characteristics <sup>c</sup>   | results <sup>d</sup>  |  | reference                              |
|---|----------------------------|---|---|---|--|--|
|   |                            |   |   | with AC   | without AC   |  |
| continuous mixed and aerated reactor; HRT: 3.75; BC: 2000   | activated sludge           | PAC (Panreac PR); d: 74–88; cc: 0.5                             | SW: Acid Orange 7 (c: 20); peptone (c: 160); COD: 250   | X <sub>col</sub> : 0.97<br>X <sub>cod</sub> : ~0.75   | n.m.   | Márquez and Costa (1996)               |
| aerobic sequencing batch reactor; HRT: 72 (SW) and 120 (TW) | bio-sludge                 | GAC (CGC-11, C. Gigan Co.); S <sub>BET</sub> : 1050–1150; cc: 1 | SW: Disperse Red 60 (c: 80); glucose (c: 1875); COD: 2008<br>SW: Disperse Blue 60 (c: 80); glucose (c: 1875); COD: 2008<br>TW: mixed disperse dyes; COD: 1517       | X <sub>col</sub> : 0.942<br>X <sub>cod</sub> : 0.974<br>X <sub>col</sub> : 0.845<br>X <sub>cod</sub> : 0.973<br>X <sub>col</sub> : 0.930<br>X <sub>cod</sub> : 0.922      | X <sub>col</sub> : 0.881<br>X <sub>cod</sub> : 0.962<br>X <sub>col</sub> : 0.762<br>X <sub>cod</sub> : 0.959<br>X <sub>col</sub> : 0.877<br>X <sub>cod</sub> : 0.908 | Sirianuntapiboon and Srisornsak (2007) |
| aerobic sequencing batch reactor; HRT: 72 (SW) and 180 (TW) | bio-sludge                 | GAC (CGC-11, C. Gigan Co.); S <sub>BET</sub> : 1050–1150; cc: 1 | SW: Direct Red 23 (c: 40); glucose (c: 1875); COD: 2000<br>SW: Direct Blue 201 (c: 40); glucose (c: 1875); COD: 2000<br>TW: mixed direct dyes; COD: 1615            | X <sub>col</sub> : 0.810<br>X <sub>cod</sub> : 0.983<br>X <sub>col</sub> : 0.848<br>X <sub>cod</sub> : 0.972<br>X <sub>col</sub> : 0.571<br>X <sub>cod</sub> : 0.636      | X <sub>col</sub> : 0.756<br>X <sub>cod</sub> : 0.967<br>X <sub>col</sub> : 0.799<br>X <sub>cod</sub> : 0.959<br>X <sub>col</sub> : 0.511<br>X <sub>cod</sub> : 0.609 | Sirianuntapiboon et al. (2007)         |
| aerobic stirred tank reactor; V.L: 3                        | <i>Pseudomonas putida</i>  | GAC (Filtrisorb 400); S <sub>BET</sub> : 1050–1200; cc: ~1.6    | TW: mixed direct dyes; glucose (c: 890); COD: 2438<br>SW: mixture of Tectilon Blue 4R-01, Tectilon Red 2B and Tectilon Orange 3G (c: 3x33); CM1 nutrient broth (5%) | X <sub>col</sub> : 0.760<br>X <sub>cod</sub> : 0.862<br>k <sub>AV</sub> (TB4R): 8.297 (6 h)<br>k <sub>AV</sub> (TR2B): 6.090 (6 h)<br>k <sub>AV</sub> (TO3G): 12.58 (6 h) | k <sub>AV</sub> (TB4R): 0.918 (6 h)<br>k <sub>AV</sub> (TR2B): 0.240 (6 h)<br>k <sub>AV</sub> (TO3G): 0.558 (6 h)  | Walker and Weatherley (1999b)          |
| aerobic fluidized-bed reactor; HRT: 20                      | <i>Trametes versicolor</i> | PAC; d: 37–150; cc: ~ 50  | SW: Acid Violet 7 (c: 100); glucose (c: 5000)   | X <sub>col</sub> : 0.55 (after 7 d)   | n.m.   | Zhang and Yu (2000)                    |
| upflow anaerobic sludge blanket reactor; HRT: 5–5.5         | activated granular sludge  | GAC (Norit SA-4); cc: 10<br>GAC (Norit SA-4); cc: 0.4           | SW: H. Reactive Red 2 (c: 42); VFA mixture (COD: 1500)  | X <sub>col</sub> : ~0.90 (after 130 d)<br>X <sub>col</sub> : ~0.43 (after 112 d)  | X <sub>col</sub> : ~0.35 (after 130 d)   | Van der Zee et al. (2003)              |

**Table 2.3.** Selected results of AC-amended biological dye removal studies. (cont.)

| reactor system <sup>a</sup>                                  | organisms used             | AC characteristics <sup>b</sup>  | wastewater characteristics <sup>c</sup>                                   | results <sup>d</sup> |            | reference               |
|--|----------------------------|--|---|----------------------|------------|-------------------------|
|  |                            |  |   | with AC              | without AC |                         |
| upflow anaerobic stirred packed-bed reactor; $V_{PB}$ : ~2   | mixed bacterial consortium | GAC (Merck); d: 300–700; ccv: ~0.5   | SW: Orange II (c: 100); sodium acetate (c: 200)                           | k: 2.46              | n.m.       | Mezőhegyi et al. (2009) |
|  |                            |  | SW: Acid Red 88 (c: 100); sodium acetate (c: 200)                         | k: 2.63              |            |                         |
| upflow anaerobic stirred packed-bed reactor; $V_{PB}$ : ~2–3 | mixed bacterial consortium | GAC (Norit ROX 0.8); d: 300–700; ccv: ~0.5; $S_{BET}$ : 1055; $pH_{PZC}$ : 8.3; CO: 911                | SW: H. Reactive Black 5 (c: 100); sodium acetate (c: 200)                 | k: 3.51              |            | Mezőhegyi et al. (2010) |
|  |                            |  | SW: H. Reactive Black 5 (c: 100); sodium acetate (c: 200)                 | k: 2.83              | n.m.       |                         |
|  |                            |  | GAC mod: gas. (BO: 28); d: 300–700; ccv: ~0.4; $S_{BET}$ : 1097; CO: 1136 | k: 5.70              |            |                         |
|  |                            |  | GAC mod: gas. (BO: 50); d: 300–700; ccv: ~0.3; $S_{BET}$ : 1336; CO: 1448 | k: 9.05              |            |                         |
|  |                            | GAC mod: $HNO_3$ ; d: 300–700; ccv: ~0.5; $S_{BET}$ : 1004; $pH_{PZC}$ : 4.5; CO: 2041                 |   | k: 4.85              |            |                         |
|  |                            | GAC mod: $HNO_3$ /heat under $N_2$ ; d: 300–700; ccv: ~0.5; $S_{BET}$ : 977; $pH_{PZC}$ : 8.6; CO: 106 |   | k: 5.21              |            |                         |

<sup>a</sup> Abbreviations: HRT, hydraulic residence time, h; BC, biomass concentration,  $mg L^{-1}$ ; SW, simulated wastewater; TW, textile wastewater;  $V_L$ , volume of treated dye solution, L;  $V_{PB}$ , apparent volume of the packed-bed, mL. <sup>b</sup> Abbreviations: d, AC particle size,  $\mu m$ ; cc: carbon concentration in the liquid phase,  $g L^{-1}$ ;  $S_{BET}$ , BET surface area,  $m^2 g^{-1}$ ; ccv, carbon concentration in the packed-bed volume,  $g mL^{-1}$ ;  $pH_{PZC}$ , point of zero charge; CO, amount of CO-emitting groups on AC surface,  $\mu mol g^{-1}$ ; mod, modified; gas., gasification; BO, AC burn-off, %. <sup>c</sup> Abbreviations: c, inlet concentration,  $mg L^{-1}$ ; COD, chemical oxygen demand,  $mg L^{-1}$ ; H., hydrolysed; VFA, volatile fatty acid. <sup>d</sup> Abbreviations:  $X_{COD}$ , colour removal;  $X_{COD}$ , COD removal; n.m., not measured;  $k_{AV}$ , average reaction rate constant,  $mg h^{-1}$ ; k, kinetic constant of the model suggested by Mezőhegyi et al. (2008),  $mmol g_{AC}^{-1} min^{-1}$ .

(Ong et al., 2008a), SBR filled with BAC (Ong et al., 2008b) or combined GAC-packed column/SBR (Ong et al., 2005a). Moreover, GAC inoculated with single species of *Bacillus OY1-2* was able to reduce the azo dye Red B in a packed reactor under anoxic conditions (Li et al., 2004).

## 4.2. AC-catalysed bioreduction of azo dyes

The anaerobic reduction of several azo colourants usually proceeds rather slowly making the process insufficient from practical aspects. Bacterial azo reduction is generally considered as a non-specific reduction process that can be helped by redox mediators, shuttling electrons from bacteria to the azo dyes (Keck et al., 1997). Therefore, the use of such agents is a logical strategy for accelerating anaerobic decolourisation. Quinone-like compounds have been reported to catalyse the decolourisation of azo dyes (Van der Zee et al., 2001; Rau et al., 2002; Van der Zee and Cervantes, 2009). However, continuous dosing of the redox mediator results additional process costs. This problem can be avoided by immobilising the electron mediator in the bioreactor. For this purpose, AC was considered as it can be retained in the reactor for prolonged time and it generally contains carbonyl/quinone sites on its surface.

The first study considering AC as catalytic redox mediator in an advanced reduction process (ARP) was reported by Van der Zee et al. (2003) treating the hydrolysed azo dye Reactive Red 2 in a lab-scale UASB reactor and using volatile fatty acids as electron donors. Mixing of AC with the granular sludge greatly improved both the dye removal and the formation of its reduction product aniline, giving evidence of AC's catalytic behaviour. Moreover, batch experiments with azo dye Acid Orange 7 proved that chemical reduction of the dye was accelerated by AC addition. These results suggested that AC could accept electrons from the microbial oxidation of organic acids and transfer the reducing equivalents to the azo dye, thereby accelerating the process. Recently, some studies examined the different aspects of AC-catalysed ARPs of azo dyes. Mezohegyi et al. (2007) investigated the anaerobic reduction of Acid Orange 7 in different reactor systems, in the presence of solid electron mediators. Batch experiments with graphite, incorporated with the sludge, showed that electron-mediating capability of the solid particles contributed to higher decolourisation rates. The use of AC in a continuous upflow packed-bed bioreactor (UPBR) resulted in rather fast dye conversion, up to 99% in 2 min of space time (~5.4 min of HRT). The continuous reactor with AC was found to be more effective than the identical reactor working with graphite, proving the importance of AC's beneficial surface properties in biological azo reduction. Compared to the UPBR, an improvement in Acid Orange 7 conversion was achieved by using a novel-type upflow stirred packed-bed reactor (USPBR) containing BAC (Mezohegyi et al., 2008). The USPBR provided more reproducible data to make kinetic modeling of azo dye bioreduction possible and the

experimental points of dye conversion fitted well to Michaelis–Menten kinetics, independently from the inlet dye concentration. The electrochemical characteristics of the azo dyes were a key factor in ARPs: the bioreducibility of azo colourants could be predicted by their reduction potential values in the catalytic USPBR system, independently of the azo dye type, complexity and adsorption affinity (Mezőhegyi et al., 2009). As for the AC characteristics, the biological removal of azo dyes Orange II and Reactive Black 5 in USPBRs was significantly affected by the AC textural properties and the reduction rate constants were proportional to the AC surface area (Mezőhegyi et al., 2010). Variation of the AC surface chemistry seemed to have less effect on dye conversion rates, even though the hypothesis of AC catalysis by the carbonyl/quinonic sites in the ARP was confirmed. Nevertheless, an other mechanism influenced the catalytic decolourisation too, particularly in the absence of significant densities of surface oxygen-containing groups, whereas not the quinonic groups but rather the delocalised  $\pi$ -electrons were involved in the reduction (Mezőhegyi et al., 2010). González-Gutiérrez et al. (2009) proposed pathways for the anaerobic degradation of azo dye Reactive Red 272 in a fixed-bed reactor containing BAC and, similarly, considered AC besides extracellular enzymes or coenzymes to transfer electrons by means of its quinonic groups.

## 5. Conclusions

Activated carbon plays an important role in both physico-chemical and biological dye decolourisation techniques. Although it generally has a high affinity to adsorb dyes, AC adsorption is by far not the only mechanism that contributes to higher dye removal rates in the hybrid processes. Most of the colour-reducing methods having been reported in the literature could be auspiciously combined with the beneficial properties of AC, resulting in a synergetic increase in dye removal and, in many cases also, mineralisation efficiencies. The advantageous roles of AC or advanced (activated) carbon materials in advanced dye oxidation processes (generally, catalysing the formation of  $\cdot\text{OH}$  radicals) and in advanced (azo) dye reduction methods (transferring electrons) make these treatments attractive choices for economically improving textile/dye wastewater technologies.





## **Effective anaerobic decolorization of azo dye Acid Orange 7 in continuous upflow packed-bed reactor using biological activated carbon system**

### **Abstract**

The anaerobic reduction of azo dye Acid Orange 7 (AO7) was investigated in a continuous upflow packed-bed reactor (UPBR) containing biological activated carbon (BAC). Preliminary batch experiments using graphite proved the catalytic effect of using a solid electron mediator in the reactor. Before the start of continuous experiments, AO7 adsorption studies were done to control adsorption effects on initial decolorization rates. In a continuous UPBR-BAC system, high azo dye conversion rates were achieved during very short space times ( $\tau$ ) up to 99% in 2.0 min. In order to know which are the crucial and most influencing properties of BAC in AO7 reduction, other materials –graphite and alumina– with different properties were also tested in UPBRs. The results show that both electron-mediating capability and specific surface area of activated carbon contribute to higher reduction rates. Compared to other continuous and biological processes treating azo dyes, UPBR-BAC seems to be a very effective and promising system for anaerobic azo dye degradation.

<Published as: Mezohegyi G, Kolodkin A, Castro UI, Bengoa C, Stuber F, Font J, Fabregat A, Fortuny A. (2007). *Industrial & Engineering Chemistry Research* 46(21): 6788–6792.>

## 1. Introduction

Azo dyes are chemical substances commonly used in textile, pharmaceutical, and food industries and characterized by the N=N bond. Their production is more than 1 million tons per year in the world, and during dyeing processes, about 40% of this huge amount of azo dyes ends up in wastewaters. In addition, about 40–65 L of textile effluent is generated per kg of cloth produced (Manu and Chaudhari, 2002). There is no adequate process to treat these wastewaters at high concentrations and at soft conditions on the industrial scale for the time being, and the release of these compounds into the environment presents serious problems of pollution related to both aesthetic reasons and their toxicity.

Several methods have been found to treat azo dye wastewaters (Forgacs et al., 2004). Removal techniques for dyes include coagulation, advanced oxidation processes, membrane processes, and adsorption. These physical and chemical treatments are effective for color removal but use more energy and chemicals than biological processes (Ong et al., 2005b) and, in addition, some of them produce large amounts of secondary waste solids or streams that require further treatment or disposal (Georgiou et al., 2005). Among all of the existing techniques, the most economic and environmentally friendly are biological treatments. Because of the fact that azo dyes are artificial compounds and especially designed to be resistant in the natural environment, their biological degradation has serious obstacles. Investigations of the biodegradability of water-soluble azo dyes by an activated sludge process have indicated that, in most cases, these dyes could not be degraded under aerobic conditions. On the other hand, azo reduction can be relatively easily achieved under anaerobic conditions (Beydilli et al., 2005). Moreover, most of the products created by breaking of the N=N bond could be successfully degraded under aerobic conditions. These suggest a sequential anaerobic–aerobic process as the reasonable scheme of treating wastewaters containing azo dyes (Kalyuzhnyi and Sklyar, 2000). The bottleneck of this process is the anaerobic reduction, so by having an efficient first step in azo dye degradation, the more complete sequential treatment can be carried out.

The only, but serious, disadvantage of the anaerobic biological techniques is the need for long hydraulic residence times. Several studies indicate that reduction of many azo dyes is a relatively slow process (Brás et al., 2005; Kapdan et al., 2003; Manu and Chaudhari, 2003; Méndez-Paz et al., 2005a,b; Rajaguru et al., 2000; Sponza and İşik, 2002). However, by using an appropriate catalyst during the reduction, anaerobic biodegradation could be speeded up, resulting in much higher efficiency. In different experimental systems, redox mediators, like quinones and flavine-based compounds, have been demonstrated to accelerate azo dye reduction (Cervantes et al., 2001; Dos

Santos et al., 2005; Field and Brady, 2003; Rau et al., 2002; Van der Zee et al., 2001). These electron mediators shuttle reducing equivalents from an electron-donating cosubstrate to the azo linkage. Although the effective redox mediator dosage levels are low, continuous dosing implies continuous expenses. Therefore, it is desirable to immobilize the redox mediator in the bioreactor. For this purpose, activated carbon (AC) was considered (Figure 3.1) since it is known to contain surface quinonic structures (Van der Zee et al., 2003). Despite these facts, only a very few studies have been done using activated carbon as a catalyst for azo dye biodegradation (Van der Zee et al., 2003; Pasukphun and Vinitnantharat, 2003; Walker and Weatherley, 1999).

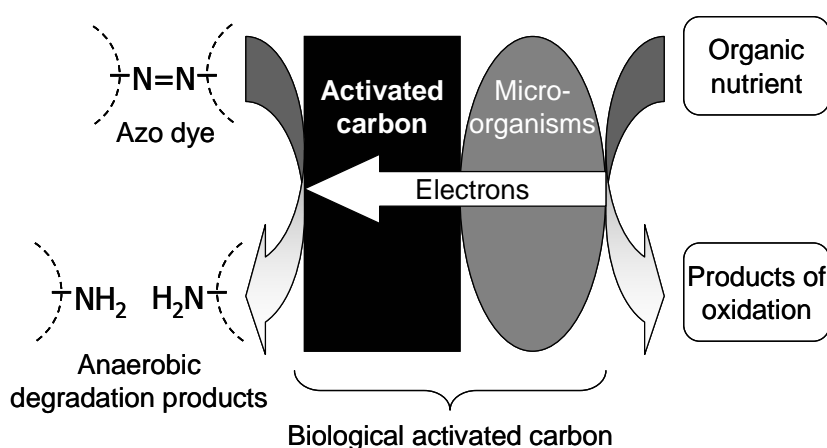


**Figure 3.1.** Role of activated carbon in anaerobic azo dye degradation.

Considering the amount of azo dye wastewaters mainly originated from the textile industry, it is clear that continuous systems have to be designed for treating these effluents. The main objective of this study was to investigate the anaerobic decolorization of azo dye Acid Orange 7 (Figure 3.2) using a continuous upflow packed-bed reactor (UPBR) filled with biological activated carbon (BAC). This system was compared with UPBRs using different support materials such as graphite or alumina to evaluate the significant role of activated carbon in anaerobic degradation of Acid Orange 7 (AO7).

## 2. Materials and methods

### 2.1. Chemicals

Azo dye Orange II (C.I. Acid Orange 7) Sodium Salt (dye content 99%, Sigma, ref. O8126) was selected as a model compound since, on the one hand, this azo dye is representative of a large class of azo dyes used commercially and, on the other hand, quantitative determination of one of its anaerobic degradation products, sulfanilic acid, is relatively easy. Sulfanilic acid (SA) was supplied by Sigma (min. 99%, ref. S5263).

Sodium acetate (99%, Aldrich, ref. 11019-1) was used as the carbon source for sludge and also as the source of reductive equivalents for azo dye reduction. Acetic acid (99.8%, Aldrich, ref. 10908-8) was used for batch experiments as the continuous carbon source and also as a pH controller. Alumina (Norton S.A., ref. 6275) with granule size of 25–50 mesh (0.3–0.7 mm), graphite flakes (Aldrich, particles of 75+ mesh, ref. 33246-1), and activated carbon (Merck, granules of 2.5 mm, ref. 1.02518.1000) were used as support materials for biodegradation. Activated carbon was crushed, and granules of 25–50 mesh size were separated, washed with distilled water, dried at 104 °C for 15 h, and stored under normal conditions until use. Carborundum granules (Carlo Erba Reagents, ref. 434766) were used as inert diluent for the activated carbon catalyst. The basal media contained the following compounds ( $\text{mg L}^{-1}$ ):  $\text{MnSO}_4 \cdot \text{H}_2\text{O}$  (0.155),  $\text{CuSO}_4 \cdot 5\text{H}_2\text{O}$  (0.285),  $\text{ZnSO}_4 \cdot 7\text{H}_2\text{O}$  (0.46),  $\text{CoCl}_2 \cdot 6\text{H}_2\text{O}$  (0.26),  $(\text{NH}_4)_6\text{Mo}_7\text{O}_{24}$  (0.285),  $\text{MgSO}_4 \cdot 7\text{H}_2\text{O}$  (15.2),  $\text{CaCl}_2$  (13.48),  $\text{FeCl}_3 \cdot 6\text{H}_2\text{O}$  (29.06),  $\text{NH}_4\text{Cl}$  (190.9),  $\text{KH}_2\text{PO}_4$  (8.5),  $\text{Na}_2\text{HPO}_4 \cdot 2\text{H}_2\text{O}$  (33.4), and  $\text{K}_2\text{HPO}_4$  (21.75).

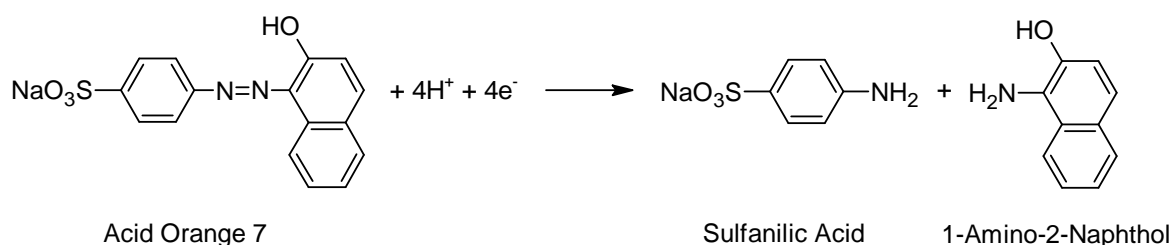


**Figure 3.2.** Anaerobic degradation of Acid Orange 7.

## 2.2. Batch experiment

For batch experiments, a stirred-tank reactor was used with a useful volume of 1.2 L maintained at a constant temperature of 35 °C. The mixed culture of anaerobic sludge was obtained by partial digestion of aerobic sludge under anaerobic conditions. The reactor was agitated by a magnetic stirrer only for 20 s/per experiment –to avoid destruction of biofilm on the catalyst surface– immediately after changing 300 mL of decolorized dye solution for a fresh one. Acetic acid (4.0% v/v) was continuously fed not just to keep the acetate level nearly constant in the batch but also to help keep the pH level between 6.7 and 7.2. Anaerobic conditions were maintained by continuous bubbling of helium into the reactor. The redox potential was continuously monitored.

The batch contained 20 g of graphite as an electron-conducting catalyst. In fact, the reason of using graphite instead of activated carbon was that graphite has no adsorption properties; thus, dye degradation in the batch reactor could be clearly followed. In the case of AC, which can easily adsorb a higher amount of azo dyes, it is more difficult to

examine adsorption and catalytic effects separately since adsorption is not constant and depends both on azo dye concentration in the liquid phase and on contact time.

The objective of the batch experiment was to compare Acid Orange 7 anaerobic degradation in traditional and discontinuous biological systems –operating with high contact times– with a batch containing a solid electron mediator.

### 2.3. Continuous experiments

Figure 3.3 shows schematically our continuous system. The upflow packed-bed reactor has a diameter of 15 mm with a useful volume of 9 mL. It is filled with the mixture of 10 g of carborundum granules –its inert property was previously tested, and carborundum did not show any positive effect on decolorization rates– and 1 g of activated carbon with the size of 25–50 mesh. To prevent washing out of AC, two filters were placed into the top and bottom of the reactor. The UPBR was working at a constant temperature of 35 °C. The entering feed was 100 mg L<sup>-1</sup> Acid Orange 7 solution containing 200 mg L<sup>-1</sup> of sodium acetate as substrate and the basal media with microelements. The flow rate of the feed was varied between 25 and 70 mL h<sup>-1</sup>. The pH of the outlet solution varied between 6.8 and 7.2. The anaerobic condition in the feeding bottle (5 L) was maintained by both cooling of the solution (at 5 °C) and bubbling of helium. The redox potential was continuously monitored and remained below –500 mV (referred to Ag<sup>+</sup>/AgCl electrode).

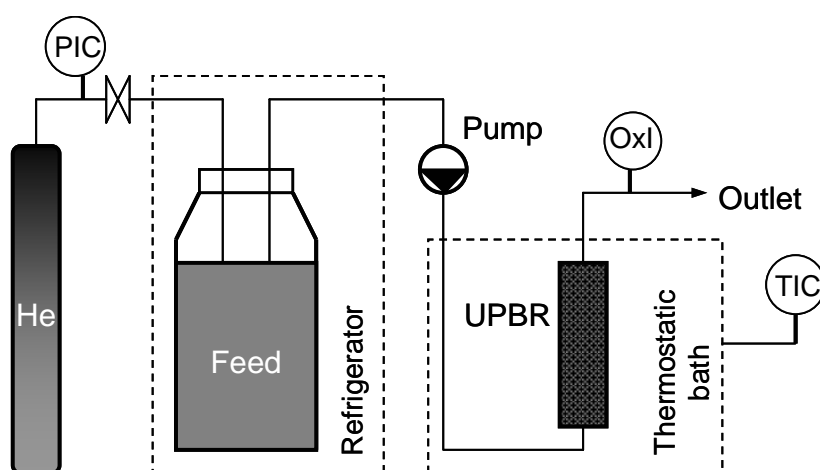


**Figure 3.3.** Continuous and anaerobic upflow packed-bed reactor setup.

To prepare the biological system, anaerobic sludge was filtered by a filter with a pore size of 20–25 μm to only have single cells and spores. This filtrate was pumped through the activated carbon for a week. During this period, the biofilm was immobilized on the AC surface, resulting in the so-called biological activated carbon. Then the biofilm was adapted to AO7 by continuous flowing of the dye solution containing both the basal media and the carbon source through the reactor. To maintain the same culture of sludge, every

new reactor was set by using the outlet of an already operated reactor as the inlet to the new one.

In order to know what are the crucial and most influencing properties of the BAC system in AO7 reduction, different materials –graphite and alumina– with different conducting and surface properties were also tested in UPBRs. These reactors were set up in the same way as the one with AC.

## 2.4. Adsorption experiments

Before starting experiments in UPBRs, all reactors with activated carbon, graphite, and alumina were saturated with azo dye to avoid the influence of initial dye adsorption during the initial period of operation. To know exactly the sorption capacities of these materials and the time of saturation needed, adsorption experiments were done. Nine bottles, each of them containing 100 mg of activated carbon, were filled with 100 mL of AO7 solution in different initial concentrations between 150 and 600 mg L<sup>-1</sup>. Adsorption was allowed to run for 16 days, and then samples were taken. For alumina, graphite, and AC, dye adsorption was also examined as a function of time. Bottles containing 100 mg of either alumina or graphite or AC and 100 mL of AO7 solution with an initial concentration of 400 mg L<sup>-1</sup> were left for 16 days, and during that period, samples were taken 10 times. All solutions were slowly stirred for 30 s each day. The pH of the solutions was always adjusted to be between 7.0 and 7.5.

## 2.5. Analytical methods

Acid Orange 7, sulfanilic acid, and acetate were measured by high-performance liquid chromatography (HPLC) on a C<sub>18</sub> Hypersil ODS column in a gradient of methanol–water mobile phase with a flow rate of 1 mL min<sup>-1</sup>. AO7 was determined on 487 nm (at a retention time (RT) = 17.55 min), sulfanilic acid was determined on 252 nm (RT = 2.18 min) and acetate was determined on 210 nm (RT = 3.68 min). 1-Amino-2-naphthol (1A2N), the other product generated during the anaerobic degradation of AO7, was not determined because of its partial precipitation.

# 3. Results and discussion

## 3.1. Adsorption kinetics

In the cases of alumina and graphite, Acid Orange 7 adsorption was found to be almost zero. On the contrary, activated carbon showed a strong adsorption capacity for AO7. Azo

dye adsorption as a function of time is shown in Figure 3.4. Adsorption fits very well to a second-order kinetic model (Órfão et al., 2006) (eq. 1),

$$Q = \frac{K \cdot Q_E^2 \cdot t_A}{1 + K \cdot Q_E \cdot t_A} \quad (1)$$

where  $Q$  ( $\text{mg g}_{\text{AC}}^{-1}$ ) represents the AO7 concentration in the solid phase,  $Q_E$  ( $\text{mg g}_{\text{AC}}^{-1}$ ) is the corresponding value at equilibrium,  $t_A$  (days) is the contact time, and  $K$  ( $\text{g}_{\text{AC}} \text{mg}^{-1} \text{day}^{-1}$ ) is the adsorption rate constant. Values of  $Q$  can be obtained from (eq. 2),

$$Q = \frac{(C_{0A} - C_A) \cdot V}{m_{\text{AC}}} \quad (2)$$

where  $C_A$  ( $\text{mg L}^{-1}$ ) is the AO7 concentration in the solution,  $C_{0A}$  ( $\text{mg L}^{-1}$ ) is the initial dye concentration,  $V$  (L) is the volume of solution, and  $m_{\text{AC}}$  (g) is the mass of activated carbon. After linearization of eq. 1,  $Q_E$  and  $K$  values were found to be  $340 \text{ mg g}_{\text{AC}}^{-1}$  and  $2.59 \times 10^{-3} \text{ g}_{\text{AC}} \text{mg}^{-1} \text{day}^{-1}$ , respectively.

### 3.2. Equilibrium adsorption isotherm

The sorption process is well-described by the Langmuir isotherm (Figure 3.5). According to the model (eq. 3),

$$Q_E = \frac{Q_L \cdot K_L \cdot C_E}{1 + K_L \cdot C_E} \quad (3)$$

where the variables  $Q_E$  ( $\text{mg g}_{\text{AC}}^{-1}$ ) and  $C_E$  ( $\text{mg L}^{-1}$ ) are the azo dye equilibrium concentrations in the solid and liquid phases,  $Q_L$  ( $\text{mg g}_{\text{AC}}^{-1}$ ) is the maximum adsorbance capacity according to the Langmuir model, and  $K_L$  ( $\text{L mg}^{-1}$ ) is the Langmuir-constant; a maximum adsorption of  $339 \text{ mg g}_{\text{AC}}^{-1}$  with a  $K_L$  value of  $0.242 \text{ L mg}^{-1}$  was found by using the linearized form of eq. 3. Before the start of continuous experiments, more than 6 times this amount of dye was pumped through the reactors to ensure avoidance of initial adsorption effects on outlet dye concentration.

### 3.3. Batch experiment

Initial concentrations of Acid Orange 7, sulfanilic acid, and acetate in the batch reactor were 48, 41.5, and  $110 \text{ mg L}^{-1}$ , respectively. The pH of the solution at the start was 6.8 and at the end was 6.7. Figure 3.6 shows AO7 conversion vs time. When using graphite in the batch, after 20 h, azo dye degradation was about 88%. In our previous study,



operating with the same initial parameters but having no catalyst in the reactor, no decolorization was observed during the first 24 h (data not shown). This means that using graphite together with anaerobic sludge results in a significant increase of color removal. Moreover, in different traditional and discontinuous biological systems –using different initial dye concentrations– high Acid Orange 7 conversion (> 90%) has generally required longer contact times (Table 3.1). Although it is difficult to compare decolorization efficiencies of these systems to ours since wastewater characteristics could be rather different, considering the required contact times, it also implies that using a solid electron mediator in the bioreactor can speed up AO7 degradation.

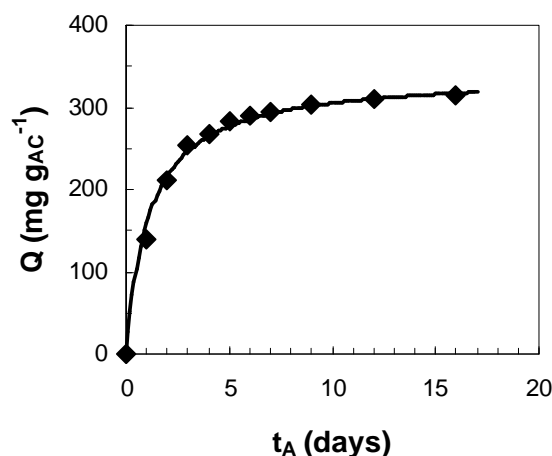


**Figure 3.4.** Acid Orange 7 adsorption on activated carbon predicted by a second-order kinetic model (line).

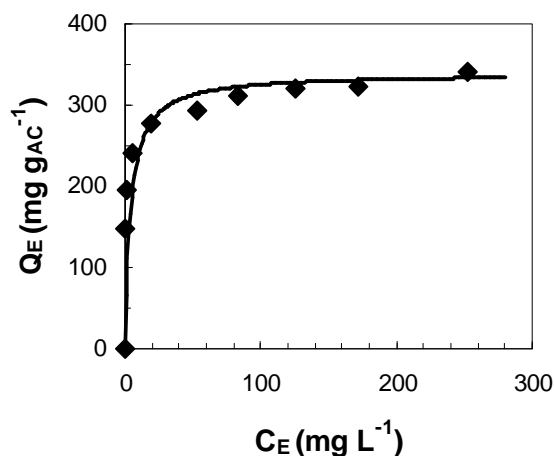


**Figure 3.5.** Acid Orange 7 equilibrium adsorption on activated carbon predicted by Langmuir isotherm (line).

In earlier studies, it was found that 1-amino-2-naphthol (1A2N) is a redox mediator that plays a significant role in the transport of electrons to the dye, thus giving to the whole process an autocatalytic nature (Méndez-Paz et al., 2003; Van der Zee et al., 2000). For this, a second-order kinetic model –supposing autocatalysis– was proposed by Van der Zee et al. (2000) in which  $X$  varies as a function of time according to (eq. 4),

$$X = \frac{1 - (k_2 \cdot c_0 + k_1)}{k_1 \cdot \exp(k_2 \cdot t \cdot c_0 + k_1 \cdot t) + k_2 \cdot c_0} \quad (4)$$

where  $X$  is the dye conversion,  $c_0$  ( $\text{mmol L}^{-1}$ ) is the initial azo dye concentration,  $t$  (h) is the elapsed time, and  $k_1$  ( $\text{h}^{-1}$ ) and  $k_2$  ( $\text{L mmol}^{-1} \text{h}^{-1}$ ) are the first-order and second-order kinetic constants, respectively. As Figure 3.6 shows, the model fits very well the experimental points. Significant deviations from the model can only be observed in the period of first 4 h of decolorization, which can be explained by having a certain concentration of 1A2N in the batch at initial conditions and, also, having higher redox potential values at the start because of the initial mixing of fresh and decolorized solution.

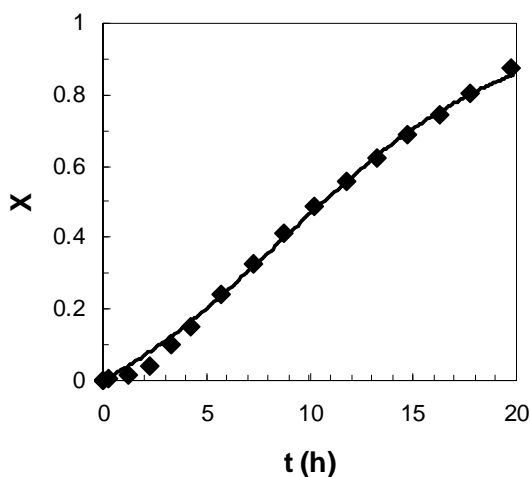


**Figure 3.6.** Acid Orange 7 conversion in batch reactor using graphite as solid electron-mediator catalyst. Line shows the fitting to second-order autocatalytic model.

### 3.4. Continuous experiments

In the case of continuous packed-bed reactors working with catalysts, it is better to examine conversion values as a function of space time rather than of hydraulic residence time, since the crucial factor in these reactions is the amount of catalyst rather than the reactor volume. Space time ( $\tau$ , min) is defined by (eq. 5),

$$\tau = \frac{m_C}{F_V \cdot \rho} \quad (5)$$

where  $m_C$  (g) is the mass of catalyst in the reactor,  $F_V$  ( $\text{mL min}^{-1}$ ) is the volumetric flow rate of azo dye solution, and  $\rho$  ( $\text{g mL}^{-1}$ ) is the density of the solution.

AC is not just a redox mediator having the ability to conduct electrons; it also has important functional groups on its surface. To test the importance of all these properties in azo dye decolorization, graphite, which is an electron conductor having no specific surface properties, and alumina, having neither functional groups on its surface nor conductive properties, were also used in a UPBR to compare them with the BAC system. Results are shown in Figure 3.7. Using alumina in the anaerobic reactor did not result in high values of AO7 conversion, even at high space time. Only 33% of decolorization was achieved at a space time of 15.8 min, which cannot be considered as an effective treatment. A UPBR working with graphite showed much higher decolorization rates than that in the case of alumina. 77% of AO7 conversion was achieved at a  $\tau$  of 9.7 min. The difference in efficiencies of these two systems suggests that the conductive property of the support material strongly affects azo dye decolorization.

On the other hand, Figure 3.7 also shows that the BAC system definitely gave higher azo dye conversions than the UPBR with graphite. This can be explained by the different structural and adsorption properties of these two materials. While graphite has a structure that consists of only aromatic rings with delocalized electrons –causing its electron-mediating property– and has no adsorption capability for AO7, the activated carbon structure contains both aromatic rings and surface functional groups. These specific quinonic groups are capable of transporting electrons by the way of keto–enol tautomerism that results in a more efficient reducing equivalent transfer compared with that of the delocalized electron system. In addition, in the case of AC, the strong adsorption capacity of AO7 and its high concentration on the carbon surface also help the electron transport from the electron donor acetate to the azo linkage.

In UPBR-BAC, almost complete decolorization was achieved at short space time. AO7 conversion was about 95% at 1.6 min, and 2.0 min of  $\tau$  resulted in 99% of decolorization. These values of space time correspond to extremely short hydraulic residence times of about 4.4 min and 5.4 min (with packed-bed porosity of 0.3), respectively. By comparing these with hydraulic residence times applied in other continuous biological systems using similar initial dye concentrations (Table 3.1), it seems that UPBR-BAC requires one of the shortest times needed to achieve almost complete decolorization of AO7.

**Table 3.1.** Anaerobic degradation of Acid Orange 7: selected results of studies reported in the literature.

| reactor type <sup>a</sup> | main influent characteristics <sup>b</sup>                      | C <sub>INDYE</sub> (mg L <sup>-1</sup> ) | time (h) <sup>c</sup> | color removal or removal rate constant <sup>d</sup> | reference                 |
|---------------------------|---|--|-----------------------|---|---------------------------|
| semicont.                 | simulated textile wastewater                                    | 100                                      | 240                   | 82–100%   | Manu and Chaudhari (2002) |
| SBR                       | COD = 2.66–5.32 g L <sup>-1</sup> day <sup>-1</sup>             | 50–100                                   | 21.5                  | 30–80%  | Ong et al. (2005b)        |
| batch                     | COD = 0.30–3.00 g L <sup>-1</sup>                               | 100                                      | >10                   | >75%  | Brás et al. (2001)        |
| batch                     | glucose = 1.80–2.60 g L <sup>-1</sup>                           | 25–320                                   | 48–120                | 100%  | Méndez-Paz et al. (2005a) |
| UASB                      | glucose = 2.00 g L <sup>-1</sup>                                | 100–200                                  | 10–80                 | 92–98%  | Méndez-Paz et al. (2005b) |
| UASB                      | COD = 5.3 g L <sup>-1</sup> day <sup>-1</sup><br>AQDS = 0–30 μM | 100                                      | 6                     | >85%  | Cervantes et al. (2001)   |
| batch                     | glucose: 1.8–2.6 g L <sup>-1</sup>                              | 100–300                                  |                       | 0.72–1.11 day <sup>-1</sup>                         | Méndez-Paz et al. (2003)  |
| batch                     | sulphide = 0.6–0.7 mM<br>1A2N = 0.0–1.0 mM                      | 80–100                                   |                       | 0.09–1.2 day <sup>-1</sup>                          | Van der Zee et al. (2000) |

<sup>a</sup>Reactor types: UASB, upflow anaerobic sludge blanket; SBR, sequencing batch reactor. <sup>b</sup>Abbreviations: COD, chemical oxygen demand; AQDS, anthraquinone-2,6-sulphonic acid; 1A2N, 1-amino-2-naphthol. <sup>c</sup>Time corresponds either to contact time (batch) or to hydraulic residence time (continuous-type reactors). <sup>d</sup>Removal rate constant refers to first-order kinetics.

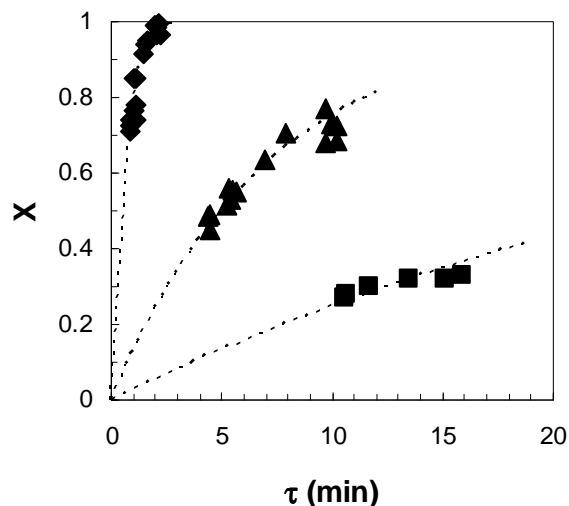


**Figure 3.7.** Acid Orange 7 conversion in continuous UPBR using different support materials: (◆) activated carbon, (▲) graphite, and (■) alumina.

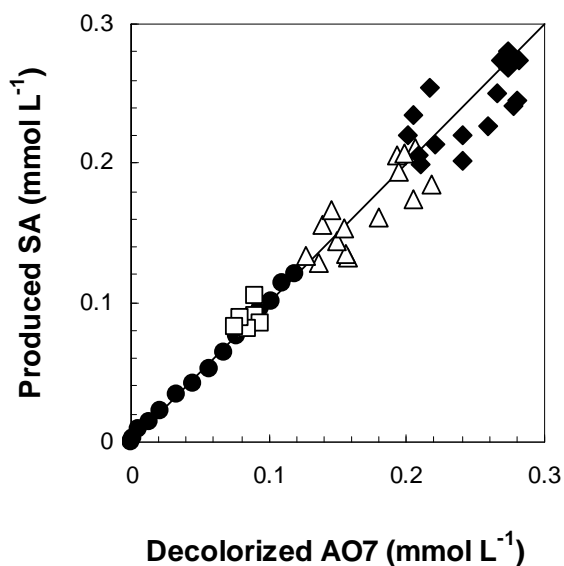


**Figure 3.8.** Ratio between destroyed Acid Orange 7 and produced sulfanilic acid in different reactor systems: (●) batch with graphite, (□) UPBR with alumina, (△) UPBR with graphite, and (◆) UPBR with BAC.

### 3.5. AO7–SA ratio

As was shown in Figure 3.2, during the anaerobic degradation of Acid Orange 7, sulfanilic acid (SA) and 1-amino-2-naphthol are produced. To confirm the proposed reaction and check if only the azo bond was broken in the dye molecule or whether there were subsequent reactions, SA concentration in the outlet was also determined.

Figure 3.8 shows sulfanilic acid concentrations as a function of degraded AO7. It can be seen that the amount of produced SA is proportional to the amount of decolorized azo dye in the ratio of 1:1 –independent of the reactor system– giving evidence that the proposed reaction takes place. In addition, sulfanilic acid adsorption on the support materials or its possible consumption by microorganisms as a carbon source can be neglected.

## **4. Conclusions**

To the best of our knowledge, a continuous upflow packed-bed reactor with biological activated carbon was applied, for the first time, for anaerobic azo dye decolorization. High conversion rates of Acid Orange 7 were achieved at very short space times, corresponding to extremely short hydraulic residence times. Different support materials were also used to determine the crucial roles of BAC in azo dye reduction. The results show that both electron conductivity and specific carbon surface with functional groups contribute to higher reduction rates. Compared to other continuous and biological processes treating azo dyes, UPBR with BAC seems to be one of the most effective and promising systems for anaerobic azo dye degradation.



# 4

## **Novel bioreactor design for decolourisation of azo dye effluents**

### **Abstract**

The anaerobic decolourisation of azo dye Acid Orange 7 (AO7) was studied in a continuous upflow stirred packed-bed reactor (USPBR) filled with biological activated carbon (BAC). Special stirring of BAC and different biodegradation models were investigated. The application of appropriate stirring in the carbon bed resulted in an increase of azo dye bioconversion up to 96% in 0.5 min, compared to unstirred reactor system with ensuring high dye degradation rates at very short space times. In addition, USPBR provided much more reproducible data to make kinetic modeling of AO7 biodegradation. First-order, autocatalytic and Michaelis–Menten models were found to describe the decolourisation process rather well at lower initial dye concentration. AO7 showed significant inhibition effect to biomass beyond inlet dye concentrations of 300 mg L<sup>-1</sup>. Expanding Michaelis–Menten kinetics by a substrate inhibition factor resulted in a model giving good fitting to experimental points, independently on the initial colourant concentration. Processing at very low hydraulic residence time together with higher initial dye concentration resulted in toxicity to bacteria.

<Published as: Mezohegyi G, Bengoa C, Stuber F, Font J, Fabregat A, Fortuny A. (2008). *Chemical Engineering Journal* 143(1–3): 293–298.>



## 1. Introduction

Azo colourants make up the largest and most versatile class of dyes with more than 2000 different azo dyes being currently used (Stolz, 2001). A typical drawback of azo dye colouration –mainly occurred in textile industry– is that large amounts of the dyestuff are directly spilt to wastewater. These chemicals and their degradation products may cause serious problems of environmental pollution and, in addition, the increased demand for textile products have made textile industry one of the main sources of severe environmental problems worldwide (Vandevivere et al., 1998). Relevant factories have deficiencies of treating efficiently these effluents on industrial scale, particularly at higher dye concentrations and at lower energy consumptions.

Up to now, several methods have been found to treat azo dye wastewaters (Slokar and Marechal, 1998; Robinson et al., 2001; Forgacs et al., 2004). However, among the diverse colour removal techniques, biological methods seem to be the most economic and environmental friendly. Many reviews are available on microbiological decolourisation of dyes and azo dyes (Stolz, 2001; Pearce et al., 2003; Banat et al., 1996; Delée et al., 1998; Van der Zee and Villaverde, 2005). While latter ones can be reduced to the corresponding amines by bacteria under anaerobic conditions, they are difficult to completely breakdown aerobically (Nigam et al., 1996). On the other hand, the anaerobic breakdown products of azo dyes are more susceptible to biodegradation under aerobic conditions rather than under anaerobic conditions. Complete treatment and efficient biomineralisation process can, thus, be obtained by a sequential anaerobic–aerobic process (Delée et al., 1998).

These sequential reactor studies have shown that a generally high extent of colour removal can be obtained (Lourenço et al., 2001) and several of them furthermore provide evidence for removal of aromatic amines (O'Neill et al., 2000a; Rajaguru et al., 2000). However, anaerobic reduction of many azo dyes can be considered as a relatively slow process (Nigam et al., 1996; O'Neill et al., 2000; Rajaguru et al., 2000; Supaka et al., 2004) that is, practically the only, but serious disadvantage of biological azo dye decolourisation. To overcome this problem, by using redox mediators during the reduction, anaerobic biodegradation can be enhanced resulting in much higher removal rates. During last years, evidences have been accumulated that quinoid compounds and humic substances can play important roles as redox mediators in anaerobic reduction processes such as biotransformation of azo dyes, polyhalogenated pollutants and nitroaromatics (Field et al., 2000). Among quinones, mostly applied compounds in azo dye degradation as catalytic mediators have been anthraquinone-2,6-disulfonate (Cervantes et al., 2001; Van der Zee et al., 2001; Rau et al., 2002; Dos Santos et al., 2004) and anthraquinone-2-sulfonate (Rau et al., 2002; Dos Santos et al., 2004), both resulting highly efficient azo dye decolourisation. However, homogeneous reaction

requires continuous dosing of the redox mediator resulting additional process costs. This problem can be avoided by immobilizing the electron mediator in the bioreactor. Aside from immobilized anthraquinone (Guo et al., 2007), activated carbon as a possible solid redox mediator containing surface quinonic structures, was reported to be able to accelerate azo dye reduction (Van der Zee et al., 2003; Mezohegyi et al., 2007).

The role of activated carbon as catalyst is diverse in different reactions, related to oxidation, combination and decomposition but not to reduction (Stüber et al., 2005). Research for dye wastewater treatments by BAC system under anaerobic conditions have not been so widespread either. Upflow anaerobic sludge blanket reactors have been the most commonly used high-rate anaerobic systems that could be used for treatment of dye wastes (O'Neill et al., 2000b). To our knowledge, packed-bed-type reactors using biological activated carbon system have never been applied for anaerobic azo dye decolourisation by other authors.

In our previous study (Mezohegyi et al., 2007) the results cleared the efficiency of using a solid electron mediator in both continuous upflow packed-bed reactors (UPBR) and discontinuous reactors during anaerobic Acid Orange 7 (AO7) reduction. Moreover, evidences were given that in UPBR with BAC system, the electron conductivity of the active carbon and its specific surface with both functional groups and the carbon's strong adsorption capacity for Acid Orange 7, contribute together to higher azo dye decolourisation rates. Recent study similarly concerns with testing the anaerobic biodegradation of azo dye AO7 in packed-bed reactors containing biological activated carbon. Differences in goals of present study were to develop UPBR reactors (USPBR) to both have more effective treatment and make kinetic modeling possible; to investigate the effect of stirring of BAC; and, to develop a possible model to describe anaerobic azo dye biodegradation in USPBR–BAC system.

## 2. Materials and methods

### 2.1. Chemicals

Azo dye Orange II (C.I. Acid Orange 7) sodium salt (dye content 99%, Sigma, ref. O8126), an acid dye widely used in textile processes, was selected as model azo colourant. Sulfanilic acid, one of the anaerobic degradation products of Acid Orange 7 was supplied by Sigma (min. 99%, ref. S5263). Sodium acetate (99%, Aldrich, ref. 11019-1) was used as co-substrate being both the carbon source for sludge and electron donor for azo reduction. Activated carbon (Merck, granules of 2.5 mm, ref. 1.02518.1000) was used as catalytic support material in upflow stirred packed-bed reactors. Activated carbon was crushed and granules of 25–50 mesh size were separated, washed with

distilled water, dried at 104 °C for 15 h and stored under normal conditions. Carborundum granules (Carlo Erba Reagents, ref. 434766) were used as inert diluent for activated carbon. The basal media contained the following compounds (mg L<sup>-1</sup>): MnSO<sub>4</sub>·H<sub>2</sub>O (0.155), CuSO<sub>4</sub>·5H<sub>2</sub>O (0.285), ZnSO<sub>4</sub>·7H<sub>2</sub>O (0.46), CoCl<sub>2</sub>·6H<sub>2</sub>O (0.26), (NH<sub>4</sub>)<sub>6</sub>Mo<sub>7</sub>O<sub>24</sub> (0.285), MgSO<sub>4</sub>·7H<sub>2</sub>O (15.2), CaCl<sub>2</sub> (13.48), FeCl<sub>3</sub>·6H<sub>2</sub>O (29.06), NH<sub>4</sub>Cl (190.9), KH<sub>2</sub>PO<sub>4</sub> (8.5), Na<sub>2</sub>HPO<sub>4</sub>·2H<sub>2</sub>O (33.4), K<sub>2</sub>HPO<sub>4</sub> (21.75).

## 2.2. Upflow stirred packed-bed reactor setup

Figure 4.1 shows schematically the continuous and anaerobic experimental system. The upflow stirred packed-bed reactor has a diameter of 15 mm with a volume of 10 mL. It is filled with the mixture of 10 g of carborundum granules as inert and 1 g of activated carbon with size of 25–50 mesh. The reasons of using an inert diluent for activated carbon are that on the one hand, it is required to test unit amount of catalyst, and on the other hand, because of technological reasons, since the stirring system in USPBR requires a minimal bed volume of about 10 mL while 1 g of AC has only about 3 mL of apparent volume. The packed-bed porosity is about 0.3. Two filters were placed into the top and bottom of the reactor to prevent washing out of AC. The temperature was kept constant at 35 °C. The entering feed was 100 mg L<sup>-1</sup> Acid Orange 7 solution containing 200 mg L<sup>-1</sup> sodium acetate and the basal media with microelements. The flow rate of the feed was varied between 25 and 350 mL h<sup>-1</sup> and was ensured by a micro pump (Bio-chem Valve Inc., ref. 120SP2420-4TV). The pH of the outlet solution varied between 6.7 and 7.4 and was measured by a Crison lab pH-meter with a Slimtrode pH electrode (Hamilton, ref. 238150). The anaerobic condition in the feeding bottle (5 L) was maintained by both cooling of the solution (at 5 °C) and bubbling of helium. The establishment of low oxidation–reduction potentials ( $\leq -400$  mV) for the system, under anaerobic conditions, is necessary for high colour removal rates (Lourenço et al., 2001). The redox potential was continuously monitored (measured where the outlet immediately left the USPBR) and remained below  $-500$  mV (referred to Ag<sup>+</sup>/AgCl electrode). The reactor was built together with a stirring system that makes possible to apply a very fine and slow agitation (1 revolution per hour) in the biological activated carbon bed.

## 2.3. Biological activated carbon system

To prepare the biological system, anaerobic sludge with mixed culture was filtered by a microfilter with a pore size of 20–25  $\mu$ m to only have single cells and spores. This filtrate was pumped through the activated carbon for a week. During this period the biofilm was immobilized on AC surface resulting in the so-called biological activated carbon. Then the biofilm was adapted to AO7 by continuous flowing of the dye solution containing both the basal media and carbon source through the reactor. To maintain the same culture of

sludge, every new reactor was set by using the outlet of an already operated reactor as the inlet to the new one.

The use of mixed culture instead of a specific strain is reasonable. The large number of azo dyes that can be reduced by many different bacteria indicates that azo dye reduction is a non-specific reaction. So far, no strain has been reported being able to decolourise a wide range of azo dyes. Therefore, the use of specific strains on anaerobic biodegradation does not make much sense in treating textile wastewaters, which are composed of several kinds of dyes.

## 2.4. Analytical methods

Acid Orange 7, sulfanilic acid and acetate were measured by HPLC on a C<sub>18</sub> Hypersil ODS column in a gradient of methanol–water mobile phase with a flow rate of 1 mL min<sup>-1</sup>. AO7 was determined at 487 nm, sulfanilic acid at 252 nm and acetate at 210 nm. Sulfanilic acid generation is not represented in results, the only reason of measuring that was to check if the AO7 degradation/sulfanilic acid production ratio was appropriate and the colourant and by-products were not used as a carbon source. The other product generated during the anaerobic degradation of AO7, 1-amino-2-naphthol (1A2N), was not determined due to its partial precipitation.

## 3. Results and discussion

### 3.1. Stirring of BAC in packed-bed reactor

#### 3.1.1. *Agitation effects on biomass*

The reason of testing this novel-type reactor is complex. Uncontrolled BAC may lead to an overproduction in biomass that may result head losses because of clogging phenomena and high bacteria levels in the effluent may also be observed (Scholz and Martin, 1997). On the other hand, higher density of biomass in the bed pores can inhibit biodegradation near to the activated carbon surface. It was found that after a certain process time, the pressure loss in USPBR was significantly less than in UPBR, meaning that the stirred reactor contained less amount of biomass than the simple packed-bed reactor, supposing no significant activated carbon wash-out. Thus, the stirred packed-bed holds less resistance to the flow and slow agitation of BAC together with continuous flow of dye solution through the bed can help removing the 'superfluous' amount of biomass from the reactor. Moreover, agitation can help keeping a nearly constant amount of biomass in the

packed-bed and, also helps eliminating isolated layers of microorganisms, thus, enhancing the performance of the activated carbon.

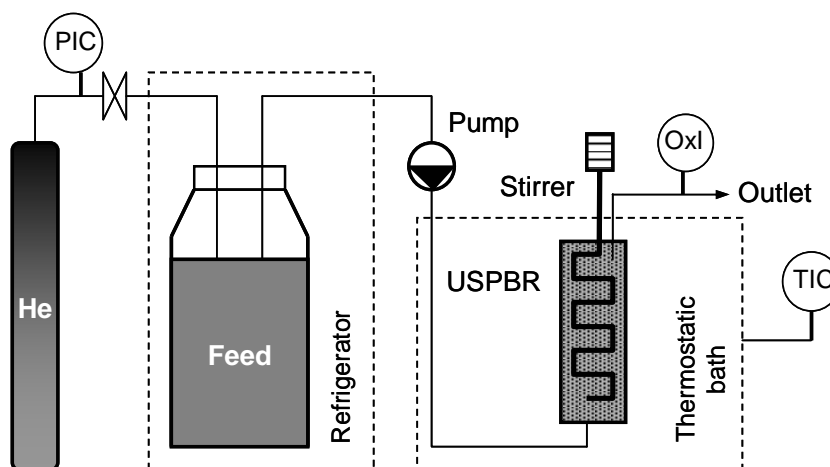


**Figure 4.1.** Anaerobic upflow stirred packed-bed reactor setup.

### 3.1.2. Periodical stirring

Continuous packed-bed reactors working with catalysts –supposing that the amount of catalyst is rather decisive in the reaction than the reactor volume– can be better characterized by space time than by hydraulic residence time. In upflow packed-bed reactors used in our previous study (Mezohegyi et al., 2007), slow but monotonous decreasing of dye conversion values was observed over the time. This can be explained by the isolation of metabolically active organisms from the activated carbon surface by continuous expansion of biofilm around the catalyst. To avoid this problem, appropriate stirring of BAC was applied in the packed-bed reactor.

The effect of slow agitation was examined in two identical USPBRs. Figure 4.2 shows AO7 conversions and referred space times in function of time on stream. During the first 30 days, both reactors were saturated with azo dye to avoid the influence of initial dye adsorption during the initial period of operation. Stirring was first applied on day 39 and 38 in *USPBR-1* and *USPBR-2*, respectively, and was stopped after 1 day of operation. It can be clearly seen that azo dye conversion increased by applying 24-hour long stirring in both reactors. *USPBR-1* worked with space times of 0.47–0.56 min ( $105\text{--}125\text{ mL h}^{-1}$ ) and *USPBR-2* with space times of 0.39–0.72 min ( $85\text{--}155\text{ mL h}^{-1}$ ). In case of *USPBR-1*, stirring resulted 10% increase of AO7 conversion at a space time of 0.54 min ( $110\text{ mL h}^{-1}$ ) while 55% of increase at space time of 0.40 min ( $150\text{ mL h}^{-1}$ ) was observed in *USPBR-2*. When stirring was stopped, conversion started decreasing in both reactors, thus, confirming the positive effect of slow agitation of BAC on decolourisation rates. However, before application of stirring, different conversions of AO7 were found at same space time

in the two reactors. This can be explained by having different concentrations of biomass in them. It is very difficult to control biomass growth in the BAC bed. On the other hand, after stirring, similar dye conversions were observed at same space time in both reactors (e.g., 90–95% at a space time of 0.5 min). According to these, an optimal amount of biomass exists that can be mostly ensured by using agitation in the biological activated carbon.

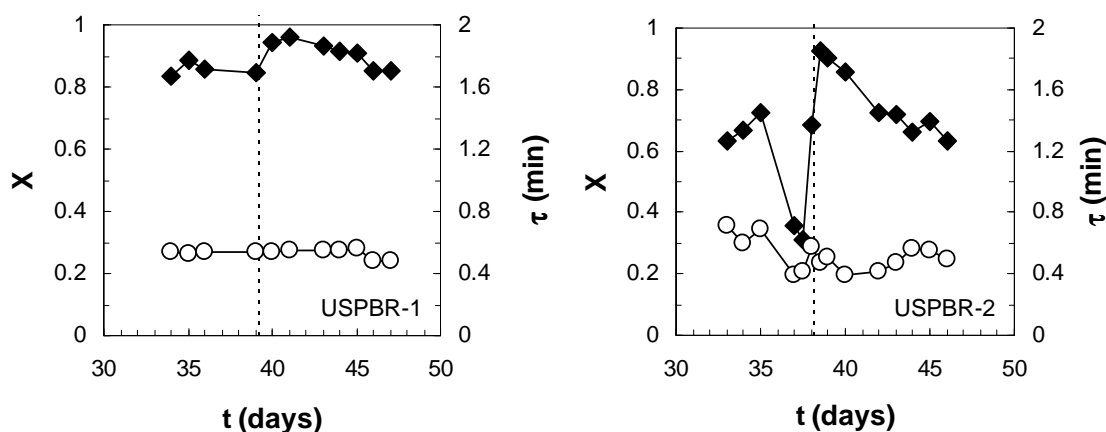


**Figure 4.2.** Effect of stirring in BAC in the packed-bed reactors: (◆) AO7 conversion (X); (○) space time ( $\tau$ ); dotted line represents the start of 24-hour agitation period.

### 3.1.3. Continuous stirring

Since decolourisation rates slowly decreased by time in UPBRs and, in addition, the microbial concentration may vary depending on both the lifetime of the reactor and the applied flow rate of azo dye solution, it was not possible to examine process kinetics in unstirred reactor accurately. In *USPBR-3* –identical as *USPBR-1* and *USPBR-2*– AO7 decolourisation was tested at a certain space time of 0.5 min (HRT of 1.4 min calculated from the reactor hold-up). Results are shown on Figure 4.3. During long time of continuous operation, no significant change in dye conversion was observed. Moreover, nearly the same conversions (90–96%) were achieved than in case of the other two stirred reactors at same space time. These suggest that USPBR gives more representative results for AO7 degradation than UPBR and, in addition, stirred reactor could provide more exact data for kinetic modeling.

## 3.2. Modeling AO7 anaerobic biodegradation in USPBR

### 3.2.1. Determination of reaction rate

The mole balance for the packed-bed reactor is given by (eq. 1):

$$\frac{dF_{AO7}}{dm_C} = -r'_{AO7} = \frac{d(c_{AO7} \cdot F_V)}{d(\tau \cdot F_V \cdot \rho)} \quad (1)$$

where  $F_{AO7}$  ( $\text{mmol min}^{-1}$ ) is the molar flow of azo dye solution,  $m_C$  (g) is the mass of catalyst in the reactor,  $r'_{AO7}$  ( $\text{mmol min}^{-1} \text{g}^{-1}$ ) is the rate of the reaction,  $c_{AO7}$  ( $\text{mmol L}^{-1}$ ) is the dye concentration,  $F_V$  ( $\text{L min}^{-1}$ ) is the volumetric flow,  $\tau$  (min) is the space time and  $\rho$  ( $\text{g L}^{-1}$ ) is the density of solution. If the flow rate of azo dye solution is kept constant and the density difference between the dye solution and water is neglected, the reaction rate  $r_{AO7}$  ( $\text{mmol min}^{-1} \text{L}^{-1}$ ) will finally be (eq. 2):

$$\frac{dc_{AO7}}{d\tau} = -r_{AO7} \quad (2)$$

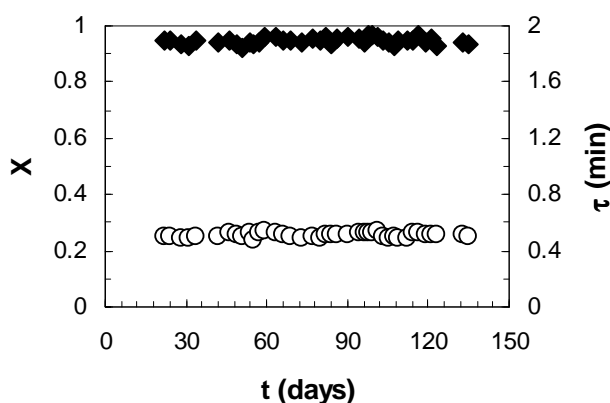


**Figure 4.3.** Effect of continuous stirring in BAC in *USPBR-3*: (◆) Acid Orange 7 conversion ( $X$ ); (○) space time ( $\tau$ ).

### 3.2.2. Kinetic models

To make kinetic modeling possible, a new reactor, *USPBR-4*, was built since in the former ones solely high AO7 conversion values were found even at maximum flow rates of the system (up to  $350 \text{ mL h}^{-1}$ ). The reactor *USPBR-4* contained 250 mg of activated carbon. More than one kinetic model was found to describe rather well Acid Orange 7 anaerobic biodegradation in the upflow stirred packed-bed reactor (Figure 4.4), namely, first-order model, Michaelis–Menten (MM) model and a second-order autocatalytic model (Van der Zee et al., 2000). Table 4.1 shows the kinetic parameters encountered for these models. The simple first-order model fits well the experimental points (Figure 4.4a). According to the standard deviations associated to the model fits (Table 4.1) although, there are no significant differences among them, the autocatalytic model was found to be the most appropriate to describe AO7 biodegradation (Figure 4.4b). This can be explained by the autocatalytic nature of 1-amino-2-naphthol (Van der Zee et al., 2000; Méndez-Paz

et al., 2003), being one of the anaerobic degradation products of Acid Orange 7. On the other hand, Michaelis–Menten model is also expected to describe AO7 biodecolourisation since it is a biological process and, also, the amount of consumed acetate by bacteria – providing the electrons to azo reduction– is directly proportional to dye conversion. Indeed, MM kinetics seems to be applicable for modeling Acid Orange 7 degradation in our reactor system (Figure 4.4c). According to the very good fitting of all the models, the reaction rate predicted by all then should be similar. This is accomplished when comparing the first-order and autocatalytic model, since the first-order constants are similar and the second part of the autocatalytic model gives relatively small values because of the second-power function of the small dye concentration used. The reaction rates of the first-order and MM model are similar as well, since the first-order constants are similar and the Michaelis-constant is rather big relatively to the outlet dye concentrations, thus MM reduces to first-order model in this case.

**Table 4.1.** Kinetic data of models used for anaerobic AO7 degradation in *USPBR-4*.

| Model type                             | Model equation   | Kinetic constants   | S.D. <sup>a</sup>                   |
|--|--|---|-------------------------------------|
| First-order                            | $r_{AO7} = -k \cdot c_{AO7}$   | $k = 10.1 \text{ min}^{-1}$   | 0.048                               |
| Autocatalytic                          | $r_{AO7} = -k_1 \cdot c_{AO7} - k_2 \cdot c_{AO7} \cdot (c_0 - c_{AO7})$ | $k_1 = 10.8 \text{ min}^{-1}$<br>$k_2 = 1.05 \text{ L mmol}^{-1} \text{ min}^{-1}$  | 0.047                               |
| Michaelis–Menten                       | $r_{AO7} = -\frac{k_1 \cdot c_{AO7}}{k_2 + c_{AO7}}$                     | $k_1 = 10.8 \text{ mmol L}^{-1} \text{ min}^{-1}$<br>$k_2 = 0.94 \text{ mmol L}^{-1}$   | 0.054                               |
| Michaelis–Menten with substrate inhib. | $r_{AO7} = -\frac{k_1 \cdot c_{AO7}}{k_2 + c_{AO7} + (c_{AO7}^2/k_i)}$   | $k_1 = 11.7 \text{ mmol L}^{-1} \text{ min}^{-1}$<br>$k_2 = 1.15 \text{ mmol L}^{-1}$<br>$k_i = 4.38 \text{ mmol L}^{-1}$<br>$k_1' = 6.18 \text{ mmol L}^{-1} \text{ min}^{-1}$<br>$k_2' = 0.55 \text{ mmol L}^{-1}$<br>$k_i' = 0.09 \text{ mmol L}^{-1}$ | 0.048<br><br><br>0.056 <sup>b</sup> |

<sup>a</sup>Standard deviation associated to the model fitting:  $s.d. = \sqrt{\sum (x - x^{MOD})^2 / (n - 1)}$  where  $n$  is the number of experimental points. <sup>b</sup>Standard deviation associated to  $k'$  values calculated from experimental points involving both initial dye concentrations of 0.286 and 0.857 mmol L<sup>-1</sup> (100 and 300 mg L<sup>-1</sup>, respectively).

Many azo dyes may have strong adsorption affinity to activated carbons depending on the surface chemistry of the carbon (Pereira et al., 2003). It can be interesting to mention that the so-called Langmuir–Hinshelwood equation –describing the rate law for surface catalysed reactions where the overall reaction rate is proportional to the surface coverage of the substrate over the catalyst– is analogous with the MM model and differences only are between the kinetic constants. Hereby, the former equation may also be used to describe our system suggesting that strong adsorption capacity of the carbon for AO7 can play an important role during this complex biological decolourisation process.



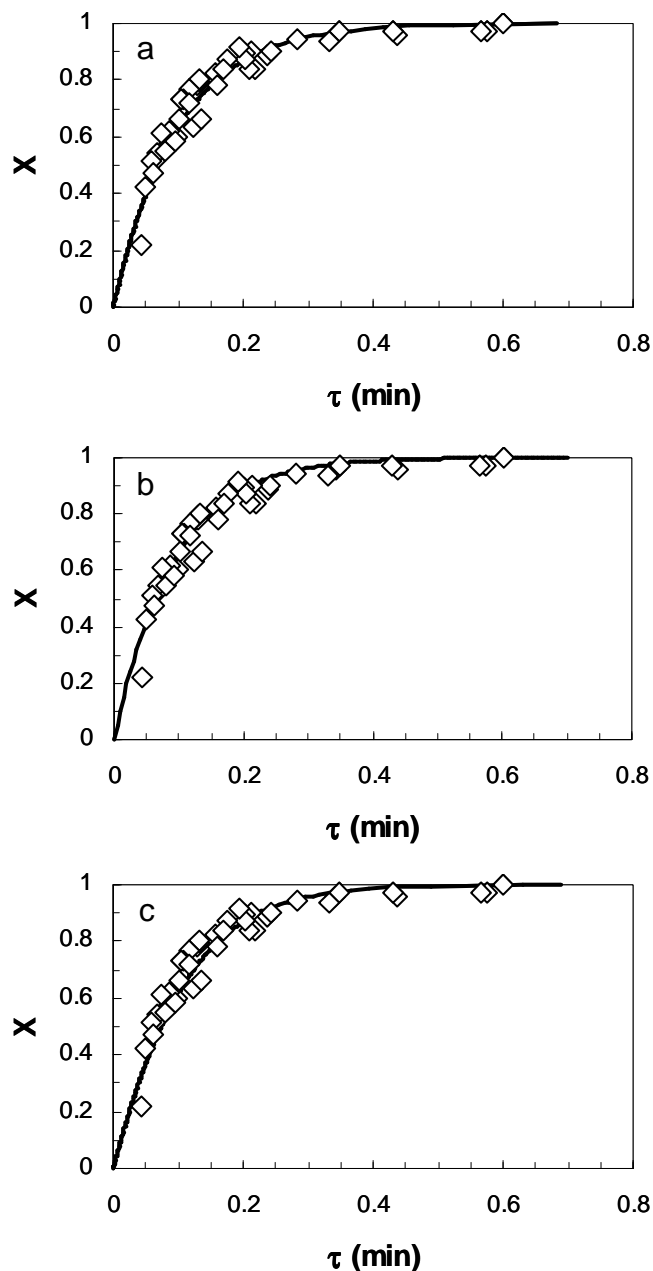


**Figure 4.4.** Kinetic modeling of Acid Orange 7 anaerobic biodegradation in *USPBR-4*: line shows the fitting to (a) first-order kinetic model, (b) autocatalytic model and (c) Michaelis–Menten model.

### 3.3. Substrate inhibition and toxicity effects

50 days after measuring experimental points in *USPBR-4*, the reproducibility of the reactor system was checked by measuring AO7 conversions again, at certain space times. The previously determined Michaelis–Menten model fitted still well the newly measured points. After that, the inlet dye concentration was increased from  $100 \text{ mg L}^{-1}$  to  $300 \text{ mg L}^{-1}$  to check if higher AO7 concentrations may have inhibition or toxicity effects to

the biomass. Figure 4.5 shows that the MM model set before shows significant deviation from experimental points at initial concentration of  $300 \text{ mg L}^{-1}$ . This suggests that AO7 possesses concentration-dependent inhibition effects for bacteria in the reactor. For this, MM model was expanded by an inhibition factor and this model with 3 kinetic constants describes well the degradation process, independently on the initial dye concentrations (Figure 4.5). The substrate inhibition was found to be significant since the value of the constant ratio  $k_i/k_2$  is less than 10. Table 4.1 also shows the standard deviation value associated to experimental points involving both initial dye concentrations of 100 and  $300 \text{ mg L}^{-1}$ . However, the recalculated kinetic constants –including both inlet concentrations– differ from the former ones. This can be explained by having not only inhibition but also toxicity effects to the biomass at higher inlet dye concentrations. Indeed, using very high flow rate in *USPBR-4* at  $300 \text{ mg L}^{-1}$  of initial dye concentration resulted toxicity, i.e., the redox potential was increased from  $-485 \text{ mV}$  up to  $-180 \text{ mV}$  in 3 h after changing the flow of dye solution from  $150$  to  $260 \text{ mL h}^{-1}$ . Then, to avoid the irreversible deactivation of microbes, the flow was set back to  $55 \text{ mL h}^{-1}$  and, in addition, after 2 days the initial AO7 concentration was changed back to  $100 \text{ mg L}^{-1}$ . After 5 more days, the redox potential decreased back to  $-486 \text{ mV}$  and AO7 conversion nearly returned to the value as it was before the toxicity to biomass (Figure 4.5).

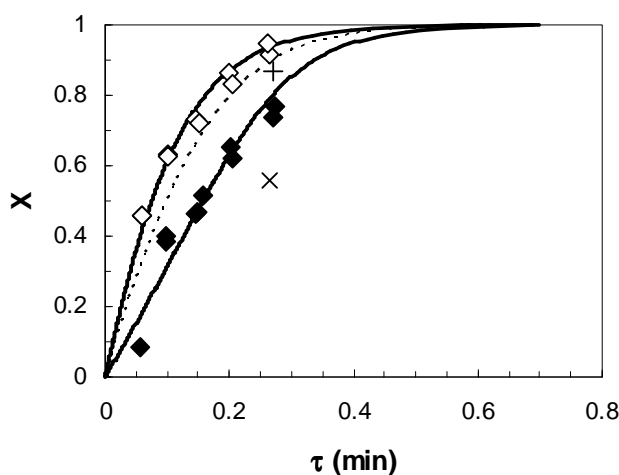


**Figure 4.5.** Substrate inhibition and toxicity effects during Acid Orange 7 decolourisation in *USPBR-4*: ( $\diamond$ ) shows repeated experimental points with initial AO7 concentration of  $100 \text{ mg L}^{-1}$ ; ( $\blacklozenge$ ) shows experimental points with initial AO7 concentration of  $300 \text{ mg L}^{-1}$ ; ( $\times$ ) shows AO7 conversion, 1 day after biomass toxicity; (+) shows AO7 conversion, 6 days after biomass toxicity; dotted line represents the Michaelis–Menten model supposing no substrate inhibition at initial AO7 concentration of  $300 \text{ mg L}^{-1}$ ; continuous lines show the fitting to expanded Michaelis–Menten model with inhibition factor at initial AO7 concentrations of  $100$  and  $300 \text{ mg L}^{-1}$ .

It is worth to mention that sulfanilic acid is a toxic product of anaerobic reduction of AO7 –even more toxic than the initial azo dye itself– such as many aromatic amines, originating from the anaerobic degradation of several azo dyes. Recent study only focuses on the reduction of an azo dye as being the first step of a sequential process. The following step of the complete treatment is to remove the (often) toxic anaerobic degradation products that can be done either by aerobic biodegradation or chemical/physical oxidation processes.

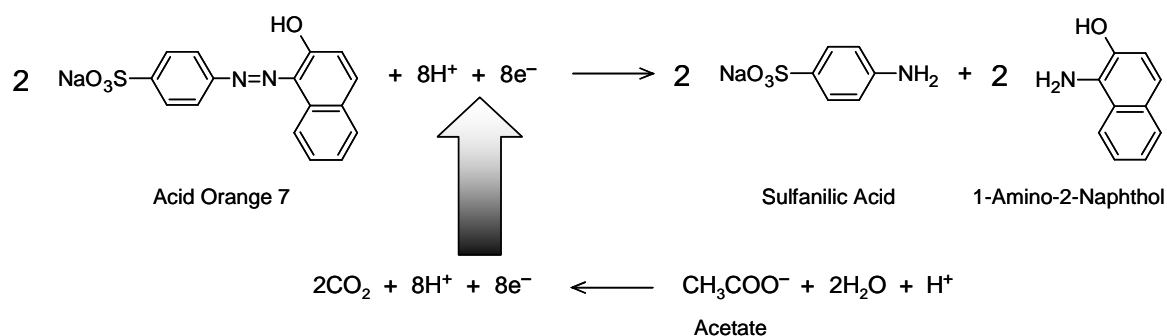


**Figure 4.6.** Theoretical consumption of acetate for Acid Orange 7 reduction.

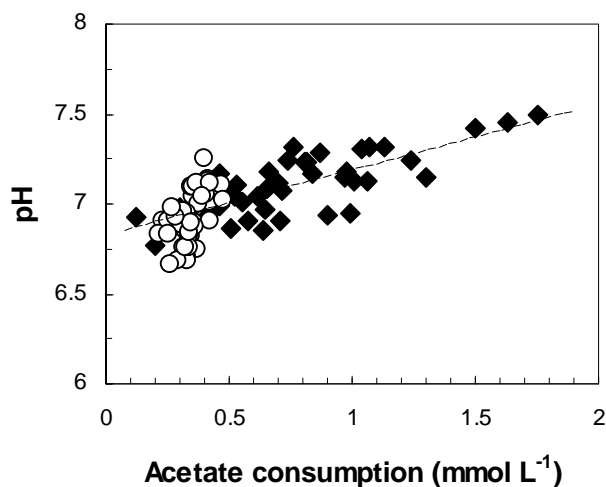


**Figure 4.7.** The change of pH of the outlet solution at different acetate consumptions in *USPBR-3* (○) and *USPBR-4* (◆).

### 3.4. Acetate consumption

Azo dye decolourisation should linearly increase with the consumption of acetate by bacteria. Theoretically, 0.5 mol of acetate is needed for 1 mol AO7 to decolourise (Figure 4.6) that means an acetate consumption:AO7 reduction molar ratio of 0.5. In *USPBR-3*, working with dye solution flow rate of about 120 mL h<sup>-1</sup> (space time of 0.5 min),

this ratio was found to be higher than the expected one. Probably, acetate consumption was overestimated since 200 mg L<sup>-1</sup> of sodium-acetate concentration was supposed to be in the feeding bottle. However, this concentration could be lower by time since anaerobes could consume acetate. Some analysis of the feed solution supported this fact and acetate was found to be totally consumed in 5–6 days in the bottle. To confirm the proposed electron transfer (Figure 4.6) both in *USPBR-3* and *USPBR-4*, the pH of the outlets were measured. Figure 4.7 clearly shows that higher acetate consumptions resulted higher pH values, thus, suggesting the consumption of H<sup>+</sup> during the oxidation of the electron donor.

## 4. Conclusions

To the best of our knowledge, a continuous upflow stirred packed-bed reactor with biological activated carbon was applied for the first time for anaerobic azo dye decolourisation. The application of special stirring in the carbon bed resulted in an increase of Acid Orange 7 bioconversion compared to unstirred reactor system with ensuring high dye degradation rates at very short space times/hydraulic residence times. Moreover, USPBR provided much more reproducible data to make kinetic modeling of AO7 biodegradation possible. First-order, autocatalytic and Michaelis–Menten models were all found to give good fittings to experimental points of dye conversion at lower inlet dye concentration. On the other hand, AO7 showed significant inhibition effects to the biomass at higher initial concentration and, also, processing at very low hydraulic residence times together with high initial dye concentration resulted in toxicity to bacteria. It can be assumed that a general model, describing the anaerobic biodegradation of diverse azo dyes in USPBR-BAC system, will be made up of the combination of dye inhibition and possible autocatalytic effects together with Michaelis–Menten kinetics.



## **Advanced bioreduction of commercially important azo dyes: Modeling and correlation with electrochemical characteristics**

### **Abstract**

The anaerobic biodegradability of some commercially important colorants was investigated in upflow stirred packed-bed reactors (USPBR) containing biological activated carbon (BAC) system. Decolorization with very high reduction rates took place in the case of azo dyes. At least 80% of conversion was achieved for these dyes at a space time ( $\tau$ ) of 2.0 min or higher corresponding to a residence time of about 1.8 min at the most. On the contrary, nonazo xanthene dye was not converted in the anaerobic bioreactor system. A simple model was proposed to predict azo dye decolorization involving both heterogeneous catalysis and biological degradation. Adsorption studies for the dyes revealed that their adsorption affinity to activated carbon is not the key factor in the reduction process. Results from voltammetric experiments show that a correlation exists between electrochemical characteristic and anaerobic biodegradability of different azo dyes in the continuous USPBR-BAC catalytic system.

<Published as: Mezohegyi G, Fabregat A, Font J, Bengoa C, Stuber F, Fortuny A. (2009). *Industrial & Engineering Chemistry Research* 48(15): 7054–7059.>

## 1. Introduction

Wastewaters containing azo colorants –making up the largest class of dyes– are released into the environment by many diverse sources such as textile, food, pharmaceutical, paper, and cosmetic industries. Their discharge into the hydrosphere presents a significant source of pollution due to both their visibility –even at very low concentration– and recalcitrance (Hastie et al., 2006), giving undesirable color to the water, reducing sunlight penetration, resisting photochemical and biological attack, and, also, with many dyes and their degradation products, being toxic or even mutagenic (Van der Zee and Villaverde, 2005). So far, the efficient and low-cost treatment of these hazardous effluents at industrial sites has been doubtful.

The most physicochemical dye-removal techniques (adsorption, electrochemical degradation, advanced oxidation processes, photocatalytic oxidation, etc.) appear to face several limitations since they are financially and often also methodologically demanding (Eichlerová et al., 2005). Alternatively, bioremediation-based solutions for azo dye transformation (Van der Zee and Villaverde, 2005; Banat et al., 1996; Stolz, 2001) have considerable interest since they are both economic and environmentally suitable. One possible strategy for efficient biomineralization of these azo compounds is a sequential anaerobic–aerobic process (Delée et al., 1998) that can provide complex removal of azo colorants by reduction together with their degradation products, aromatic amines by oxidation (O'Neill et al., 2000a).

However, the unspecific anaerobic reduction of many azo dyes usually proceeds rather slowly. Several studies have been conducted investigating anaerobic dye decolorization and providing rather low azo degradation rates for practical aspects. As for the bacterial azo reduction, the most generally accepted hypothesis is that it is a nonspecific reduction process through a redox mediator that shuttles electrons from bacteria to the azo dye (Keck et al., 1997). Therefore, the use of agents that help transferring the electrons from a donor to the azo bond is the logical way to accelerate the anaerobic biodegradation. Quinone-like compounds have been reported to catalyze different reduction processes such as denitrification (Aranda-Tamaura et al., 2007), biotransformation of nitroaromatics (Field et al., 2000), and decolorization of azo dyes (Van der Zee et al., 2001; Rau et al., 2002; Dos Santos et al., 2003). However, the immobilization of the redox mediator in the bioreactor still represents a challenge. Promising results have been obtained to enhance anaerobic azo dye degradation by the use of activated carbon as a solid electron mediator in the bioreactor (Van der Zee et al., 2003; Mezohegyi et al., 2007,2008).

During the anaerobic azo dye reduction in continuous systems, several parameters may have an influence on the decolorization rate such as biomass composition, chemistry of dyes, operating parameters (residence time, temperature, redox potential, and system

of contact), and feed properties (pH, dye concentration, and chemical oxygen demand (COD)). Most of these parameters can be optimized in order to reach appropriate process efficiency. However, chemical properties of all colorants are specific, and the degradation rate in the bioreactors can vary with each of the compounds. This means that common trends have to be determined that give valuable information about the biodegradability of different azo dyes. Some studies investigated the effect of chemical structures of azo dyes on their biodegradation under aerobic (Suzuki et al., 2001) and anaerobic conditions (Hsueh and Chen, 2008) based on the variation of substituents on the aromatic ring and concluded the important role of electrochemical characteristics of dye molecules in their decolorization. Moreover, correlation was reported between the reduction potentials and both the times of maximum decolorization of sulfonated azo dyes by yeast (Zille et al., 2004) and the anaerobic degradation rates of similar-structured and Acid Yellow-type azo dyes in batch tests (Guo et al., 2006). However, comparison of biodegradation kinetics of diverse azo compounds in continuous and catalytic reactor system on a wide redox potential scale, to our knowledge, has not yet been reported. Cyclic voltammetry can be an appropriate tool for determining reduction potential values of azo colorants (Zille et al., 2004; Guo et al., 2006; Guaratini et al., 2001; Chandra et al., 2008).

In a previous study of the authors (Mezohegyi et al., 2008), a novel-type anaerobic bioreactor was developed for azo dye reduction that provided highly efficient decolorization of Acid Orange 7 at lower initial dye concentration. The aim of recent study was to set evidence for the goodness of the upflow stirred packed-bed reactor (USPBR) by testing several commercially important dyes and, also, to propose a simple method for predicting anaerobic biodegradability of azo dyes in the continuous and catalytic USPBR system. Degradation rates of the colorants with process modeling were discussed, and correlations between reduction capability and electrochemical characteristics of the dyes were demonstrated.

The current and important role of the selected dyes (Figure 5.1) at industrial scale is worth mentioning. Considering both the volume generated and the effluent composition, textile industry wastewater is rated as the most polluting among all industrial sectors. The two acid azo dyes Orange II (OII) and Acid Red 88 (AR88) and the diazo dye Reactive Black 5 (RB5) are widely used at the textile sites, and various treatments of wastewaters containing these colorants have been thoroughly investigated. The use of synthetic dyes in the food industry is unambiguous since they are cheaper, more stable, more available, and have a greater coloring range and intensity than natural dyes (Prado and Godoy, 2002). Thus, Tartrazine (E102) and Sunset Yellow FCF (SY) are present in thousands of foods and drugs. However, despite the Food Standards Agency's recent call for a ban on the use of certain artificial azo colorants (including SY and E102) in food products causing hyperactivity in children (Food Standards Agency, 2008), they are still in use and large amounts of these compounds end up in wastewaters as well. Orange G (OG) is used in many staining formulations. As one important representative of xanthene dyes,



Rhodamine 6G (R6G) is famous for its good stability as dye laser material. Although it is not an azo dye, its contingent anaerobic decolorization was also tested for demonstration purposes.

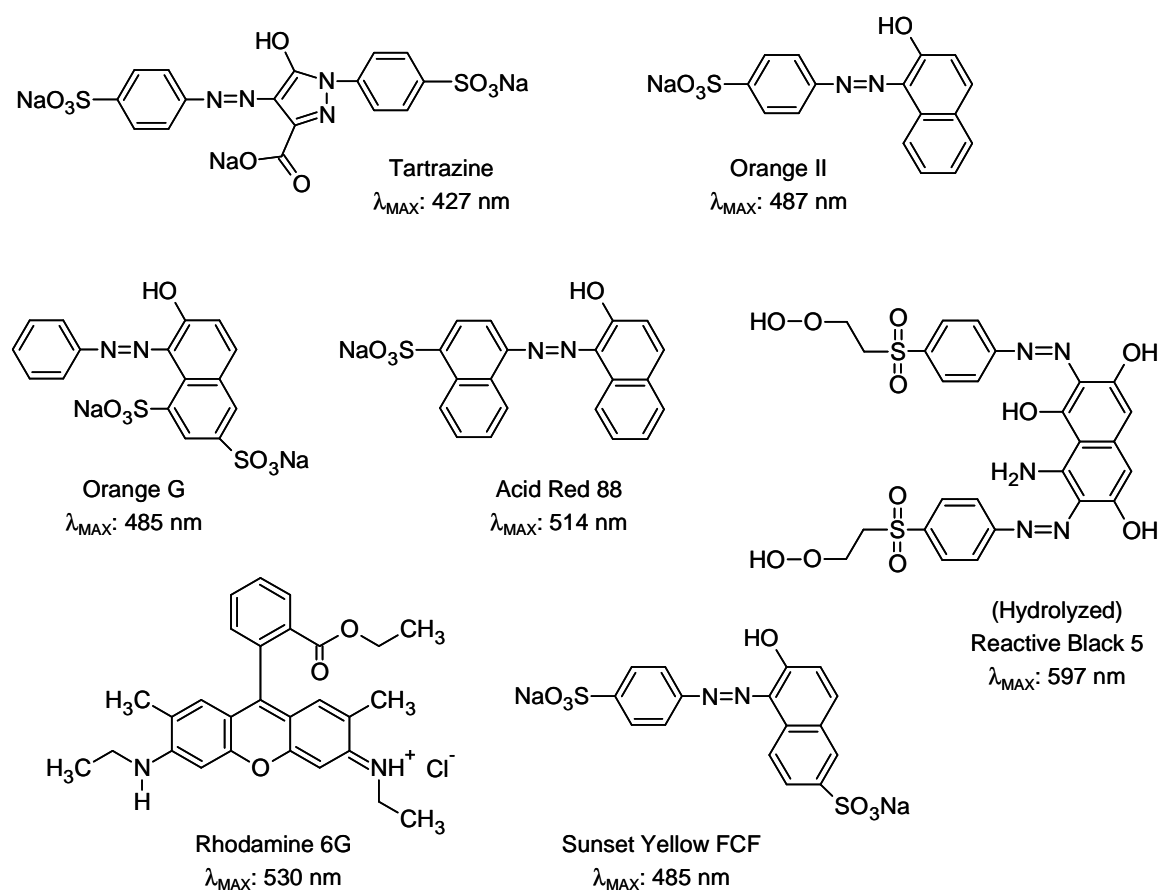


Figure 5.1. Chemical structures of the dyes investigated.

## 2. Materials and methods

### 2.1. Chemicals

Azo dyes Orange II sodium salt (dye content 93%, Sigma, ref. O8126), Orange G (97%, Sigma-Aldrich, ref. O1625), Sunset Yellow FCF (96%, Aldrich, ref. 465224), Acid Red 88 (75%, Sigma-Aldrich, ref. 195227), Tartrazine (85%, Manuel Vilaseca, S.A.), Reactive Black 5 (55%, Sigma-Aldrich, ref. 306452), and nonazo Rhodamine 6G (95%, Sigma, ref. R4127) were selected as model dyes. Sodium acetate (99%, Aldrich, ref. 11019-1) was used as cosubstrate, being both the carbon source for microorganisms and the electron donor for azo reduction. Activated carbon (Merck, 2.5 mm granules, ref. 1.02518.1000) for the biological carbon bed was previously crushed and granules of 25–50 mesh size (0.7–0.3 mm) were separated, washed with distilled water, dried at

104 °C for 15 h, and stored at room conditions until use. The basal media contained several compounds ( $\text{mg L}^{-1}$ ):  $\text{MnSO}_4 \cdot \text{H}_2\text{O}$  (0.155),  $\text{CuSO}_4 \cdot 5\text{H}_2\text{O}$  (0.285),  $\text{ZnSO}_4 \cdot 7\text{H}_2\text{O}$  (0.46),  $\text{CoCl}_2 \cdot 6\text{H}_2\text{O}$  (0.26),  $(\text{NH}_4)_6\text{Mo}_7\text{O}_{24}$  (0.285),  $\text{MgSO}_4 \cdot 7\text{H}_2\text{O}$  (15.2),  $\text{CaCl}_2$  (13.48),  $\text{FeCl}_3 \cdot 6\text{H}_2\text{O}$  (29.06),  $\text{NH}_4\text{Cl}$  (190.9),  $\text{KH}_2\text{PO}_4$  (8.5),  $\text{Na}_2\text{HPO}_4 \cdot 2\text{H}_2\text{O}$  (33.4), and  $\text{K}_2\text{HPO}_4$  (21.75).

## 2.2. Feed and bioreactor system

The USPBR system and operating parameters used in this study were similar to those described in a former study of the authors (Mezőhegyi et al., 2008). The reduction of dyes was tested in two identical reactors, both containing 1 g of activated carbon with the immobilized microorganisms originated from a nonspecific anaerobic mixed culture (Mezőhegyi et al., 2007). The reactors had a diameter of 15 mm with a useful volume of ~2 mL. The packed-bed porosity was ~0.3. Two filters, placed into the top and bottom of the reactor, prevented washing out of the carbon. The temperature was kept constant at 35 °C. The entering dye concentration was  $100 \text{ mg L}^{-1}$  in the case of each dye. The feed also contained  $200 \text{ mg L}^{-1}$  of sodium acetate and the basal media with microelements. The flow rate of the feed was varied between 25 and  $250 \text{ mL h}^{-1}$  and was ensured by a micropump (Biochem Valve Inc., ref. 120SP2420-4TV). The anaerobic condition in the feeding bottle (5 L) was maintained by both cooling of the solution (at 5 °C) and bubbling of helium. The redox potential was continuously monitored and remained below  $-500 \text{ mV}$  (referred to  $\text{Ag}^+/\text{AgCl}$  electrode). Agitation of the biomass was applied for 1 h/day, and sampling was done immediately after or during this period.

Preparing the dye solution of Acid Red 88 (AR88) resulted in difficulties since it partly precipitated with several microelements, making the set of its initial concentration difficult. To have  $100 \text{ mg L}^{-1}$  of initial AR88 concentration, the solution had to be prepared with  $230 \text{ mg L}^{-1}$  azo dye, which was then separated from precipitation before use. In order to simulate dye-bath effluents from dyeing processes with azo reactive dyes, hydrolysis of the dye Reactive Black 5 (RB5H) was accomplished by dissolving it in distilled water, adjusting the pH to 12.0 with 1 M NaOH, boiling for 2 h, cooling the solution down, setting the pH to 7.0 with 1M/0.1 M HCl, and adjusting the necessary volume of prepared stock solution with distilled water.

## 2.3. Adsorption experiments

Before starting experiments in USPBRs, the activated carbon bed was saturated with the azo dyes at  $100 \text{ mg L}^{-1}$  concentration to avoid the influence of initial dye adsorption during the initial period of operation. Adsorption kinetic experiments were run to evaluate the sorption affinities of colorants onto the activated carbon surface. One bottle for each dye, containing 100 mg of activated carbon, was filled with 100 mL of a  $500 \text{ mg L}^{-1}$  dye

solution. Adsorption took place for 15 days, and during this period, samples were taken each second day. The solutions were smartly stirred for a few seconds each day. To avoid a certain increase of basicity during the experiment, pH of the solutions was always adjusted with 0.1 M HCl to be between 7.2 and 7.8.

## 2.4. Voltammetric experiments

Cyclic voltammetry measurements were performed on a PC-controlled PGSTAT12 potentiostat (Autolab) with an in-built frequency response analyzer FRA2 module using a standard three-electrode configuration (reference electrode, Ag/AgCl<sub>(sat)</sub>; counterelectrode, Pt-wire; working electrode,  $\phi = 1$  mm gold disk). Before experiments, the working electrode was polished with 0.5  $\mu\text{m}$  alumina slurry followed by sonication in Milli-Q water. Between experiments with the different dyes, the electrode was washed with acetone and water. The supporting electrolyte was 80 mM H<sub>2</sub>SO<sub>4</sub>. The concentrations of dye samples were 100 mg L<sup>-1</sup>. Before the measurements, dye solutions were saturated by N<sub>2</sub> for 1 min. Cyclic voltammograms were carried out in the potential range of 0.1 to -0.5 V at a scan rate of 0.1 V s<sup>-1</sup>.

## 2.5. Analytical methods

All dyes, acetate, and the monoazo reduction product of RB5H (RB5H<sub>M</sub>) were measured by high-performance liquid chromatography (HPLC) on a C<sub>18</sub> Hypersil ODS column. For azo dyes and acetate, a gradient of methanol–water (M/W) mobile phase was applied (M/W solvent ratios (%) were 0:100 for acetate; 45:55 for RB5H; 60:40 for OG, SY, and E102; 70:30 for OII; and 80:20 for AR88), whereas Rhodamine 6G was detected using a buffered (CH<sub>3</sub>COONa/CH<sub>3</sub>COOH, pH 4.0) acetonitrile–water mobile phase (80:20) with a flow rate of 1 mL min<sup>-1</sup>. Acetate was determined at 210 nm, and RB5H<sub>M</sub> was determined at 530 nm. The applied wavelengths for the colorants are given in Figure 5.1.

# 3. Results and discussion

## 3.1. Adsorption kinetics of dyes

The data obtained from dye adsorption experiments is summarized in Table 5.1. In the cases of all dyes, adsorption was found to fit very well to a second-order kinetic model (Mezohegyi et al., 2007) (eq. 1):

$$Q = \frac{k \cdot Q_E^2 \cdot t}{1 + k \cdot Q_E \cdot t} \quad (1)$$

where  $Q$  ( $\text{mg g}_{\text{AC}}^{-1}$ ) represents the dye concentration in the solid phase,  $Q_E$  ( $\text{mg g}_{\text{AC}}^{-1}$ ) is the corresponding value at equilibrium,  $t$  (days) is the contact time, and  $k$  ( $\text{g}_{\text{AC}} \text{mg}^{-1} \text{day}^{-1}$ ) is the adsorption rate constant. Values of  $Q$  can be calculated from (eq. 2):

$$Q = \frac{(C_{0A} - C_A) \cdot V}{m_{\text{AC}}} \quad (2)$$

where  $C_A$  ( $\text{mg L}^{-1}$ ) is the dye concentration in solution at a time  $t$ ,  $C_{0A}$  ( $\text{mg L}^{-1}$ ) is the initial dye concentration,  $V$  (L) is the volume of solution, and  $m_{\text{AC}}$  (g) is the mass of activated carbon.  $C_{0A}$  was chosen to be quite high ( $500 \text{ mg L}^{-1}$ ) at which concentration the adsorption equilibria of OII (the smallest dye in this study) is nearly equal to its maximum adsorption affinity to the Merck carbon (Mezohegyi et al., 2007). The equilibrium adsorption capacity of activated carbon at this  $C_{0A}$  value can be evaluated by using this simple kinetic model.

All dyes showed high adsorption affinity onto the carbon surface. A nonsignificant linear correlation can be found between maximum adsorption values and the inverse values of molar masses; the smaller dye molecules generally promote a higher adsorption rate. This can be reasonable because of the porous structure of activated carbon. On the other hand, weakness of the correlation was expected because of the existence of other factors influencing dye adsorption onto the same carbon, such as the chemical structure of dyes.

**Table 5.1.** Adsorption, biodecolorization kinetic, and electrochemical data of dyes used in this study.

| dye  | M<br>( $\text{mg mmol}^{-1}$ ) | $Q_E$<br>( $\text{mg g}_{\text{AC}}^{-1}$ ) | $10^4 k$<br>( $\text{g}_{\text{AC}} \text{mg}^{-1} \text{d}^{-1}$ ) | $k_1$<br>( $\text{mmol g}_{\text{AC}}^{-1} \text{min}^{-1}$ ) | $k_2$<br>( $\text{mmol L}^{-1}$ ) | $E_R$<br>(mV)     |
|------|--------------------------------|---|---|---|-----------------------------------|-------------------|
| OII  | 350                            | 369   | 10.5  | 2.46  | 0.88                              | -194              |
| OG   | 452                            | 327   | 13.6  | 1.05  | 0.90                              | -256              |
| SY   | 452                            | 302   | 14.8  | 1.35  | 0.91                              | -248              |
| E102 | 534                            | 211   | 19.0  | 0.91  | 0.85                              | -339              |
| AR88 | 400                            | 383   | 6.7   | 2.63  | 0.90                              | -175              |
| RB5H | 648                            | 110   | 62.6  | 3.51  | 0.96                              | -44               |
| R6G  | 479                            | 188   | 9.8   | n.r. <sup>a</sup>   | n.r. <sup>a</sup>                 | n.p. <sup>b</sup> |

<sup>a</sup>No reduction was observed. <sup>b</sup>No reduction peak was found in the negative potential range.

### 3.2. Reduction of (azo) dyes

Dye reduction in the upflow stirred packed-bed reactor with biological activated carbon (USPBR-BAC) system can be described by a model (Mezohegyi et al., 2008) involving both heterogeneous catalysis and biological decolorization with Michaelis–Menten-like kinetics (eq. 3):

$$\frac{dc_{\text{DYE}}}{\rho \cdot d\tau} = -\frac{k_1 \cdot c_{\text{DYE}}}{k_2 + c_{\text{DYE}}} \quad (3)$$

where  $c_{\text{DYE}}$  (mmol L<sup>-1</sup>) is the dye concentration,  $\tau$  (min g<sub>AC</sub> g<sup>-1</sup>) is the space time,  $\rho$  (g L<sup>-1</sup>) is the density of solution, and  $k_1$  (mmol g<sub>AC</sub><sup>-1</sup> min<sup>-1</sup>) and  $k_2$  (mmol L<sup>-1</sup>) are the kinetic parameters. Using space time with the expanded units (including the mass of activated carbon) gives more information about the reactor. As Figure 5.2(a–f) shows, all azo dyes were highly degraded at short space times and the model fits well the experimental points. Dye conversion values above 80% were achieved in the case of each azo dye at a  $\tau$  of 2.0 min or higher, corresponding to a hydraulic residence time of about 1.8 min at the most (calculated from the reactor holdup).

Appropriate agitation in the biological activated carbon bed has a positive effect on azo dye conversion rate since it helps both controlling the amount of biomass in the packed bed and eliminating isolated layers of microorganisms, thus enhancing the performance of the activated carbon (Mezohegyi et al., 2008). On the other hand, the effect of dye conversion drop after agitation stop is probably due to mass transfer limitations. Beside OII, AR88 conversion showed the most significant deviations from model when sampling was accidentally done out of the 1-h-long agitation period (Figure 5.2e). At a constant flow of 77 mL h<sup>-1</sup> ( $\tau = 0.78$  min), Acid Red conversion dropped by 35%; only 12 hours after that the stirring was interrupted. According to these, reduction of the two dyes mentioned depends stronger on the reactor system than of the other colorants. Considering this, the autocatalytic nature of 1-amino-2-naphthol (Van der Zee et al., 2000) (1A2N), one of the reduction products of both AO7 and AR88, may be relevant. When agitation in the packed bed is eliminated, 1A2N either may get stucked there by adsorption or may be partially degraded, resulting in loss of its autocatalytic ability. However, this hypothesis could not be confirmed because of aminonaphthol partial precipitation and its autoxidation in the outlet.

During the reduction of diazo RB5H, a colored monoazo product is formed (RB5H<sub>M</sub>) that finally is partly reduced. The decolorization of the diazo dye can be modeled easily (Figure 5.2f) using eq. 3. On the other hand, the two sequential reductions can be considered as a series reaction, and the outlet concentration of RB5H<sub>M</sub> depends on the first azo bond reduction rate as well. The second reduction rate can be given as eq. 4:

$$\frac{dc_{\text{RB5HM}}}{\rho \cdot d\tau} = \frac{k_1 \cdot c_{\text{DYE}}}{k_2 + c_{\text{DYE}}} - \frac{k_3 \cdot c_{\text{RB5HM}}}{k_4 + c_{\text{RB5HM}}} \quad (4)$$

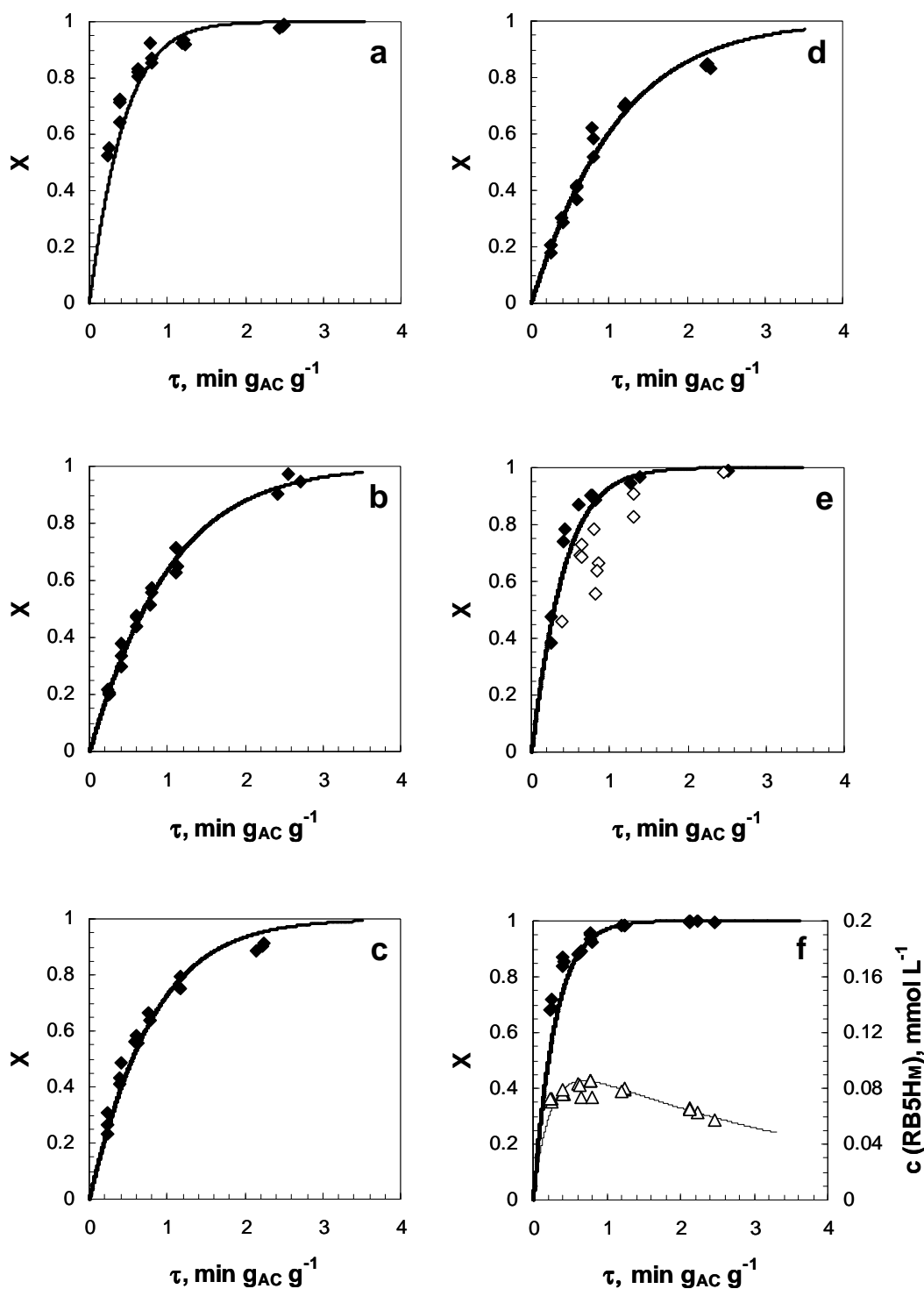
where  $c_{\text{RB5HM}}$  (mmol L<sup>-1</sup>) is the monoazo product concentration,  $c_{\text{DYE}}$  (mmol L<sup>-1</sup>) is the actual diazo (RB5H) concentration,  $\tau$  (min) is the space time, and  $k$  values ( $k_{1,3}$ : mmol g<sub>AC</sub><sup>-1</sup> min<sup>-1</sup>;  $k_{2,4}$ : mmol L<sup>-1</sup>) are the referred kinetic constants. Equation 4 can be easily

solved numerically using e.g., the Euler method. The best model fit for RB5H<sub>M</sub> reduction (Figure 5.2f) supposes significantly –over 10-fold– smaller rate constant for the second reduction ( $k_3 = 0.24 \text{ mmol g}_{\text{AC}}^{-1} \text{ min}^{-1}$ ) than for the first one ( $k_1 = 3.51 \text{ mmol g}_{\text{AC}}^{-1} \text{ min}^{-1}$ ), implying quite poor RB5H<sub>M</sub> decolorization rates. Otherwise, the model (eq. 4) fits the experimental points well and may be applied to describe the second azo reduction in other diazo dyes.

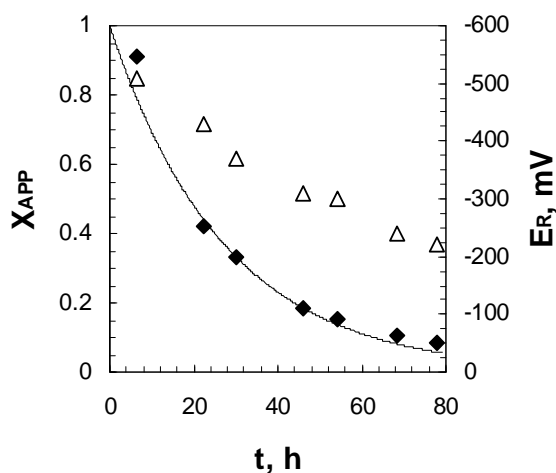
The problem of quantitative determination of RB5H<sub>M</sub> has to be noticed. Since this monoazo compound probably does not exist at the market, its calibration has to be done –together with the final reduction compound– according to the referred HPLC peak areas. Since the final aminonaphthol derivative partially precipitates, the outlet concentration of RB5H<sub>M</sub> can be underestimated. To preclude this error, RB5H<sub>M</sub> concentration was determined by using the *Solver* function of Microsoft Excel. When searching for the kinetic constants of the model ( $k_3$ ,  $k_4$ ), an auxiliary constant was introduced to the equation system that was equal to the RB5H<sub>M</sub> concentration/peak area ratio (that is, in fact, always a constant value when analyzing in the applied concentration interval). Thus, the best model fit finally gave both the kinetic constants of biodegradation and the real outlet concentration values of the monoazo compound.

Table 5.1 shows the kinetic parameters of azo dye biodecolorization encountered for the model. According to  $k_1$  kinetic constants, the mostly biodegradable azo dye is the reactive (and hydrolyzed) RB5H. Since this dye presented the poorest adsorption rate onto the activated carbon among all colorants, it can be concluded that the adsorption affinity of dyes is not the decisive factor in biodecolorization. It is interesting to mention that the reduction products of the more biodegradable dyes (RB5H, AR88, and AO7) possess autocatalytic properties (Van der Zee et al., 2000; Wang et al., 2008). The Michaelis–Menten constant ( $k_2$ ) is an indicator of the affinity that the biomass has for the cosubstrate (acetate) and was found practically to be the same in each case of dye reduction ( $0.90 \pm 0.06 \text{ mmol L}^{-1}$ ). This means that similar biomass culture was obtained in both upflow stirred packed-bed reactors since the same electron donor was used in each process and the reactors operated under the same conditions (pH,  $T$ ).

Nonazo dye Rhodamine could not be degraded in the anaerobic bioreactor (Figure 5.3). In 80 h of feeding the  $100 \text{ mg L}^{-1}$  dye solution to the USPBR at a constant flow rate of  $24 \text{ mL h}^{-1}$ , the apparent conversion dropped under 10% accompanied by the monotone decrease of the redox potential. The falling trend of apparent conversion can be approached exponentially and if calculating the curve improper integral, the activated carbon adsorption capacity for this dye is roughly given, confirming Rhodamine's nonbiodegradable characteristic in anaerobic environment.



**Figure 5.2.** Kinetic modeling of azo dye anaerobic biodecolorization in USPBR: (a) Orange II, (b) Orange G, (c) Sunset Yellow FCF, (d) Tartrazine, (e) Acid Red 88, and (f) hydrolyzed Reactive Black 5; ( $\blacklozenge$ ) shows azo dye conversion ( $X$ ); ( $\diamond$ ) shows conversion values of AR88 when sampling was done out of the agitation period; ( $\triangle$ ) shows outlet concentration values of the monoazo degradation product of RB5H ( $\text{RB5H}_M$ ); lines represent the fitting to the model (eq. 3); thin line (f) shows  $\text{RB5H}_M$  reduction evaluated by the series reaction model (eq. 4).



**Figure 5.3.** Disappearance of Rhodamine in the anaerobic USPBR: (◆) apparent dye conversion ( $X_{APP}$ ); (△) redox potential ( $E_R$ ); line represents an exponential approach to apparent conversion decrease.

### 3.3. Role of redox characteristics in bioreduction

Cyclic voltammetric responses of each azo dye are presented in Figure 5.4. As expected, reduction peaks occurred at negative potentials, between 0 and  $-400$  mV. One reduction peak was found for each monoazo dye, and two peaks were found in the case of the diazo reactive dye. Table 5.1 shows the potential values at which the azo dyes were reduced. According to these, the first azo bond in Reactive Black requires mild anaerobic conditions for reduction, while Tartrazine is only able to biodegrade in the strict absence of oxygen. The more negative the reduction potential of the azo dye is, the more difficult it is to anaerobically biodecolorize it. This hypothesis is confirmed when plotting the azo dye decolorization constants ( $k_1$ ) in function of reduction potentials (Figure 5.5). The correlation can be fitted to a straight line in the given potential interval. The reduction potential of RB5H<sub>M</sub> ( $-257$  mV) predicts its significantly higher degradation rate than the calculated value ( $0.24 \text{ mmol g}_{AC}^{-1} \text{ min}^{-1}$ ), although this prediction does not take into account that this is not the initial compound to be reduced but an intermediate of a series reduction. In the case of nonazo R6G, no reduction peak was found in the negative potential range, thus confirming again its resistance to bioreduction, in the conditions tested.

### 3.4. Biomass sensitivity

The efficacy of the USPBR-BAC system referred to azo dye anaerobic decolorization has been proved, and according to the rate constants achieved, one of the most problematic disadvantages of biological azo degradation, i.e., the slowness of the process, was eliminated. However, there are factors that will always limit the biomass efficiency in azo reduction, independently from bioreactor types. Parameters such as



temperature, pH of solution, and dye concentration can have important impacts on dye conversion rates, depending on the culture tolerance. Orange II was selected as model azo dye to test some of these variables. As Table 5.2 shows, biomass activity (i.e., azo dye reduction) strongly depends on several operating factors. The mixed culture thrives under mesophilic conditions and is adapted to the process temperature (35 °C). The biomass mostly tolerates neutral pH, and a slight change into acidic or basic environment ( $\text{pH } 7.0 \pm 1.5$ ) already causes a significant decrease in dye conversion. Acetate, a cosubstrate widely used as an electron source in decolorization processes (Van der Zee and Villaverde, 2005), did not show any inhibition effects to microorganisms, even at higher concentrations. On the other hand, at an inlet acetate concentration of  $20 \text{ mg L}^{-1}$ , all the carbon source was consumed and was found to be insufficient to provide the necessary amount of protons and electrons for higher azo dye reduction rates. The dye concentration, as it was reported in earlier works (Van der Zee and Villaverde, 2005; Mezohegyi et al., 2008), also affects the biodecolorization process. Higher dye conversion at the applied hydraulic residence time (0.4 min, calculated from the reactor holdup) can be ensured only at lower initial concentrations, whereas higher inlet colorant concentrations inhibit microbial activity. On the other hand, operating with higher dye concentrations and/or high flow rates may cause not only inhibition but also toxicity to the biomass (Mezohegyi et al., 2008).

**Table 5.2.** Microbial sensitivity for temperature, inlet pH, acetate concentration, and dye concentration at a  $\tau$  of  $0.50 \pm 0.02$  min.

| operation factor                             |     | dye conversion |
|--|-----|----------------|
| temperature (°C)                             | 25  | 0.66           |
|  | 30  | 0.75           |
|  | 35  | 0.84           |
|  | 40  | 0.83           |
| pH   | 5.5 | 0.66           |
|  | 6.0 | 0.83           |
|  | 6.5 | 0.77           |
|  | 7.0 | 0.75           |
|  | 7.5 | 0.72           |
|  | 8.0 | 0.67           |
| acetate concentration ( $\text{mg L}^{-1}$ ) | 8.5 | 0.46           |
|  | 20  | 0.19           |
|  | 50  | 0.77           |
|  | 100 | 0.78           |
|  | 200 | 0.80           |
| dye concentration ( $\text{mg L}^{-1}$ )     | 500 | 0.78           |
|  | 50  | 0.88           |
|  | 100 | 0.79           |
|  | 200 | 0.70           |
|  | 300 | 0.60           |
|  | 400 | 0.52           |
|  | 500 | 0.14           |

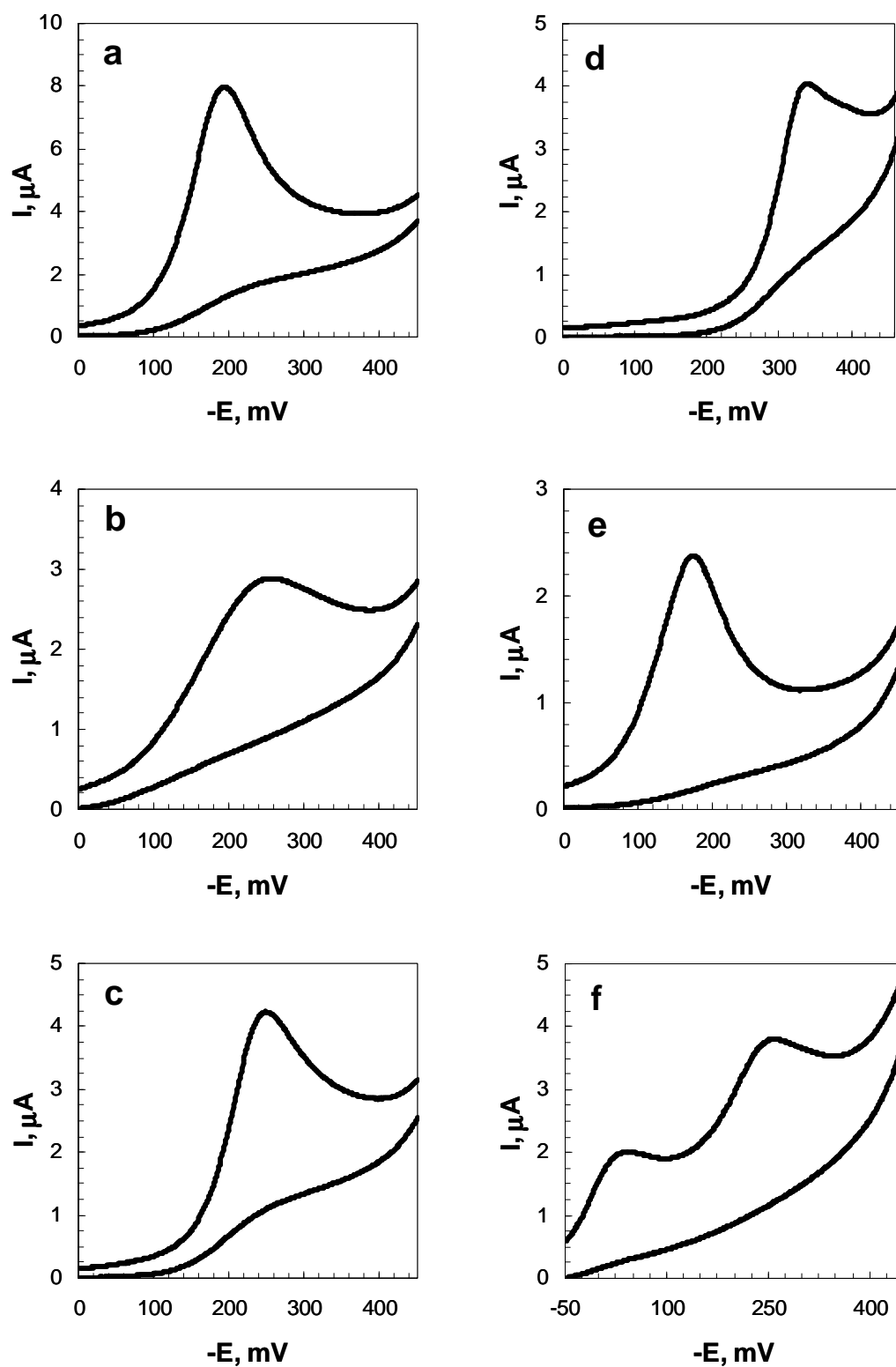


**Figure 5.4.** Cyclic voltammograms of azo dyes in 80 mM  $\text{H}_2\text{SO}_4$  at 0.1 V/s scan rate: (a) Orange II, (b) Orange G, (c) Sunset Yellow FCF, (d) Tartrazine, (e) Acid Red 88, and (f) hydrolyzed Reactive Black 5.

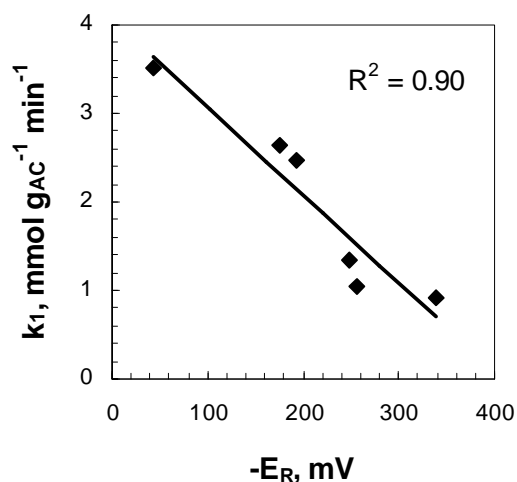


**Figure 5.5.** Correlation between kinetic constants ( $k_1$ ) and the reduction potentials of azo dyes.

## 4. Conclusions

Anaerobic decolorization of some commercially important dyestuffs was investigated in upflow stirred packed-bed reactors with biological activated carbon system. Reduction of the nonazo xanthene dye Rhodamine did not take place even at very low flow rates. On the contrary, all mono- and diazo dyes were efficiently reduced and their decolorization was successfully predicted by a simple model involving both heterogeneous catalysis by activated carbon and biological degradation. Activated carbon high capacity for these dyes was found not to be the crucial promoter of reduction. The electrochemical characteristic of azo dyes, however, was found to be a key factor in their decolorization. A linear correlation was found between the kinetic constants of the model and the reduction potentials of the dyes. According to these results, anaerobic biodegradability of an azo dye can be predicted by its reduction potential value in this continuous reactor system, independently from the azo colorant type and complexity. The biomass was found to be sensitive to some operating factors that require appropriate control and limitation in order to ensure an efficient biodecolorization process.

# 6

## **Tailored activated carbons as catalysts in biodecolourisation of textile azo dyes**

### **Abstract**

Anaerobic reduction of two textile azo dyes (Orange II and Reactive Black 5) was investigated in upflow stirred packed-bed reactors (USPBRs) with biological activated carbon (BAC) system. The bioreactors were prepared with tailored activated carbons (ACs) having different textural properties and various surface chemistries. A kinetic model proposed previously was able to describe the catalytic azo reduction in all cases. Decolourisation with very high reduction rates took place in the case of each AC. Best dye removals were ensured by the AC having the highest surface area: conversion values above 88% were achieved in the case of both azo dyes at a space time of 0.23 min or higher, corresponding to a very short hydraulic residence time of about 0.30 min at the most. The decolourisation rates were found to be significantly influenced by the textural properties of AC and moderately affected by its surface chemistry. The results confirmed the catalytic effects of carbonyl/quinone sites and, in addition, delocalized  $\pi$ -electrons seemed to play a role in the catalytic reduction in the absence of surface oxygen groups.

<Published as: Mezohegyi G, Gonçalves F, Órfão JJM, Fabregat A, Fortuny A, Font J, Bengoa C, Stuber F. (2010). *Applied Catalysis B: Environmental* 94: 179–185.>

## 1. Introduction

Textile industry is one of those industries that consume large amounts of water in the manufacturing process (Lin and Chen, 1997) and, also, discharge great amounts of effluents with synthetic dyes to the environment causing public concern and legislation problems. Azo dyes, that make up the majority (60–70%) of the dyes applied in textile processing industries (Van der Zee et al., 2001) are considered to be serious health-risk factors. Apart from the aesthetic deterioration of water bodies, many azo colourants and their breakdown products are toxic to aquatic life (Chung and Stevens, 1993) and can cause harmful effects to humans (Weisburger, 2002; Oliveira et al., 2007). Several physico-chemical and biological methods for dye removal from wastewater have been investigated (Forgacs et al., 2004; Robinson et al., 2001; Van der Zee and Villaverde, 2005; Vandevivere et al., 1998) and seems that each technique faces the facts of technical and economical limitations (Van der Zee and Villaverde, 2005). However, microbial decolourisation of dyes (Van der Zee and Villaverde, 2005; Banat et al., 1996; Pearce et al., 2003; Stolz, 2001) is one of the most attractive technologies considering its economic, environmentally suitable and methodologically relatively simple features.

Azo dyes are xenobiotic compounds and due to their electron withdrawing nature, they tend to persist under aerobic environment (Knackmuss, 1996). However, under anaerobic conditions, decolourisation is achieved while the aromatic amines produced from such azo cleavage can be removed aerobically (Işık and Sponza, 2006). These predicted the efficacy of an anaerobic–aerobic reactor sequence for complete azo dye treatment (Işık and Sponza, 2006; O'Neill et al., 2000b). The most serious drawback of azo dye reduction by bacteria used to be the slowness of the process. A few study have cleared that certain electron mediators such as quinone-like compounds can greatly accelerate decolourisation rates in homogeneous reactions (Van der Zee and Villaverde, 2005; Dos Santos et al., 2004; Rau et al., 2002). On the other hand, heterogeneously catalyzed azo bioreduction by a solid redox mediator such as activated carbon (AC), has been reported to be a very promising process (Van der Zee et al., 2003; Mezohegyi et al., 2007, 2008,2009).

In catalysis, ACs have been mainly used as support, but their use as catalysts on their own is growing quickly (Figueiredo and Pereira, 2009; Radovic and Rodríguez-Reinoso, 1997; Fortuny et al., 1998; Rivera-Utrilla and Sánchez-Polo, 2002; Suarez-Ojeda et al., 2005). One of the advantages of ACs is the possibility of tailoring their physical and/or chemical properties in order to optimise their performance for specific applications (Pereira et al., 2004). This means that both their pore structure and surface chemistry can be varied (Pereira et al., 2004; Figueiredo et al., 1999; Pereira et al., 1999) to meet the demands of the catalytic reaction considered. In textile and dye wastewater treatments, the role of activated carbon has been often limited to dye adsorption. If AC is considered

as a catalyst in biological azo dye decolourisation, its specific modification may increase dye removal rates. In the present study, several activated carbons with modified pore structures or surface chemistries were applied for the first time in anaerobic upflow stirred packed-bed reactors (Mezőhegyi et al., 2008) for azo dye reduction, and the effects of AC texture and surface chemical group variation on decolourisation rates were discussed.

## 2. Experimental

### 2.1. Preparation of activated carbons

#### 2.1.1. Activated carbons with different textural properties

The initial material selected (sample AC<sub>0</sub>) was the commercial activated carbon Norit Rox 0.8, which was supplied in the form of cylindrical pellets of 0.8 mm diameter and 5 mm length. The activated carbons with larger porosities were obtained by CO<sub>2</sub> gasification of sample AC<sub>0</sub> previously impregnated with 3.5% of cobalt. The role of cobalt was to catalyze the gasification of carbon, thereby promoting the formation of mesopores (Pereira et al., 2004). The impregnation was carried out by mixing the previously vacuum-degassed sample AC<sub>0</sub> with an aqueous solution of Co(NO<sub>3</sub>)<sub>2</sub>·6H<sub>2</sub>O. The resulting suspension was shaken for 2 h. Then the sample was washed with distilled water and dried at 100 °C overnight in an oven.

The gasification experiments were carried out in a tubular vertical reactor under the following experimental conditions: heating from room temperature to 900 °C at 10 °C min<sup>-1</sup> under a flow of 100 cm<sup>3</sup> min<sup>-1</sup> of N<sub>2</sub>; at 900 °C the gas was changed to CO<sub>2</sub> maintaining the flow rate and the sample was gasified during 40 min (AC<sub>T1</sub>) or 120 min (AC<sub>T2</sub>) and finally cooled down to room temperature under a flow of 100 cm<sup>3</sup> min<sup>-1</sup> of N<sub>2</sub>. These carbons were subsequently washed with a 2 M HCl-solution to remove cobalt, followed by washing with distilled water until reaching neutral pH and dried in the oven at 100 °C. To make comparison with the starting carbon possible, AC<sub>0</sub> was also heated up to 900 °C and was kept at this temperature for 40 min under a flow of 100 cm<sup>3</sup> min<sup>-1</sup> of N<sub>2</sub> (AC<sub>T0</sub>) to ensure similar surface chemistry to the gasificated samples. Since the quinonic surface groups are supposed to play an important role during anaerobic biodecolourisation of azo dyes by biological activated carbon, and a significant amount of these groups were removed by the heat treatment, a slight oxidation was applied for samples AC<sub>T0</sub>, AC<sub>T1</sub> and AC<sub>T2</sub>. These carbons were heated up to 425 °C at 10 °C min<sup>-1</sup> under a flow of 75 cm<sup>3</sup> min<sup>-1</sup> of N<sub>2</sub>; when the given temperature was reached, air was added to the gas flow to have 5% (v/v) of O<sub>2</sub>; this gaseous mixture was passed for 4 h. When cooling started, the gas was set back only to N<sub>2</sub>. After cooling to room temperature,

all the carbon samples were crushed and granules of 25–50 mesh size (0.7–0.3 mm) were separated and stored under normal conditions.

### *2.1.2. Activated carbons with different surface chemistries*

The treatments outlined below were carried out in order to obtain materials with different surface chemistries, while maintaining the original textural properties as far as possible.

Liquid-phase oxidation of AC<sub>0</sub> with HNO<sub>3</sub> was performed using a 250 cm<sup>3</sup> Soxhlet extraction apparatus. Initially, 400 cm<sup>3</sup> of 5 M HNO<sub>3</sub> were introduced into a 500 cm<sup>3</sup> Pyrex round bottom flask and heated to boiling temperature with a heating mantle. The Soxhlet with a certain amount of activated carbon was connected to the boiling flask and to the condenser. The reflux was stopped after 6 h. The AC was then washed with distilled water to neutral pH and dried in an air convection oven at 100 °C for 24 h (sample AC<sub>1</sub>).

Sequentially, the sample AC<sub>1</sub> was altered by thermal treatments; the starting material had to present a large amount of surface groups that were to be removed in different amounts (and types) by applying different temperatures. In every case, 3 g of sample AC<sub>1</sub> were placed into a fused silica tubular reactor. The heating was done under a flow of N<sub>2</sub> at 100 cm<sup>3</sup> min<sup>-1</sup> and the heating rate was 10 °C min<sup>-1</sup>. The carbon samples were heated up to 400 °C (AC<sub>2</sub>), 600 °C (AC<sub>3</sub>), 750 °C (AC<sub>4</sub>) and 1100 °C (AC<sub>5</sub>). AC<sub>5</sub> was kept at 1100 °C for 1 h. Posteriorly, one additional sample was prepared from AC<sub>0</sub> by heating it up to 750 °C under a flow of N<sub>2</sub> at 100 cm<sup>3</sup> min<sup>-1</sup> and heating rate of 10 °C min<sup>-1</sup> (AC<sub>02</sub>). After cooling to room temperature under the same atmosphere, all the carbon samples were crushed and granules of 25–50 mesh size (0.3–0.7 mm) were separated and stored under normal conditions.

## 2.2. Characterization of activated carbons

### *2.2.1. Textural characterization*

The textural characterization of the materials was principally important in the case of pore size-modified activated carbons, but it was also checked if there had been notable textural changes after the surface chemistry modifications, including the thermal treatments. This characterization was based on the N<sub>2</sub> adsorption isotherms, determined at 77 K with a Coulter Omnisorp 100 CX gas adsorption analyser. The micropore volume ( $V_{\mu}$ ) and the non-microporous surface area ( $S_{\neq\mu}$ ) were calculated by the *t*-method, using the standard isotherms for carbon materials proposed by Rodriguez-Reinoso et al. (1987). The BET surface areas ( $S_{\text{BET}}$ ) of the samples were also calculated for comparison purposes.

### 2.2.2. Surface chemistry characterization

The temperature-programmed desorption (TPD) profiles of the samples were obtained in an Altamira AMI-200 characterization unit, working with a U-shaped tubular microreactor, placed inside an electrical furnace. The flow of the helium carrier gas was  $25 \text{ cm}^3 \text{ min}^{-1}$ , the temperature was programmed to linearly rise up to  $1100 \text{ }^\circ\text{C}$  at a heating rate of  $5 \text{ }^\circ\text{C min}^{-1}$ . The amounts of CO and  $\text{CO}_2$  desorbed from the carbon samples (100 mg) were determined by an Ametek Dymaxion mass spectrometer. The relative molecular masses monitored for all samples were 2 ( $\text{H}_2$ ), 16 (O), 18 ( $\text{H}_2\text{O}$ ), 28 (CO) and 44 ( $\text{CO}_2$ ).

The determination of  $\text{pH}_{\text{PZC}}$  (point of zero charge) of the samples was similarly carried out as reported by Órfão et al. (2006):  $20 \text{ cm}^3$  of 0.01 M NaCl solution was placed in a closed Erlenmeyer flask. The pH was adjusted to a value between 2 and 10 by adding HCl 0.1 M or NaOH 0.1 M solutions. Then, 0.05 g of each sample was added and the final pH measured after 48 h under agitation at room temperature. The  $\text{pH}_{\text{PZC}}$  is the point where the curve  $\text{pH}_{\text{final}}$  vs.  $\text{pH}_{\text{initial}}$  crosses the line  $\text{pH}_{\text{initial}} = \text{pH}_{\text{final}}$ . Blank tests without carbon were also made in order to eliminate the influence of  $\text{CO}_2$  from air on pH.

### 2.3. Chemicals

Azo dyes Orange II sodium salt (dye content 93%, Sigma, ref. O8126) and Reactive Black 5 (55%, Sigma–Aldrich, ref. 306452) were selected as model textile dyes. In order to simulate dye-bath effluents from dyeing processes with azo reactive dyes, hydrolysis of Reactive Black (RB5H) was accomplished by: dissolving it in distilled water, adjusting the pH to 12.0 with 1 M NaOH, boiling for 2 h, cooling the solution down, setting the pH to 7.0 with 1 M/0.1 M HCl and adjusting the necessary volume of prepared stock solution with distilled water. Sodium acetate (99%, Aldrich, ref. 11019-1) was used as co-substrate being both the carbon source for microorganisms and electron donor for azo reduction. The basal media contains several compounds ( $\text{mg L}^{-1}$ ):  $\text{MnSO}_4 \cdot \text{H}_2\text{O}$  (0.155),  $\text{CuSO}_4 \cdot 5\text{H}_2\text{O}$  (0.285),  $\text{ZnSO}_4 \cdot 7\text{H}_2\text{O}$  (0.46),  $\text{CoCl}_2 \cdot 6\text{H}_2\text{O}$  (0.26),  $(\text{NH}_4)_6\text{Mo}_7\text{O}_{24}$  (0.285),  $\text{MgSO}_4 \cdot 7\text{H}_2\text{O}$  (15.2),  $\text{CaCl}_2$  (13.48),  $\text{FeCl}_3 \cdot 6\text{H}_2\text{O}$  (29.06),  $\text{NH}_4\text{Cl}$  (190.9),  $\text{KH}_2\text{PO}_4$  (8.5),  $\text{Na}_2\text{HPO}_4 \cdot 2\text{H}_2\text{O}$  (33.4), and  $\text{K}_2\text{HPO}_4$  (21.75).

### 2.4. Feed and bioreactor system

The upflow stirred packed-bed reactor (USPBR) system and operating parameters used in this study were similar to those described in a former study of the authors (Mezohegyi et al., 2008). The reduction of dyes was tested in reactors containing 1 g of activated carbon with the immobilized microorganisms (Figure 6.1) originated from a non-specific anaerobic mixed culture (Mezohegyi et al., 2007). The reactor had a diameter of



15 mm with a useful volume of about 2 cm<sup>3</sup>. The packed-bed porosity was about 0.3. Two filters, placed into the top and bottom of the reactor, prevented washing out of the carbon. The temperature was kept constant at 35 °C. The entering concentration of dyes was 100 mg L<sup>-1</sup>. The feed also contained 200 mg L<sup>-1</sup> of sodium acetate and the basal media with microelements. The flow rate of the feed was varied between 25 and 250 mL h<sup>-1</sup> and was ensured by a micro pump (Bio-chem Valve Inc., ref. 120SP2420-4TV). The anaerobic condition in the feeding bottle (5 L) was maintained by both cooling of the solution (at 5 °C) and bubbling of helium. The redox potential was continuously monitored and remained below -500 mV (referred to a combined Pt//Ag/AgCl redox electrode). Agitation of the biomass was applied for 1 hour/day and sampling was done immediately after or during this period. Before starting experiments in USPBRs, the activated carbon bed was saturated with the azo dyes at 100 mg L<sup>-1</sup> concentration to avoid the influence of initial dye adsorption during the initial period of operation.

## 2.5. Analytical methods

Both dyes and the monoazo reduction product of RB5H (RB5H<sub>M</sub>) were measured by HPLC on a C<sub>18</sub> Hypersil ODS column. A gradient of methanol–water (M:W) mobile phase was applied (M:W solvent ratios (%) were: 45:55 for RB5H and 70:30 for OII). OII, RB5H and RB5H<sub>M</sub> were determined at 487, 597 and 530 nm, respectively.

## 3. Results and discussion

### 3.1. Characterization of activated carbons

#### 3.1.1. Textural characterization

Figure 6.2 shows the N<sub>2</sub> adsorption isotherms for the activated carbon samples after textural (Figure 6.2a) and surface chemistry modification (Figure 6.2b). The shape of the isotherms denotes the presence of micropores but mainly the mesopores in the carbon samples. The textural modification of AC resulted in the enhancement of the porosity. Evidently, the longer time of gasification was applied, the higher burn-off values were reached (28% and 50% for AC<sub>T1</sub> and AC<sub>T2</sub>, respectively). Some calculated data confirms these observations and shows that the gasification time correlates to several textural factors (Table 6.1). On the other hand, surface chemistry modification by acid and consecutive thermal treatment of AC<sub>0</sub> did not cause significant textural changes, only a very slight reduction of microporosity was observed while the meso- and macroporosity remained intact; thus a possible variation in biodecolourisation rates with these carbons would be solely due to their different surface chemistries.

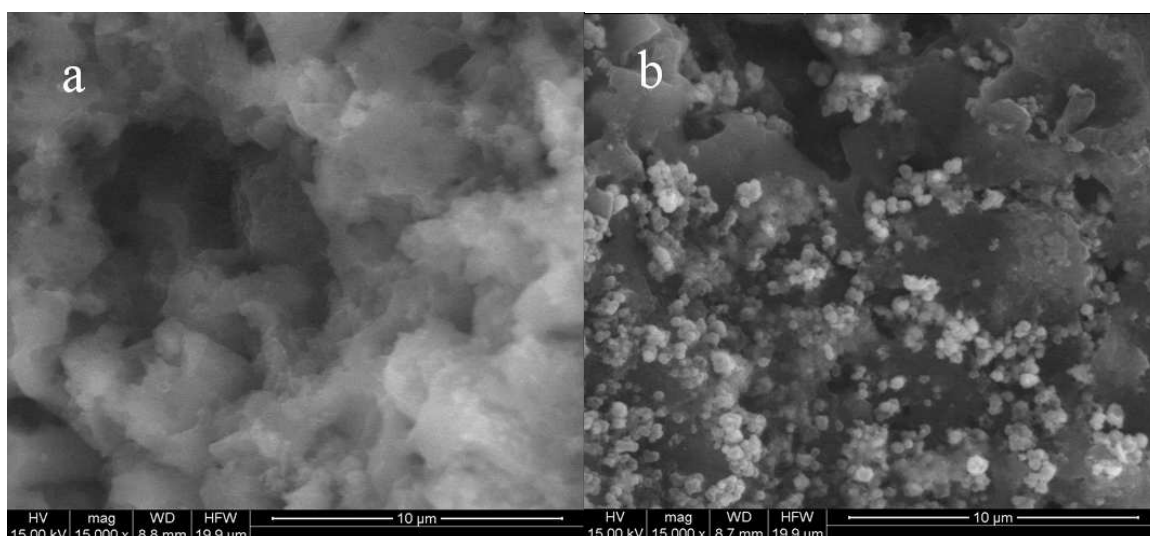


**Figure 6.1.** Activated carbon surface without (a) and with (b) biofilm (ESEM).

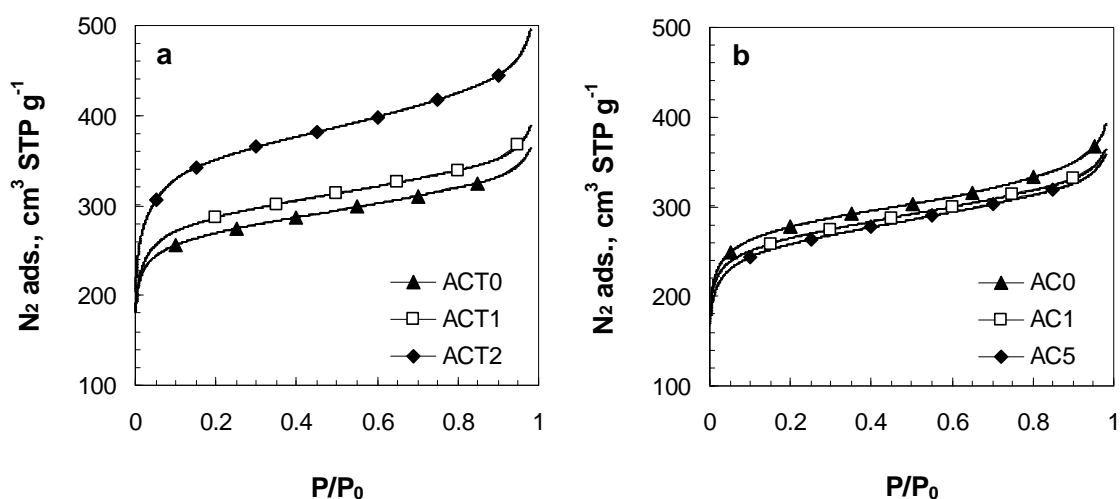


**Figure 6.2.**  $N_2$  adsorption isotherms at 77 K for activated carbons with different textural properties (a) and surface chemistries (b).

### 3.1.2. Surface chemistry characterization

The surface oxygen groups on carbon materials decompose upon heating by releasing CO and  $CO_2$  at different temperatures. A  $CO_2$  peak results from carboxylic acids at low temperatures, or lactones at higher temperatures; carboxylic anhydrides originate both a CO and a  $CO_2$  peak; phenols, ethers, and carbonyls/quinones originate CO peaks (Figueiredo et al., 1999). Figure 6.3 shows the TPD spectra of the Norit Rox activated carbon before ( $AC_0$ ) and after the textural modifications. Because of their preparation method, none of these carbon samples ( $AC_{T0}$ ,  $AC_{T1}$  and  $AC_{T2}$ ) contains significant amount of surface groups emitting  $CO_2$  (Figure 6.3a), its rate of generation was less than 0.03

$\mu\text{mol s}^{-1} \text{g}^{-1}$  in each case. The amount of CO-emitting groups is obviously higher by the increase of the activated carbon surface area (Figure 6.3b), but the specific CO-releasing groups density was found to be similar for  $\text{AC}_{\text{T}0}$ ,  $\text{AC}_{\text{T}1}$  and  $\text{AC}_{\text{T}2}$  (1.00, 1.04 and 1.08  $\mu\text{mol m}^{-2}$ , respectively). According to both the CO- and  $\text{CO}_2$ -spectra, the textural modification (followed by slight oxidation) was carried out by varying mainly the textural characteristics but not the surface chemistries of the carbon samples ( $\text{AC}_{\text{T}0}$ ,  $\text{AC}_{\text{T}1}$  and  $\text{AC}_{\text{T}2}$ ).

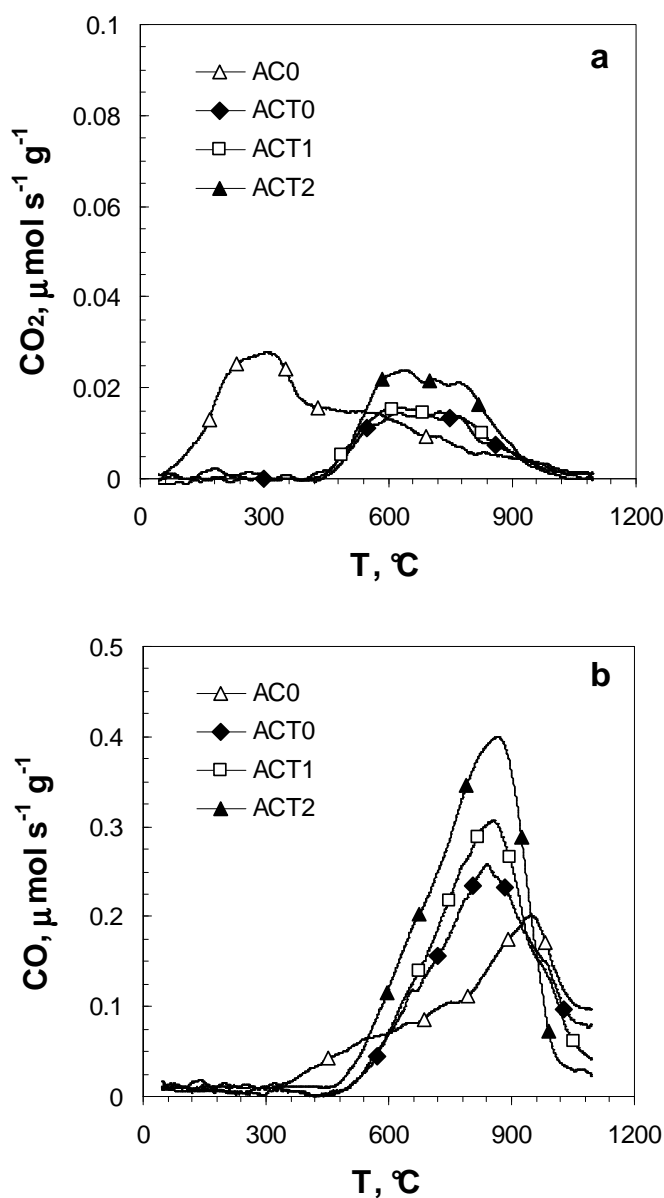


**Figure 6.3.** TPD spectra of activated carbons with different textural properties: (a)  $\text{CO}_2$  and (b) CO evolution.

Figure 6.4 shows the TPD spectra of  $\text{AC}_0$  and the samples with modified surface chemistries ( $\text{AC}_1$ – $\text{AC}_5$ ;  $\text{AC}_{02}$ ). It can be seen that the nitric acid treatment ( $\text{AC}_1$ ) increased the amount of surface groups, which is evidenced by the increase of  $\text{CO}_2$  (Figure 6.4a)

and CO (Figure 6.4b) released. Both the spectra show well the effect of thermal treatments on sample AC<sub>1</sub>; the higher temperature was applied, the more amount of surface groups were removed. In case of thermal treatment at 1100 °C (AC<sub>5</sub>), no significant amount of surface groups remained on the carbon. Table 6.2 shows the total amounts of CO and CO<sub>2</sub> released, obtained by integration of the areas under the TPD peaks, the ratio CO/CO<sub>2</sub> and the point of zero charge of the samples with different surface chemistries. A good correlation was found between the BET surface areas and the evolved amounts of CO and CO<sub>2</sub> in the case of texture-modified samples, as mentioned before.

**Table 6.1.** Textural data of selected activated carbons used in this study.

| Carbon           | <sup>a</sup> S <sub>BET</sub> (m <sup>2</sup> g <sup>-1</sup> ) | <sup>b</sup> V <sub>μ</sub> (cm <sup>3</sup> g <sup>-1</sup> ) | <sup>c</sup> S <sub>≠μ</sub> (m <sup>2</sup> g <sup>-1</sup> ) |
|------------------|---|--|--|
| AC <sub>0</sub>  | 1055  | 0.415  | 90   |
| AC <sub>1</sub>  | 1004  | 0.409  | 75   |
| AC <sub>5</sub>  | 977   | 0.401  | 76   |
| AC <sub>T0</sub> | 1027  | 0.417  | 71   |
| AC <sub>T1</sub> | 1097  | 0.444  | 74   |
| AC <sub>T2</sub> | 1336  | 0.534  | 113  |

<sup>a</sup>BET surface area. <sup>b</sup>Microporous volume. <sup>c</sup>Non-microporous surface area.

**Table 6.2.** Surface chemistry data of activated carbon samples.

| sample           | CO <sub>2</sub> (μmol g <sup>-1</sup> ) | CO (μmol g <sup>-1</sup> ) | CO/CO <sub>2</sub> | pH <sub>PZC</sub> |
|------------------|---|----------------------------|--------------------|-------------------|
| AC <sub>0</sub>  | 144                                     | 911                        | 6.3                | 8.3               |
| AC <sub>T0</sub> | 62                                      | 1023                       | 16.5               | n.m.              |
| AC <sub>T1</sub> | 68                                      | 1136                       | 16.7               | n.m.              |
| AC <sub>T2</sub> | 94                                      | 1448                       | 15.4               | n.m.              |
| AC <sub>1</sub>  | 628                                     | 2041                       | 3.2                | 4.5               |
| AC <sub>2</sub>  | 181                                     | 1808                       | 10.0               | 7.3               |
| AC <sub>3</sub>  | 51                                      | 1481                       | 29.0               | 7.6               |
| AC <sub>4</sub>  | 35                                      | 888                        | 25.4               | 8.1               |
| AC <sub>5</sub>  | n.d.                                    | 106                        | –                  | 8.6               |
| AC <sub>02</sub> | n.d.                                    | 498                        | –                  | n.m.              |

n.m., not measured; n.d., not detectable.

In order to determine the amount of individual surface groups, the deconvolution of the CO- and CO<sub>2</sub>-spectra was carried out for all carbon samples, according to the numerical calculations described by Figueiredo et al. (2007). A multiple gaussian function was used for fitting each of the TPD spectra, taking the position of the peak center as initial estimate (Figure 6.5). The numerical calculations were based on a non-linear routine which

minimized the square of the deviations, using the Simplex method to perform the iterations. Table 6.3 gives the deconvolution data of the main peaks obtained, where  $T_M$  is the temperature of the peak maximum and  $A$  is the integrated peak area. According to the individual peak data, only the sample AC<sub>1</sub> contains significant amount of CO<sub>2</sub>-releasing (acid and anhydride) groups on its surface, together with presenting the smallest CO:CO<sub>2</sub> ratio among all the carbon samples. The CO-emitting groups on each ACs are present in higher amounts and among them, carbonyl/quinone sites can be considered as the most significant ones.

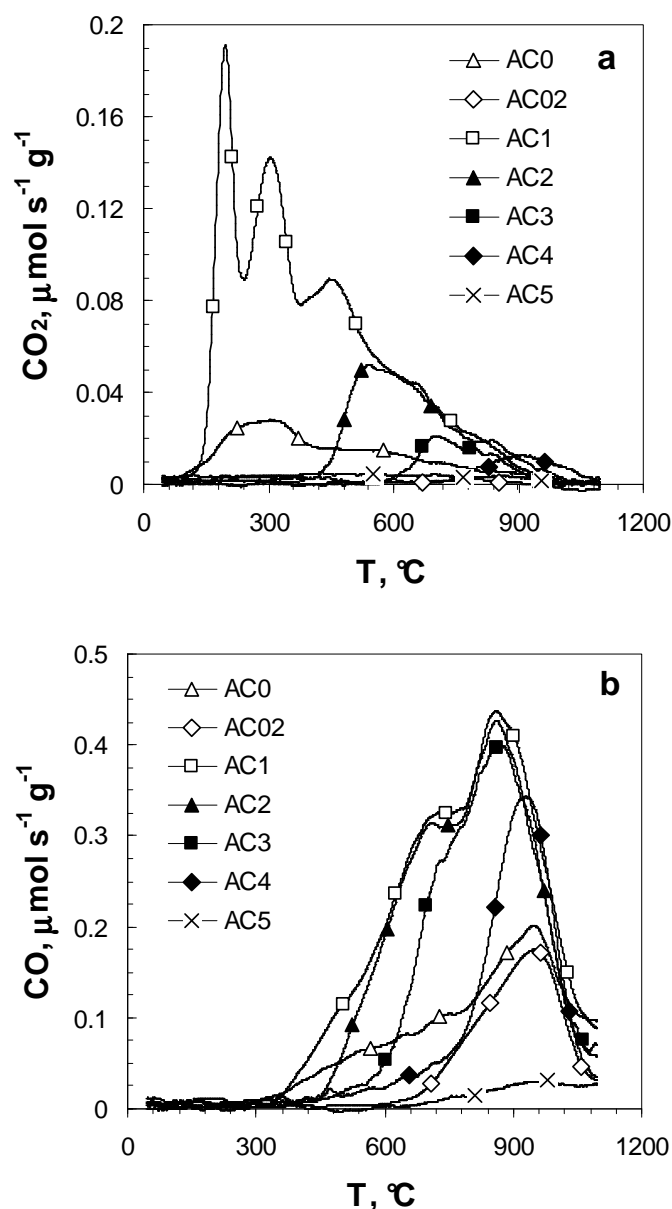


**Figure 6.4.** TPD spectra of activated carbons with different surface chemistries: (a) CO<sub>2</sub> and (b) CO evolution.

The  $\text{pH}_{\text{PZC}}$  values are consistent with the  $\text{CO}$  and  $\text{CO}_2$  evolutions (Table 6.2). The  $\text{HNO}_3$ -treatment originated a large amount of oxygen-containing surface groups having mainly acid characteristics (sample  $\text{AC}_1$ ). After thermal treatments at high temperatures ( $>700\text{ }^\circ\text{C}$ ), practically only  $\text{CO}$ -releasing groups remained on the carbon surface, which have neutral or basic properties. However, the basic characteristics associated with activated carbons submitted to thermal treatments are mainly associated with the electron-rich oxygen-free sites located on the carbon basal planes (Lewis basicity). Although  $\text{pH}_{\text{PZC}}$  is considered to have serious significance in the adsorption of dyes onto activated carbons (Faria et al., 2004), probably it is not the crucial factor in the present biological reduction process, which is rather dependent on electrochemical characteristics of the system (Mezohegyi et al., 2009).

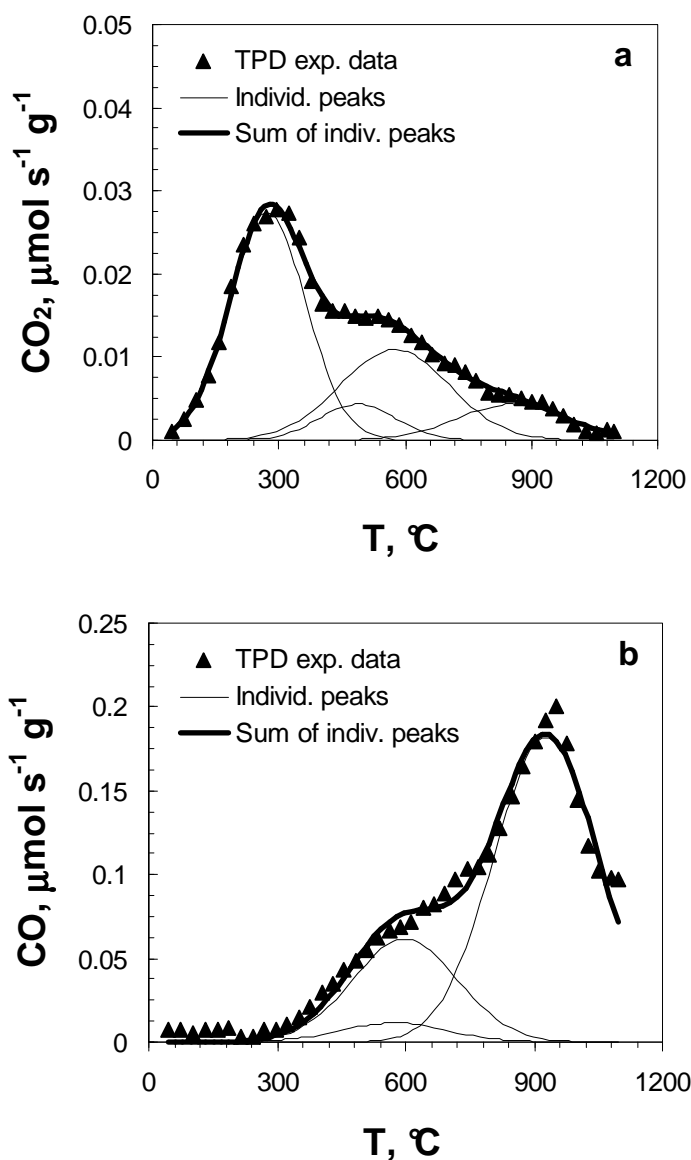


**Figure 6.5.** Deconvolution of TPD spectra: example for (a)  $\text{CO}_2$  and (b)  $\text{CO}$  evolution ( $\text{AC}_0$ ).

**Table 6.3.** Results of the deconvolution of TPD spectra.

| Sample           | Carboxylic acid |                              | Anhydride  |                              | Lactone    |                              | Phenol     |                              | Carbonyl/quinone |                              |
|------------------|-----------------|------------------------------|------------|------------------------------|------------|------------------------------|------------|------------------------------|------------------|------------------------------|
|                  | $T_M$ (°C)      | A ( $\mu\text{mol g}^{-1}$ ) | $T_M$ (°C) | A ( $\mu\text{mol g}^{-1}$ ) | $T_M$ (°C) | A ( $\mu\text{mol g}^{-1}$ ) | $T_M$ (°C) | A ( $\mu\text{mol g}^{-1}$ ) | $T_M$ (°C)       | A ( $\mu\text{mol g}^{-1}$ ) |
| AC <sub>0</sub>  | 274             | 75                           | 575        | 42                           | 853        | 17                           | 594        | 227                          | 931              | 688                          |
| AC <sub>T0</sub> | –               | –                            | 625        | 38                           | 810        | 24                           | 712        | 226                          | 874              | 735                          |
| AC <sub>T1</sub> | –               | –                            | 618        | 41                           | 809        | 27                           | 706        | 243                          | 860              | 811                          |
| AC <sub>T2</sub> | –               | –                            | 617        | 51                           | 789        | 41                           | 680        | 390                          | 856              | 945                          |
| AC <sub>1</sub>  | 299             | 211                          | 577        | 159                          | 817        | 48                           | 677        | 713                          | 890              | 1141                         |
| AC <sub>2</sub>  | –               | –                            | 575        | 128                          | 775        | 49                           | 689        | 632                          | 884              | 1019                         |
| AC <sub>3</sub>  | –               | –                            | –          | –                            | 747        | 52                           | 743        | 549                          | 898              | 886                          |
| AC <sub>4</sub>  | –               | –                            | –          | –                            | 908        | 35                           | 667        | 94                           | 923              | 780                          |
| AC <sub>5</sub>  | –               | –                            | –          | –                            | –          | –                            | 786        | 27                           | 978              | 86                           |
| AC <sub>02</sub> | –               | –                            | –          | –                            | –          | –                            | 786        | 151                          | 931              | 347                          |

## 3.2. Reduction of azo dyes

### 3.2.1. Modeling

The efficacy of the anaerobic upflow stirred packed-bed reactor with biological activated carbon system for mono- and diazo reduction was proved in an earlier study of the authors (Mezohegyi et al., 2009). The degradation model involving both heterogeneous catalysis and biological decolourisation with Michaelis–Menten-like kinetics can be given as:

$$\frac{dc_{\text{DYE}}}{\rho \cdot d\tau} = -\frac{k_1 \cdot c_{\text{DYE}}}{k_2 + c_{\text{DYE}}} \quad (1)$$

where  $c_{\text{DYE}}$  ( $\text{mmol L}^{-1}$ ) is the dye concentration,  $\tau$  ( $\text{min g}_{\text{AC}} \text{g}^{-1}$ ) is the space time,  $\rho$  ( $\text{g L}^{-1}$ ) is the density of solution, and  $k_1$  ( $\text{mmol g}_{\text{AC}}^{-1} \text{min}^{-1}$ ) and  $k_2$  ( $\text{mmol L}^{-1}$ ) are the kinetic parameters. In case of a diazo colourant (RB5H), the material balance equation for the monoazo reduction product is:

$$\frac{dc_{\text{RB5HM}}}{\rho \cdot d\tau} = \frac{k_1 \cdot c_{\text{DYE}}}{k_2 + c_{\text{DYE}}} - \frac{k_3 \cdot c_{\text{RB5HM}}}{k_4 + c_{\text{RB5HM}}} \quad (2)$$

where  $c_{\text{RB5HM}}$  ( $\text{mmol L}^{-1}$ ) is the monoazo product concentration and  $k$  values ( $k_3$ :  $\text{mmol g}_{\text{AC}}^{-1} \text{min}^{-1}$  and  $k_4$ :  $\text{mmol L}^{-1}$ ) are the referred kinetic constants. Eq. (2) can be easily solved numerically using for instance the Euler method.

### 3.2.2. Catalytic reduction by ACs with different textural properties

Figure 6.6 shows an example ( $\text{AC}_0$ ) that the kinetic models Eqs. (1) and (2) fit the experimental points of azo bioreduction well, irrespectively of the activated carbon used in the bioreactor. According to the  $k_1$  kinetic constants achieved for the carbons having different textural properties (Figure 6.7), the original sample  $\text{AC}_0$  presented the smallest decolourisation rates while  $\text{AC}_{\text{T}_2}$  with the highest surface area resulted the best azo dye removal. Although the USPBRs with each carbon appeared to be a very effective treatment system,  $\text{AC}_{\text{T}_2}$  worked extremely well: conversion values above 88% were achieved in case of both azo dyes at a  $\tau$  of 0.23 min or higher corresponding to a very short hydraulic residence time of about 0.30 min at the most (calculated from the reactor hold-up). To the author's knowledge, so far, no better removal rates of azo dyes Orange II and Reactive Black 5 have been reported in anaerobic bioreactors. The Michaelis–Menten constant ( $k_2$ ) was found to be similar in the case of both dyes reduction and of all activated carbons (0.90–0.95  $\text{mmol L}^{-1}$ ).



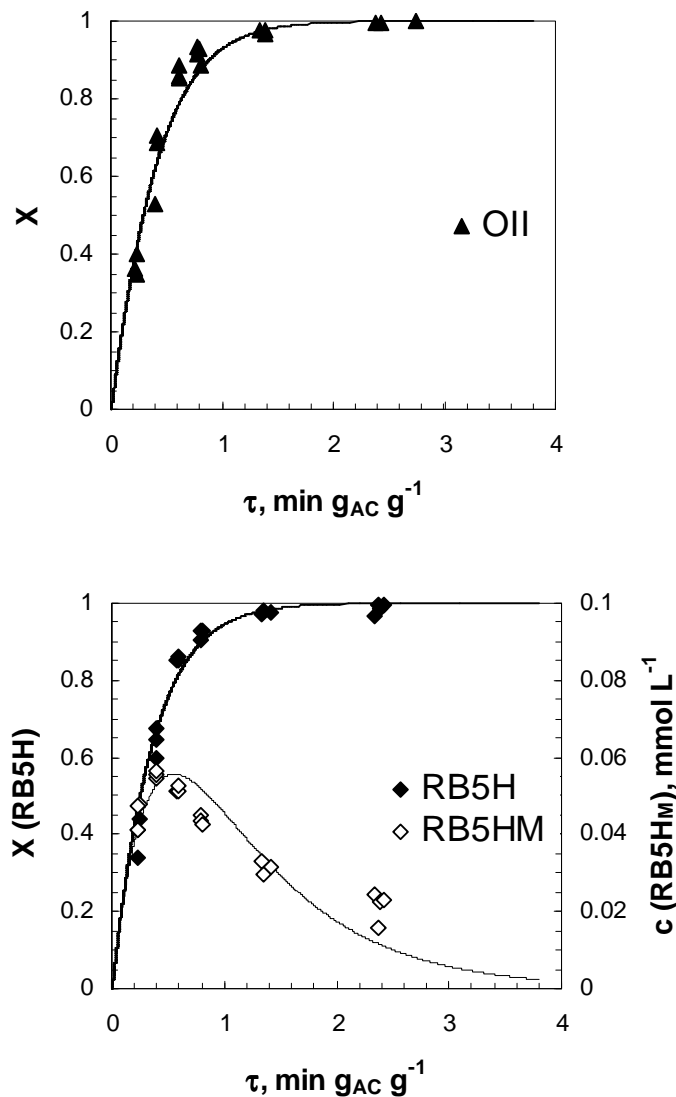


**Figure 6.6.** Example of kinetic modeling of azo anaerobic biodecolourisation in USPBR ( $\text{AC}_0$ ); lines show the model fitting to experimental points.

When plotting  $k_1$  constants against the amount of quinonic groups  $[\text{CO}_Q]$  on the referred activated carbon's surface (Figure 6.7), two important conclusions can be done. On the one hand, the dye reduction rate is proportional to the activated carbon surface area. This is evidenced when considering the data of  $\text{AC}_{\text{T}0}$ ,  $\text{AC}_{\text{T}1}$  and  $\text{AC}_{\text{T}2}$ , which have similar specific surface chemistries (referred to the  $[\text{CO}_Q]/S_{\text{BET}}$  ratios), since the amount of CO released is directly proportional to the BET surface area. On the other hand, the increase of the amount of CO-releasing groups –mostly, quinonic groups– on the activated carbon surface results higher decolourisation rates, at least, in the given range of  $[\text{CO}_Q]$ . The samples  $\text{AC}_0$  and  $\text{AC}_{\text{T}0}$  have similar textural properties with nearly the same BET surface areas. However, they slightly differ in surface chemistries and  $\text{AC}_{\text{T}0}$ , possessing a denser quinonic surface structure, gave significantly better reduction rates

than  $AC_0$  for both azo colourants. This confirms the hypothesis of quinonic catalysis in anaerobic azo dye reduction.

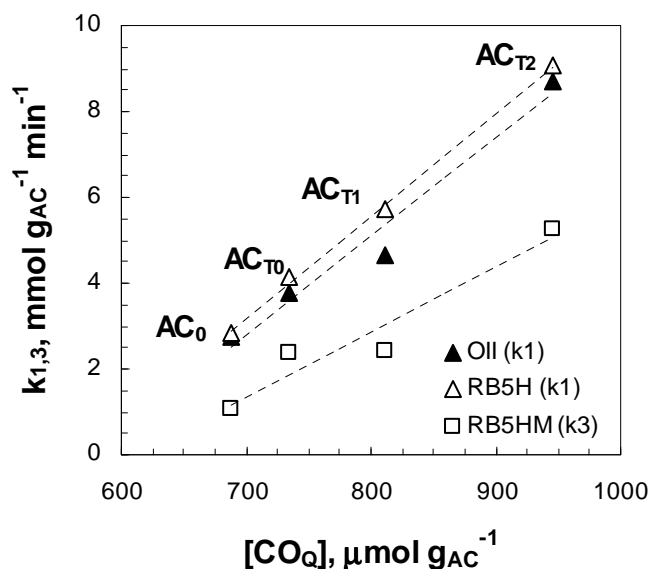


**Figure 6.7.** Correlation between catalytic azo reduction and surface quinonic densities of activated carbons with different textural properties.

### 3.2.3. Catalytic reduction by ACs with different surface chemistries

Comparing to textural modification, variation of the carbon surface groups ( $AC_1$ – $AC_5$  and  $AC_{02}$ ) seems to have less effect on dye reduction (Figure 6.8). Although different surface chemistries were obtained on  $AC_1$ ,  $AC_2$ , and  $AC_3$ , they did not present significant differences in azo dye reduction rates, probably due to their similar high carbonyl/quinonic groups surface densities (890–1140  $\mu\text{mol g}_{\text{AC}}^{-1}$ ). It is interesting to note that once the carbon surface chemistry is different, then the accessibility of the dye molecules to the pores and their interaction with the activated carbon surface are expected to be different as well, which may have a certain influence on the dye reduction. On the other hand, the decrease of quinonic groups down to smaller amounts ( $\sim 600 \mu\text{mol g}_{\text{AC}}^{-1}$ ) implied reduction of the catalytic activity of activated carbon. This means that a  $[\text{CO}_Q]$  interval exists where quinonic catalysis of azo reduction occurs. Besides the present anaerobic azo reduction process, carbonyl/quinonic groups on AC surface has also been reported as the decisive sites in different applications such as in the oxidative dehydrogenation of ethylbenzene (Pereira et al., 1999; Maciá-Agulló et al., 2005) or in electrical double layer capacitors (Bleda-Martínez et al., 2005). The  $k_2$  constants were found to be between 0.90–0.94  $\text{mmol L}^{-1}$  for all carbons.

The sample  $AC_5$  presented the highest azo dye reduction rates and this performance needs some explanation. Dye adsorption studies for the activated carbon samples

(AC<sub>1</sub>–AC<sub>5</sub>) were previously done (data not shown) and no significant difference among adsorption capacities of these ACs was found. This confirms the importance of another factor in the reduction process. The thermal treatment at 1100 °C (sample AC<sub>5</sub>) resulted only a minimal amount of carbonyl groups on the carbon surface. The density of the delocalized  $\pi$ -electrons on the graphene sheets increases upon the removal of the electronegative surface oxygen groups and hence the electrical conductivity increases (Pantea et al., 2001). Therefore AC<sub>5</sub> should have a higher conductivity than the samples AC<sub>1</sub>–AC<sub>4</sub> and AC<sub>5</sub> is probably the only sample where the  $\pi$ -electrons extensively participate in the reduction process. Considering all the activated carbon samples with different surface chemistries, their performance in dye decolourisation is probably related to two different reaction mechanisms occurring in the presence/absence of surface oxygen groups: one involves the delocalized  $\pi$ -electrons (AC<sub>5</sub> and AC<sub>02</sub>) and the other the surface quinonic functionalities (AC<sub>1</sub> to AC<sub>4</sub>). The double mechanism is better surmised when looking the reduction trend of Orange II than of the more biodegradable Reactive Black.

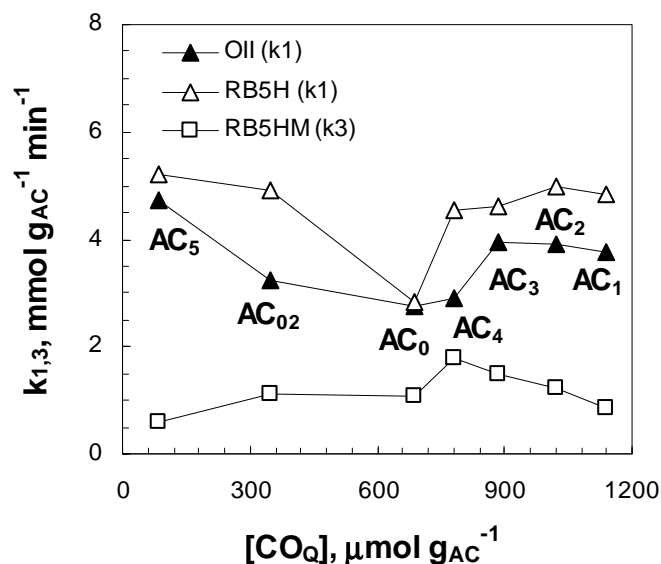


**Figure 6.8.** Correlation between catalytic azo reduction and surface quinonic densities of activated carbons with different surface chemistries.

It is interesting to mention that in case of each activated carbon, the hydrolysed reactive dye presented better biodegradability than Orange II. This result is reasonable if considering the electrochemical characteristic of these two dyes. An earlier work of the authors (Mezőhegyi et al., 2009) stated that the key factor of azo reduction was not the activated carbon high adsorption capacity for different dyes but the reduction potential value of the colourants. According to these values, the first azo bond reduction in RB5H takes place easier than the anaerobic decolourisation of the monoazo OII, irrespectively of the bioreactor system or the type of activated carbon used as a catalyst.

## 4. Conclusions

Anaerobic decolourisation of two commercially important textile azo dyes was studied in terms of activated carbon modification in upflow stirred packed-bed reactors containing biological activated carbon system. Carbons with different textural properties and various surface chemistries were prepared in order to examine their possible influence on azo dye reduction rates. Characterization of the carbon samples proved that the texturally modified ACs did not differ significantly in surface chemistries and, inversely, surface chemistry modification of ACs by acid- and thermal treatments took place with no significant textural changes. The proposed kinetic model described well the anaerobic catalytic azo reduction for all the activated carbons tested. The azo dye decolourisation rate constants were found to be proportional to the activated carbon surface area. Although variation of the AC surface chemistry seems to have less effect on dye removal rates than the textural properties, the hypothesis of catalysis by carbonyl/quinone sites in the anaerobic dye reduction process was confirmed. An other mechanism plays an important role in the catalytic decolourisation, particularly in the absence of significant densities of surface oxygen-containing groups, when not the quinonic groups but rather the delocalized  $\pi$ -electrons are involved in the reduction. Although the USPBR appears to be a very effective system for biological azo dye treatment with all the activated carbons studied, its performance can be further enhanced by appropriate tailoring of the textural and surface chemistry properties of the catalyst.



## General conclusions and future works

During the last decade, dye removal techniques were notably progressed by the involvement of AC in the operation. Most of the colour-reducing methods could be successfully combined with the beneficial properties of AC that resulted not only in a synergetic increase of decolourisation but, generally, in higher dye mineralisation rates as well. The use of AC as a catalyst in different chemical dye oxidation processes made clear that these treatments have a great potential for economically improving textile/dye wastewater technologies. On the other hand, recently, a new and promising approach have emerged for AC-amended azo dye decolourisation. The so-called advanced (bio)reduction processes (ARPs) seem very effective for colour removal and are incomparably more economic than the (advanced) oxidation treatments.

The experimental part of this thesis simultaneously focused both on the investigation of the mechanisms and crucial factors in AC-catalysed reduction of azo dyes and on the development of a high rate anaerobic reactor system in what the catalytic reaction was realised. The whole results proved that the novel continuous upflow stirred packed-bed reactor (USPBR) with the biological activated carbon (BAC) is a powerful treatment system for azo decolourisation. The reduction mechanism can be described as: (1) azo dye adsorption onto the AC surface; (2) azo bond split by electrons and  $H^+$  produced from an external carbon source by anaerobic bacteria; and (3) desorption of the generated aromatic amines from the AC surface. Apart from the basic operation parameters (e.g., feed properties, redox potential of the anaerobic environment, temperature), the most important factors strictly determining the reaction rates were the active biomass concentration in the reactor, the electrochemical characteristics of the treated colourant and the chemical and textural properties of AC.

The role of AC in the azo reduction is multiple: besides it has a high adsorption capacity for azo dyes and offers a high surface for biofilm, it acts as a redox catalyst transferring electrons from the cosubstrate (carbon source for microorganisms) to the azo linkage. Although the thesis evidenced that appropriate modification of the AC catalyst can result in dye reduction enhancement, further increase in pollutant removal may be achieved by the use of advanced carbon materials in the bioreactor, e.g., carbon

nanotubes, ordered mesoporous carbons or certain xerogels. However, the differences in the costs of these supports and in the reduction rates that they can provide, should be preliminarily analysed. Alternatively, azo dye reduction may be enhanced by impregnating the AC with appropriate (catalytic) metals but, in this case, both the microbial tolerance for these elements and their possible leaching from the AC surface have to be considered.

Although the use of AC in a biological treatment is not a recent issue, its use as a catalyst in microbial wastewater purification is a novel approach. This complex process involves both heterogeneous catalysis and biological conversion of the pollutant. As the results of the thesis showed, it is possible to establish a kinetic model to describe this type of advanced contaminant removal. Since the presence of AC in the bioreactor is more determinative than the reactor volume regarding the reduction rates, the reaction can be better described by the inclusion of space time in the kinetic model than of hydraulic residence time. The results furthermore suggested that including information about the pollutant concentration and AC properties (e.g., mass of carbon, AC surface area) in the kinetic model can significantly help to make the comparison of different bioreactor systems and/or pollutant reduction rates possible. Apart from azo dye decolourisation, the USPBR-BAC system has the potential to treat other water contaminants in different reduction processes such as dechlorination, denitrification or the reduction of nitroaromatic compounds.

The results of the thesis, in addition, propose future trends for textile azo dye production. It has to be considered that most of the colourants produced on the market should fulfil two basic requirements: on the one hand, their fixation rate during the textile dyeing process has to be high enough to avoid huge dye losses into the effluent; for instance, 10–50% of the reactive dyes end up in wastewater during the colouration of cellulose fibres (Easton, 1995); on the other hand, they should be efficiently removable from the wastewater. Considering ARPs and according to the results, the azo dyes should be manufactured with less negative reduction potentials in order to ensure their efficacious (biological) decolourisation.

It has to be noted that the biological reduction can only ensure the azo bond cleavage and is not effective in the removal of anaerobic reduction products that require further (oxidative) treatment. The application of a sequential anaerobic–aerobic process is indispensable to perform a complete removal of azo dye pollutants. Because of both the remarkable cost-efficiency of the advanced biological reduction and the oxidability of the produced aromatic amines, anaerobic decolourisation with a subsequent biological or chemical oxidation is certainly a more economic method for azo dye removal than single oxidation treatments.

## References

- Aktaş Ö, Çeçen F.** Bioregeneration of activated carbon: A review. *Int. Biodeter. Biodegr.* 2007; 59(4): 257–272.
- Al-Degs Y, Khraisheh MAM, Allen SJ, Ahmad MN.** Effect of carbon surface chemistry on the removal of reactive dyes from textile effluent. *Water Res.* 2000; 34(3): 927–935.
- Andreozzi R, Caprio V, Insola A, Marotta R.** Advanced oxidation processes (AOP) for water purification and recovery. *Catal. Today* 1999; 53(1): 51–59.
- Aranda-Tamara C, Estrada-Alvarado MI, Texier AC, Cuervo F, Gómez J, Cervantes FJ.** Effects of different quinoid redox mediators on the removal of sulphide and nitrate via denitrification. *Chemosphere* 2007; 69(11): 1722–1727.
- Banat F, Al-Bastaki N.** Treating dye wastewater by an integrated process of adsorption using activated carbon and ultrafiltration. *Desalination* 2004; 170(1): 69–75.
- Banat IM, Nigam P, Singh D, Marchant R.** Microbial decolorization of textile-dye-containing effluents: a review. *Bioresour. Technol.* 1996; 58(3): 217–227.
- Bansal RC, Goyal M.** Activated carbon adsorption. Taylor & Francis, Boca Raton FL, 2005.
- Behnajady MA, Modirshahla N, Hamzavi R.** Kinetic study on photocatalytic degradation of C.I. Acid Yellow 23 by ZnO photocatalyst. *J. Hazard. Mater.* 2006; B133(1–3): 226–232.
- Berenguer R, Marco-Lozar JP, Quijada C, Cazorla-Amorós D, Morallón E.** Effect of electrochemical treatments on the surface chemistry of activated carbon. *Carbon* 2009; 47(4): 1018–1027.
- Beydilli MI, Pavlostathis SG, Tincher WC.** Biological decolorization of the azo dye Reactive Red 2 under various oxidation-reduction conditions. *Water Environ. Res.* 2000; 72(6): 698–705.
- Bizani E, Fytianos K, Poullos I, Tsiridis V.** Photocatalytic decolorization and degradation of dye solutions and wastewaters in the presence of titanium dioxide. *J. Hazard. Mater.* 2006; 136(1): 85–94.
- Bleda-Martínez MJ, Maciá-Agulló JA, Lozano-Castelló D, Morallón E, Cazorla-Amorós D, Linares-Solano A.** Role of surface chemistry on electric double layer capacitance of carbon materials. *Carbon* 2005; 43(13): 2677–2684.
- Brás R, Ferra MIA, Pinheiro HM, Gonçalves IC.** Batch tests for assessing decolourisation of azo dyes by methanogenic and mixed cultures. *J. Biotechnol.* 2001; 89(2–3): 155–162.
- Byrappa K, Subramani AK, Ananda S, Rai KML, Sunitha MH, Basavalingu B, Soga K.** Impregnation of ZnO onto activated carbon under hydrothermal conditions and its photocatalytic properties. *J. Mater. Sci.* 2006; 41(5):1355–1362.



- Cañizares P, Gadri A, Lobato J, Nasr B, Paz R, Rodrigo MA, Saez C.** Electrochemical oxidation of azoic dyes with conductive-diamond anodes. *Ind. Eng. Chem. Res.* 2006; 45(10): 3468–3473.
- Cervantes FJ, van der Zee FP, Lettinga G, Field JA.** Enhanced decolourisation of Acid Orange 7 in a continuous UASB reactor with quinones as redox mediators. *Water Sci. Technol.* 2001; 44(4): 123–128.
- Chakraborty S, Purkait MK, DasGupta S, De S, Basu JK.** Nanofiltration of textile plant effluent for color removal and reduction in COD. *Sep. Purif. Technol.* 2003; 31(2): 141–151.
- Chandra U, Gilbert O, Swamy BEK, Bodke YD, Sherigara BS.** Electrochemical studies of Eriochrome Black T at carbon paste electrode and immobilized by SDS surfactant: A cyclic voltammetric study. *Int. J. Electrochem. Sci.* 2008; 3(9): 1044–1054.
- Choy KKH, McKay G, Porter JF.** Sorption of acid dyes from effluents using activated carbon. *Resour. Conserv. Recy.* 1999; 27(1–2): 57–71.
- Chu W.** Dye removal from textile dye wastewater using recycled alum sludge. *Water Res.* 2001; 35(13): 3147–3152.
- Chung KT, Stevens SE.** Degradation of azo dyes by environmental microorganisms and helminths. *Environ. Toxicol. Chem.* 1993; 12(11): 2121–2132.
- Cooney DO, Nagerl A, Hines AL.** Solvent regeneration of activated carbon. *Water Res.* 1983; 17(4): 403–410.
- Costa C, Márquez MC.** Kinetics of the PACT process. *Water Res.* 1998; 32(1): 107–114.
- Daneshvar N, Oladegaragoze A, Djafarzadeh N.** Decolorization of basic dye solutions by electrocoagulation: An investigation of the effect of operational parameters. *J. Hazard. Mater.* 2006; B129(1–3): 116–122.
- Delée W, O'Neill C, Hawkes FR, Pinheiro HM.** Anaerobic treatment of textile effluents: A review. *J. Chem. Technol. Biot.* 1998; 73(4): 323–335.
- Demirbas A.** Agricultural based activated carbons for the removal of dyes from aqueous solutions: A review. *J. Hazard. Mater.* 2009; 167(1–3): 1–9.
- Dos Santos AB, Bisschops IAE, Cervantes FJ, van Lier JB.** Effect of different redox mediators during thermophilic azo dye reduction by anaerobic granular sludge and comparative study between mesophilic (30 °C) and thermophilic (55 °C) treatments for decolourisation of textile wastewaters. *Chemosphere* 2004; 55(9): 1149–1157.
- Dos Santos AB, Cervantes FJ, van Lier JB.** Review paper on current technologies for decolourisation of textile wastewaters: Perspectives for anaerobic biotechnology. *Bioresour. Technol.* 2007; 98(12): 2369–2385.
- Dos Santos AB, Cervantes FJ, Yaya-Beas RE, van Lier JB.** Effect of redox mediator, AQDS, on the decolourisation of a reactive azo dye containing triazine group in a thermophilic anaerobic EGSB reactor. *Enzyme Microb. Tech.* 2003; 33(7): 942–951.
- Dos Santos AB, Traverse J, Cervantes FJ, Van Lier JB.** Enhancing the electron transfer capacity and subsequent color removal in bioreactors by applying thermophilic anaerobic treatment and redox mediators. *Biotechnol. Bioeng.* 2005; 89(1): 42–52.

- Easton JR.** The problem of colour, the dye maker's view. In: Cooper P, editor. Colour in dyehouse effluent. The Society of Dyers and Colourist, Alden Press, Oxford, 1995; p. 9–21.
- Eichlerová I, Homolka L, Lisá L, Nerud F.** Orange G and Remazol Brilliant Blue R decolorization by white rot fungi *Dichomitus squalens*, *Ischnoderma resinsum* and *Pleurotus calyprtratus*. *Chemosphere* 2005; 60(3): 398–404.
- El Qada EN, Allen SJ, Walker GM.** Adsorption of basic dyes from aqueous solution onto activated carbons. *Chem. Eng. J.* 2008; 135(3): 174–84.
- Fan HJ, Shu HY, Tajima K.** Decolorization of acid black 24 by the FeGAC/H<sub>2</sub>O<sub>2</sub> process. *J. Hazard. Mater.* 2006; B128(2–3): 192–200.
- Faria PCC, Monteiro DCM, Órfão JJM, Pereira MFR.** Cerium, manganese and cobalt oxides as catalysts for the ozonation of selected organic compounds. *Chemosphere* 2009b; 74(6): 818–824.
- Faria PCC, Órfão JJM, Pereira MFR.** Activated carbon and ceria catalysts applied to the catalytic ozonation of dyes and textile effluents. *Appl. Cat. B* 2009a; 88(3–4): 341–350.
- Faria PCC, Órfão JJM, Pereira MFR.** Adsorption of anionic and cationic dyes on activated carbons with different surface chemistries. *Water Res.* 2004; 38(8): 2043–2052.
- Faria PCC, Órfão JJM, Pereira MFR.** Mineralisation of coloured aqueous solutions by ozonation in the presence of activated carbon. *Water Res.* 2005; 39(8): 1461–1470.
- Faria PCC, Órfão JJM, Pereira MFR.** Ozone decomposition in water catalyzed by activated carbon: Influence of chemical and textural properties. *Ind. Eng. Chem. Res.* 2006; 45(8): 2715–2721.
- Field JA, Brady J.** Riboflavin as a redox mediator accelerating the reduction of the azo dye Mordant Yellow 10 by anaerobic granular sludge. *Water Sci. Technol.* 2003; 48(6): 187–193.
- Field JA, Cervantes FJ, van der Zee FP, Lettinga G.** Role of quinones in the biodegradation of priority pollutants: a review. *Water Sci. Technol.* 2000; 42(5–6): 215–222.
- Figueiredo JL, Pereira MFR.** Carbon as catalyst. In: Serp P, Figueiredo JL, editors. Carbon materials for catalysis, John Wiley and Sons, Hoboken NJ, 2009; p. 177–217.
- Figueiredo JL, Pereira MFR, Freitas MMA, Órfão JJM.** Characterization of active sites on carbon catalysts. *Ind. Eng. Chem. Res.* 2007; 46(12): 4110–4115.
- Figueiredo JL, Pereira MFR, Freitas MMA, Órfão JJM.** Modification of the surface chemistry of activated carbons. *Carbon* 1999; 37(9): 1379–1389.
- Follansbee DM, Paccione JD, Martin LL.** Globally optimal design and operation of a continuous photocatalytic advanced oxidation process featuring moving bed adsorption and draft-tube transport. *Ind. Eng. Chem. Res.* 2008; 47(10): 3591–3600.
- Food Standards Agency.** Food additives and hyperactivity. FSA 08/04/04, London, 2008.
- Forgacs E, Cserhádi T, Oros G.** Removal of synthetic dyes from wastewaters: a review. *Environ. Int.* 2004; 30(7): 953–971.

- Fortuny A, Font J, Fabregat A.** Wet air oxidation of phenol using active carbon as catalyst. *Appl. Catal. B* 1998; 19(3–4): 165–173.
- Fu Y, Viraraghavan T.** Fungal decolorization of dye wastewaters: a review. *Bioresour. Technol.* 2001; 79(3): 251–262.
- Gao Y, Liu H.** Preparation and catalytic property study of a novel kind of suspended photocatalyst of TiO<sub>2</sub>-activated carbon immobilized on silicone rubber film. *Mater. Chem. Phys.* 2005; 92(2-3): 604–608.
- Garcia J, Gomes HT, Serp P, Kalck P, Figueiredo JL, Faria JL.** Platinum catalysts supported on MWNT for catalytic wet air oxidation of nitrogen containing compounds. *Catal. Today* 2005; 102: 101–109.
- Georgi A, Kopinke FD.** Interaction of adsorption and catalytic reactions in water decontamination processes Part I. Oxidation of organic contaminants with hydrogen peroxide catalyzed by activated carbon. *Appl. Cat. B* 2005; 58(1–2): 9–18.
- Georgiou D, Hatiras J, Aivasidis A.** Microbial immobilization in a two-stage fixed-bed-reactor pilot plant for on-site anaerobic decolorization of textile wastewater. *Enzyme Microb. Tech.* 2005; 37(6): 597–605.
- Gogate PR, Pandit AB.** A review of imperative technologies for wastewater treatment I: oxidation technologies at ambient conditions. *Adv. Environ. Res.* 2004; 8(3–4): 501–551.
- Golob V, Vinder A, Simonič M.** Efficiency of the coagulation/flocculation method for the treatment of dyebath effluents. *Dyes Pigments* 2005; 67(2): 93–97.
- Gómez V, Larrechi MS, Callao MP.** Kinetic and adsorption study of acid dye removal using activated carbon. *Chemosphere* 2007; 69: 1151–1158.
- González-Gutiérrez LV, González-Alatorre G, Escamilla-Silva EM.** Proposed pathways for the reduction of a reactive azo dye in an anaerobic fixed bed reactor. *World J. Microb. Biot.* 2009; 25(3): 415–426.
- Guaratini CCI, Fogg AG, Zanoni MVB.** Studies of the voltammetric behavior and determination of diazo reactive dyes at mercury electrode. *Electroanal.* 2001; 13(18): 1535–1543.
- Guo J, Zhou J, Wang D, Tian C, Wang P, Uddin MS, Yu H.** Biocatalyst effects of immobilized anthraquinone on the anaerobic reduction of azo dyes by the salt-tolerant bacteria. *Water Res.* 2007; 41(2): 426–432.
- Guo J, Zhou J, Wang D, Xiang X, Yu H, Tian C, Song Z.** Correlation of anaerobic biodegradability and the electrochemical characteristic of azo dyes. *Biodegradation* 2006; 17(4): 341–346.
- Gupta VK, Srivastava SK, Mohan D.** Equilibrium uptake, sorption dynamics, process optimization, and column operations for the removal and recovery of malachite green from wastewater using activated carbon and activated slag. *Ind. Eng. Chem. Res.* 1997; 36(6): 2207–2218.
- Gül Ş, Özcan Ö, Erbatur O.** Ozonation of C.I. Reactive Red 194 and C.I. Reactive Yellow 145 in aqueous solution in the presence of granular activated carbon. *Dyes Pigments* 2007; 75(2): 426–431.

- Hai FI, Yamamoto K, Fukushi K.** Hybrid treatment systems for dye wastewater. *Crit. Rev. Env. Sci. Tec.* 2007; 37(4): 315–377.
- Hai FI, Yamamoto K, Nakajima F, Fukushi K.** Removal of structurally different dyes in submerged membrane fungi reactor-Biosorption/PAC-adsorption, membrane retention and biodegradation. *J. Membrane Sci.* 2008; 325(1): 395–403.
- Han Y, Quan X, Ruan X, Zhang W.** Integrated electrochemically enhanced adsorption with electrochemical regeneration for removal of acid orange 7 using activated carbon fibers. *Sep. Purif. Technol.* 2008; 59(1): 43–49.
- Hastie J, Bejan D, Teutli-León M, Bunce NJ.** Electrochemical methods for degradation of Orange II (sodium 4-(2-hydroxy-1-naphthylazo) benzenesulfonate). *Ind. Eng. Chem. Res.* 2006; 45(14): 4898–4904.
- He Z, Yang S, Ju Y, Sun C.** Microwave photocatalytic degradation of Rhodamine B using TiO<sub>2</sub> supported on activated carbon: Mechanism implication. *J. Environ. Sci.* 2009; 21(2): 268–272.
- Herrmann JM.** Heterogeneous photocatalysis: state of the art and present applications. *Top. Catal.* 2005; 34(1–4): 49–65.
- Hou Y, Qu J, Zhao X, Lei P, Wan D, Huang CP.** Electro-photocatalytic degradation of acid orange II using a novel TiO<sub>2</sub>/ACF photoanode. *Sci. Total Environ.* 2009; 407(7): 2431–2439.
- Hsueh CC, Chen BY.** Exploring effects of chemical structure on azo dye decolorization characteristics by *Pseudomonas luteola*. *J. Hazard. Mater.* 2008; 154(1–3): 703–710.
- Hu X, Lei L, Chu HP, Yue PL.** Copper/activated carbon as catalyst for organic wastewater treatment. *Carbon* 1999; 37(4): 631–637.
- Huang HH, Lu MC, Chen JN, Lee CT.** Catalytic decomposition of hydrogen peroxide and 4-chlorophenol in the presence of modified activated carbons. *Chemosphere* 2003; 51(9): 935–943.
- Ince NH, Gönenç DT.** Treatability of a textile azo dye by UV/H<sub>2</sub>O<sub>2</sub>. *Environ. Technol.* 1997; 18(2): 179–185.
- Ince NH, Hasan DA, Üstün B, Tezcanli G.** Combinative dyebath treatment with activated carbon and UV/H<sub>2</sub>O<sub>2</sub>: a case study on Everzol Black-GSP. *Water Sci. Technol.* 2002; 46(4–5): 51–58.
- Işık M, Sponza DT.** Biological treatment of acid dyeing wastewater using a sequential anaerobic/aerobic reactor system. *Enzyme Microb. Tech.* 2006; 38(7): 887–892.
- Jans U, Hoigné J.** Activated carbon and carbon black catalyzed transformation of aqueous ozone into OH-radicals. *Ozone-Sci. Eng.* 1998; 20(1): 67–90.
- Jia J, Yang J, Liao J, Wang W, Wang Z.** Treatment of dyeing wastewater with ACF electrodes. *Water Res.* 1999; 33(3): 881–884.
- Jirankova H, Cakl J, Markvartova O, Dolecek P.** Combined membrane process at wastewater treatment. *Sep. Purif. Technol.* 2007; 58(2): 299–303.
- Kalyuzhnyi S, Sklyar V.** Biomineralisation of azo dye and their breakdown products in anaerobic-aerobic hybrid and UASB reactors. *Water Sci. Technol.* 2000; 41(12): 23–30.

- Kannan N, Sundaram MM.** Kinetics and mechanism of removal of methylene blue by adsorption on various carbons - a comparative study. *Dyes Pigments* 2001; 51(1): 25–40.
- Kapdan IK, Tekol M, Sengul F.** Decolorization of simulated textile wastewater in an anaerobic-aerobic sequential treatment system. *Process Biochem.* 2003; 38(7): 1031–1037.
- Kasprzyk-Hordern B, Ziólek M, Nawrocki J.** Catalytic ozonation and methods of enhancing molecular ozone reactions in water treatment. *Appl. Catal. B* 2003; 46(4): 639–669.
- Kavitha D, Namasivayam C.** Experimental and kinetic studies on methylene blue adsorption by coir pith carbon. *Bioresour. Technol.* 2007; 98(1): 14–21.
- Keck A, Klein J, Kudlich M, Stolz A, Knackmuss HJ, Mattes R.** Reduction of azo dyes by redox mediators originating in the naphthalenesulfonic acid degradation pathway of *Sphingomonas* sp. strain BN6. *Appl. Environ. Microb.* 1997; 63(9): 3684–3690.
- Kim TH, Park C, Yang J, Kim S.** Comparison of disperse and reactive dye removals by chemical coagulation and Fenton oxidation. *J. Hazard. Mater.* 2004; B112(1–2): 95–103.
- Kimura M, Miyamoto I.** Discovery of the activated-carbon radical  $AC^+$  and the novel oxidation-reactions comprising the  $AC/AC^+$  cycle as a catalyst in an aqueous-solution. *Bull. Chem. Soc. Jpn.* 1994; 67(9): 2357–2360.
- Knackmuss HJ.** Basic knowledge and perspectives of bioelimination of xenobiotic compounds. *J. Biotechnol.* 1996; 51(3): 287–295.
- Konstantinou IK, Albanis TA.**  $TiO_2$ -assisted photocatalytic degradation of azo dyes in aqueous solution: kinetic and mechanistic investigations - A review. *Appl. Catal. B* 2004; 49(1): 1–14.
- Koparal AS, Yavuz Y, Ögütveren ÜB.** Electroadsorption of acilan blau dye from textile effluents by using activated carbon-perlite mixtures. *Water Environ. Res.* 2002; 74(6): 521–525.
- Kuai L, De Vreese I, Vandevivere P, Verstraete W.** GAC-amended UASB reactor for the stable treatment of toxic textile wastewater. *Environ. Technol.* 1998; 19(11): 1111–1117.
- Kuo WG.** Decolorizing dye wastewater with Fenton's reagent. *Water Res.* 1992; 26(7): 881–886.
- Lachheb H, Puzenat E, Houas A, Ksibi M, Elaloui E, Guillard C, Herrmann JM.** Photocatalytic degradation of various types of dyes (Alizarin S, Crocein Orange G, Methyl Red, Congo Red, Methylene Blue) in water by UV-irradiated titania. *Appl. Catal. B* 2002; 39(1): 75–90.
- Lee JW, Choi SP, Thiruvengatchari R, Shim WG, Moon H.** Evaluation of the performance of adsorption and coagulation processes for the maximum removal of reactive dyes. *Dyes Pigments* 2006a; 69(3): 196–203.
- Lee JW, Choi SP, Thiruvengatchari R, Shim WG, Moon H.** Submerged microfiltration membrane coupled with alum coagulation/powdered activated carbon adsorption for complete decolorization of reactive dyes. *Water Res.* 2006b; 40(3): 435–444.

- Legube B, Leitner NKV.** Catalytic ozonation: a promising advanced oxidation technology for water treatment. *Catal. Today* 1999; 53(1): 61–72.
- Levec J, Pintar A.** Catalytic wet-air oxidation processes: A review. *Catal. Today* 2007; 124(3–4): 172–184.
- Li JG, Lalman JA, Biswas N.** Biodegradation of Red B dye by *Bacillus* sp. OY1-2. *Environ. Technol.* 2004; 25(10): 1167–1176.
- Lin SH, Chen ML.** Treatment of textile wastewater by chemical methods for reuse. *Water Res.* 1997; 31(4): 868–876.
- Lin SH, Lai CL.** Catalytic oxidation of dye wastewater by metal oxide catalyst and granular activated carbon. *Environ. Int.* 1999; 25(4): 497–504.
- Lin SH, Lai CL.** Kinetic characteristics of textile wastewater ozonation in fluidized and fixed activated carbon beds. *Water Res.* 2000; 34(3): 763–772.
- Lin SH, Lin CM.** Treatment of textile waste effluents by ozonation and chemical coagulation. *Water Res.* 1993; 27(12): 1743–1748.
- Lin YH, Leu JY.** Kinetics of reactive azo-dye decolorization by *Pseudomonas luteola* in a biological activated carbon process. *Biochem. Eng. J.* 2008; 39(3): 457–467.
- Ling SH, Peng CF.** Treatment of textile wastewater by electrochemical method. *Water Res.* 1994; 28(2): 277–282.
- Liu H, Li G, Qu J, Liu H.** Degradation of azo dye Acid Orange 7 in water by Fe<sub>0</sub>/granular activated carbon system in the presence of ultrasound. *J. Hazard. Mater.* 2007; 144(1–2): 180–186.
- Lorenc-Grabowska E, Gryglewicz G.** Adsorption characteristics of Congo Red on coal-based mesoporous activated carbon. *Dyes Pigments* 2007; 74(1): 34–40.
- Lourenço ND, Novais JM, Pinheiro HM.** Effect of some operational parameters on textile dye biodegradation in a sequential batch reactor. *J. Biotechnol.* 2001; 89(2–3): 163–174.
- Lücking F, Köser H, Jank M, Ritter A.** Iron powder, graphite and activated carbon as catalysts for the oxidation of 4-chlorophenol with hydrogen peroxide in aqueous solution. *Water Res.* 1998; 32(9): 2607–2614.
- Macedo JS, da Costa NB, Almeida LE, Vieira EFS, Cestari AR, Gimenez IF, Carreño NLV, Barreto LS.** Kinetic and calorimetric study of the adsorption of dyes on mesoporous activated carbon prepared from coconut coir dust. *J. Colloid Interf. Sci.* 2006; 298(2): 515–522.
- Maciá-Agulló JA, Cazorla-Amorós D, Linares-Solano A, Wild U, Su DS, Schlögl R.** Oxygen functional groups involved in the styrene production reaction detected by quasi in situ XPS. *Catal. Today* 2005; 102–103: 248–253.
- Malik PK.** Use of activated carbons prepared from sawdust and rice-husk for adsorption of acid dyes: a case study of Acid Yellow 36. *Dyes Pigments* 2003; 56(3): 239–249.
- Mall ID, Srivastava VC, Agarwal NK, Mishra IM.** Removal of congo red from aqueous solution by bagasse fly ash and activated carbon: Kinetic study and equilibrium isotherm analyses. *Chemosphere* 2005; 61(4): 492–501.

- Manu B, Chaudhari S.** Anaerobic decolorisation of simulated textile wastewater containing azo dyes. *Bioresour. Technol.* 2002; 82(3): 225–231.
- Manu B, Chaudhari S.** Decolorization of indigo and azo dyes in semicontinuous reactors with long hydraulic retention time. *Process Biochem.* 2003; 38(8): 1213–1221.
- Marcucci M, Nosenzo G, Capannelli G, Ciabatti I, Corrieri D, Ciardelli G.** Treatment and reuse of textile effluents based on new ultrafiltration and other membrane technologies. *Desalination* 2001; 138(1–3): 75–82.
- Márquez MC, Costa C.** Biomass concentration in PACT process. *Water Res.* 1996; 30(9): 2079–2085.
- Méndez-Paz D, Omil F, Lema JM.** Anaerobic treatment of azo dye Acid Orange 7 under batch conditions. *Enzyme Microb. Tech.* 2005a; 36(2–3): 264–272.
- Méndez-Paz D, Omil F, Lema JM.** Anaerobic treatment of azo dye Acid Orange 7 under fed-batch and continuous conditions. *Water Res.* 2005b; 39(5): 771–778.
- Méndez-Paz D, Omil F, Lema JM.** Modeling of the Acid Orange 7 anaerobic biodegradation. *Water Sci. Technol.* 2003; 48(6): 133–139.
- Mezohegyi G, Bengoa C, Stuber F, Font J, Fabregat A, Fortuny A.** Novel bioreactor design for decolourisation of azo dye effluents. *Chem. Eng. J.* 2008; 143(1–3): 293–298.
- Mezohegyi G, Fabregat A, Font J, Bengoa C, Stuber F, Fortuny A.** Advanced bioreduction of commercially important azo dyes: Modeling and correlation with electrochemical characteristics. *Ind. Eng. Chem. Res.* 2009; 48(15): 7054–7059.
- Mezohegyi G, Gonçalves F, Órfão JJM, Fabregat A, Fortuny A, Font J, Bengoa C, Stuber F.** Tailored activated carbons as catalysts in biodecolourisation of textile azo dyes. *Appl. Cat. B* 2010; 94: 179–185.
- Mezohegyi G, Kolodkin A, Castro UI, Bengoa C, Stuber F, Font J, Fabregat A, Fortuny A.** Effective anaerobic decolorization of azo dye Acid Orange 7 in continuous upflow packed-bed reactor using biological activated carbon system. *Ind. Eng. Chem. Res.* 2007; 46(21): 6788–6792.
- Mui ELK, Ko DCK, McKay G.** Production of active carbons from waste tyres - a review. *Carbon* 2004; 42(14): 2789–2805.
- Namasivayam C, Kavitha D.** Removal of Congo Red from water by adsorption onto activated carbon prepared from coir pith, an agricultural solid waste. *Dyes Pigments* 2002; 54(1): 47–58.
- Nigam P, Banat IM, Singh D, Marchant R.** Microbial process for the decolorization of textile effluent containing azo, diazo and reactive dyes. *Process Biochem.* 1996; 31(5): 435–442.
- Oguz E, Keskinler B.** Removal of colour and COD from synthetic textile wastewaters using O<sub>3</sub>, PAC, H<sub>2</sub>O<sub>2</sub> and HCO<sub>3</sub><sup>-</sup>. *J. Hazard. Mater.* 2008; 151(2–3): 753–760.
- Oguz E, Keskinler B, Çelik C, Çelik Z.** Determination of the optimum conditions in the removal of Bomaplex Red CR-L dye from the textile wastewater using O<sub>3</sub>, H<sub>2</sub>O<sub>2</sub>, HCO<sub>3</sub><sup>-</sup> and PAC. *J. Hazard. Mater.* 2006; B131(1–3): 66–72.

- Oliveira DP, Carneiro PA, Sakagami MK, Zanoni MVB, Umbuzeiro GA.** Chemical characterization of a dye processing plant effluent - Identification of the mutagenic components. *Mutat. Res.* 2007; 626(1–2): 135–142.
- O'Neill C, Hawkes FR, Hawkes DL, Esteves S, Wilcox SJ.** Anaerobic-aerobic biotreatment of simulated textile effluent containing varied ratios of starch and azo dye. *Water Res.* 2000b; 34(8): 2355–2361.
- O'Neill C, Lopez A, Esteves S, Hawkes FR, Hawkes DL, Wilcox S.** Azo-dye degradation in an anaerobic-aerobic treatment system operating on simulated textile effluent. *Appl. Microbiol. Biot.* 2000a; 53(2): 249–254.
- Ong SA, Toorisaka E, Hirata M, Hano T.** Combination of adsorption and biodegradation processes for textile effluent treatment using a granular activated carbon-biofilm configured packed column system. *J. Environ. Sci.* 2008a; 20(8): 952–956.
- Ong SA, Toorisaka E, Hirata M, Hano T.** Granular activated carbon-biofilm configured sequencing batch reactor treatment of C.I. Acid Orange 7. *Dyes Pigments* 2008b; 76: 142–146.
- Ong SA, Toorisaka E, Hirata M, Hano T.** Treatment of azo dye Orange II in a sequential anaerobic and aerobic-sequencing batch reactor system. *Environ. Chem. Lett.* 2005a; 2(4): 203–207.
- Ong SA, Toorisaka E, Hirata M, Hano T.** Treatment of azo dye Orange II in aerobic and anaerobic-SBR systems. *Process Biochem.* 2005b; 40(8): 2907–2914.
- Órfão JJM, Silva AIM, Pereira JCV, Barata SA, Fonseca IM, Faria PCC, Pereira MFR.** Adsorption of a reactive dye on chemically modified activated carbons - Influence of pH. *J. Colloid Interf. Sci.* 2006; 296(2): 480–489.
- Pantea D, Darmstadt H, Kaliaguine S, Sümmchen L, Roy C.** Electrical conductivity of thermal carbon blacks - Influence of surface chemistry. *Carbon* 2001; 39(8): 1147–1158.
- Papić S, Koprivanac N, Božić AL, Meteš A.** Removal of some reactive dyes from synthetic wastewater by combined Al(III) coagulation/carbon adsorption process. *Dyes Pigments* 2004; 62(3): 291–298.
- Park H, Choo KH, Lee CH.** Flux enhancement with powdered activated carbon addition in the membrane anaerobic bioreactor. *Sep. Sci. Technol.* 1999; 34(14): 2781–2792.
- Park IS, Choi SY, Ha JS.** High-performance titanium dioxide photocatalyst on ordered mesoporous carbon support. *Chem. Phys. Lett.* 2008; 456(4–6): 198–201.
- Pasukphun N, Vinitnantharat S.** Degradation of organic substances and reactive dye in an immobilized-cell sequencing batch reactor operation on simulated textile wastewater. *J. Environ. Sci. Heal. A* 2003; 38(10): 2019–2028.
- Pearce CI, Lloyd JR, Guthrie JT.** The removal of colour from textile wastewater using whole bacterial cells: a review. *Dyes Pigments* 2003; 58(3): 179–196.
- Pereira MFR, Órfão JJM, Figueiredo JL.** Influence of the textural properties of an activated carbon catalyst on the oxidative dehydrogenation of ethylbenzene. *Colloid Surface A* 2004; 241(1–3): 165–171.



- Pereira MFR, Órfão JJM, Figueiredo JL.** Oxidative dehydrogenation of ethylbenzene on activated carbon catalysts. I. Influence of surface chemical groups. *Appl. Catal. A* 1999; 184: 153–160.
- Pereira MFR, Soares SF, Órfão JJM, Figueiredo JL.** Adsorption of dyes on activated carbons: influence of surface chemical groups. *Carbon* 2003; 41(4): 811–821.
- Prado MA; Godoy HT.** Validation of the methodology to determine synthetic dyes in foods and beverages by HPLC. *J. Liq. Chromatogr. R. T.* 2002; 25(16): 2455–2472.
- Purkait MK, DasGupta S, De S.** Adsorption of eosin dye on activated carbon and its surfactant based desorption. *J. Environ. Manage.* 2005; 76(2): 135–142.
- Purkait MK, Maiti A, Dasgupta S, De S.** Removal of congo red using activated carbon and its regeneration. *J. Hazard. Mater.* 2007; 145(1–2): 287–295.
- Qu GZ, Li J, Wu Y, Li GF, Li D.** Regeneration of acid orange 7-exhausted granular activated carbon with dielectric barrier discharge plasma. *Chem. Eng. J.* 2009; 146(2): 168–173.
- Quan X, Liu X, Bo L, Chen S, Zhao Y, Cui X.** Regeneration of acid orange 7-exhausted granular activated carbons with microwave irradiation. *Water Res.* 2004; 38(20): 4484–4490.
- Radovic LR, Rodríguez-Reinoso F.** Carbon materials in catalysis. In: Thrower PA, editor. *Chemistry and physics of carbon*, vol. 25, Dekker, New York, 1997; p. 243–358.
- Rajaguru P, Kalaiselvi K, Palanivel M, Subburam V.** Biodegradation of azo dyes in a sequential anaerobic-aerobic system. *Appl. Microbiol. Biot.* 2000; 54(2): 268–273.
- Ramirez JH, Maldonado-Hódar FJ, Pérez-Cadenas AF, Moreno-Castilla C, Costa CA, Madeira LM.** Azo-dye Orange II degradation by heterogeneous Fenton-like reaction using carbon-Fe catalysts. *Appl. Catal. B* 2007; 75: 312–323.
- Rau J, Knackmuss HJ, Stolz A.** Effects of different quinoid redox mediators on the anaerobic reduction of azo dyes by bacteria. *Environ. Sci. Technol.* 2002; 36(7): 1497–1504.
- Rivera-Utrilla J, Sánchez-Polo M.** Ozonation of 1,3,6-naphthalenetrisulphonic acid catalysed by activated carbon in aqueous phase. *Appl. Catal. B* 2002; 39(4): 319–329.
- Robinson T, McMullan G, Marchant R, Nigam P.** Remediation of dyes in textile effluent: a critical review on current treatment technologies with a proposed alternative. *Bioresour. Technol.* 2001; 77(3): 247–255.
- Rodríguez A, García J, Ovejero G, Mestanza M.** Wet air and catalytic wet air oxidation of several azodyes from wastewaters: the beneficial role of catalysis. *Water Sci. Technol.* 2009; 60(8): 1989–1999.
- Rodríguez A, Ovejero G, Romero MD, Díaz C, Barreiro M, García J.** Catalytic wet air oxidation of textile industrial wastewater using metal supported on carbon nanofibers. *J. Supercrit. Fluid.* 2008; 46(2): 163–172.
- Rodríguez-Reinoso F.** The role of carbon materials in heterogeneous catalysis. *Carbon* 1998; 36(3): 159–75.
- Rodríguez-Reinoso F, Martín-Martínez JM, Prado-Burguete C, McEnaney B.** A standard adsorption-isotherm for the characterization of activated carbons. *J. Phys. Chem.* 1987; 91(3): 515–516.

- Salvador F, Jiménez CS.** Effect of regeneration treatment with liquid water at high pressure and temperature on the characteristics of three commercial activated carbons. *Carbon* 1999; 37(4): 577–583.
- Sánchez-Polo M, von Gunten U, Rivera-Utrilla J.** Efficiency of activated carbon to transform ozone into ·OH radicals: Influence of operational parameters. *Water Res.* 2005; 39(14): 3189–3198.
- Sanghi R, Bhattacharya B.** Adsorption-coagulation for the decolorisation of textile dye solutions. *Water Qual. Res. J. Can.* 2003; 38(3): 553–562.
- Santiago M, Stüber F, Fortuny A, Fabregat A, Font J.** Modified activated carbons for catalytic wet air oxidation of phenol. *Carbon* 2005; 43(10): 2134–2145.
- Santos A, Yustos P, Rodríguez S, Garcia-Ochoa F, Gracia M.** Decolorization of textile dyes by wet oxidation using activated carbon as catalyst. *Ind. Eng. Chem. Res.* 2007; 46(8): 2423–2427.
- Santos VP, Pereira MFR, Faria PCC, Órfão JJM.** Decolourisation of dye solutions by oxidation with H<sub>2</sub>O<sub>2</sub> in the presence of modified activated carbons. *J. Hazard. Mater.* 2009; 162(2–3): 736–742.
- Scholz M, Martin RJ.** Ecological equilibrium on biological activated carbon. *Water Res.* 1997; 31(12): 2959–2968.
- Serp P, Corrias M, Kalck P.** Carbon nanotubes and nanofibers in catalysis. *Appl. Catal. A* 2003; 253(2): 337–358.
- Shaul GM, Barnett MW, Neiheisel TW, Dostal KA.** Activated sludge with powdered activated carbon treatment of a dyes and pigments processing wastewater. US Environmental Protection Agency EPA-600/D-83-049, Cincinnati, Ohio, 1983.
- Shen Z, Wang W, Jia J, Ye J, Feng X, Peng A.** Degradation of dye solution by an activated carbon fiber electrode electrolysis system. *J. Hazard. Mater.* 2001; B84(1): 107–116.
- Shende RV, Mahajani VV.** Wet oxidative regeneration of activated carbon loaded with reactive dye. *Waste Manage.* 2002; 22(1): 73–83.
- Shi J, Zheng J, Wu P, Ji X.** Immobilization of TiO<sub>2</sub> films on activated carbon fiber and their photocatalytic degradation properties for dye compounds with different molecular size. *Catal. Commun.* 2008; 9(9): 1846–1850.
- Shu HY, Huang CR, Chang MC.** Decolorization of mono-azo dyes in wastewater by advanced oxidation process: a case study of Acid Red 1 and Acid Yellow 23. *Chemosphere* 1994; 29(12): 2597–2607.
- Shueh CL, Huang YH, Wang CC, Chen CY.** Degradation of azo dyes using low iron concentration of Fenton and Fenton-like system. *Chemosphere* 2005; 58(10): 1409–1414.
- Silva CG, Faria JL.** Photochemical and photocatalytic degradation of an azo dye in aqueous solution by UV irradiation. *J. Photoch. Photobio. A* 2003; 155(1–3): 133–143.
- Silva CG, Wang W, Faria JL.** Photocatalytic and photochemical degradation of mono-, di- and tri-azo dyes in aqueous solution under UV irradiation. *J. Photoch. Photobio. A* 2006; 181(2–3): 314–324.

- Sirianuntapiboon S, Sadahiro O, Salee P.** Some properties of a granular activated carbon-sequencing batch reactor (GAC-SBR) system for treatment of textile wastewater containing direct dyes. *J. Environ. Manage.* 2007; 85(1): 162–170.
- Sirianuntapiboon S, Sansak J.** Treatability studies with granular activated carbon (GAC) and sequencing batch reactor (SBR) system for textile wastewater containing direct dyes. *J. Hazard. Mater.* 2008; 159(2–3): 404–411.
- Sirianuntapiboon S, Srisornsak P.** Removal of disperse dyes from textile wastewater using bio-sludge. *Bioresour. Technol.* 2007; 98(5): 1057–1066.
- Slokar YM, Le Marechal AM.** Methods of decoloration of textile wastewaters. *Dyes Pigments* 1998; 37(4): 335–356.
- Soares OSGP, Faria PCC, Órfão JJM, Pereira MFR.** Ozonation of textile effluents and dye solutions in the presence of activated carbon under continuous operation. *Sep. Sci. Technol.* 2007; 42(7): 1477–1492.
- Sobana N, Swaminathan M.** Combination effect of ZnO and activated carbon for solar assisted photocatalytic degradation of Direct Blue 53. *Sol. Energ. Mat. Sol. C* 2007; 91(8): 727–734.
- Solozhenko EG, Soboleva NM, Goncharuk VV.** Decolourization of azodye solutions by Fenton's oxidation. *Water Res.* 1995; 29(9): 2206–2210.
- Specchia V, Gianetto A.** Powdered activated carbon in an activated sludge treatment plant. *Water Res.* 1984; 18(2): 133–137.
- Sponza DT, Işik M.** Decolorization and azo dye degradation by anaerobic/aerobic sequential process. *Enzyme Microb. Tech.* 2002; 31(1–2): 102–110.
- Stolz A.** Basic and applied aspects in the microbial degradation of azo dyes. *Appl. Microbiol. Biot.* 2001; 56(1–2): 69–80.
- Stüber F, Font J, Fortuny A, Bengoa C, Eftaxias A, Fabregat A.** Carbon materials and catalytic wet air oxidation of organic pollutants in wastewater. *Top. Catal.* 2005; 33(1–4): 3–50.
- Suarez-Ojeda ME, Stüber F, Fortuny A, Fabregat A, Carrera J, Font J.** Catalytic wet air oxidation of substituted phenols using activated carbon as catalyst. *Appl. Catal. B* 2005; 58(1–2): 105–114.
- Subramani AK, Byrappa K, Ananda S, Rai KML, Ranganathaiah C, Yoshimura M.** Photocatalytic degradation of indigo carmine dye using TiO<sub>2</sub> impregnated activated carbon. *Bull. Mater. Sci.* 2007; 30(1): 37–41.
- Sun JH, Wang YK, Sun RX, Dong SY.** Photodegradation of azo dye Congo Red from aqueous solution by the WO<sub>3</sub>-TiO<sub>2</sub>/activated carbon (AC) photocatalyst under the UV irradiation. *Mater. Chem. Phys.* 2009; 115(1): 303–308.
- Supaka N, Juntongjin K, Damronglerd S, Delia ML, Strehaiano P.** Microbial decolorization of reactive azo dyes in a sequential anaerobic-aerobic system. *Chem. Eng. J.* 2004; 99(2): 169–176.
- Suzuki T, Timofei S, Kurunczi L, Dietze U, Schüürmann G.** Correlation of aerobic biodegradability of sulfonated azo dyes with the chemical structure. *Chemosphere* 2001; 45(1): 1–9.

- Tamai H, Yoshida T, Sasaki M, Yasuda H.** Dye adsorption on mesoporous activated carbon fiber obtained from pitch containing yttrium complex. *Carbon* 1999; 37(6): 983–989.
- Tanaka K, Padermpole K, Hisanaga T.** Photocatalytic degradation of commercial azo dyes. *Water Res.* 2000; 34(1): 327–333.
- Van der Zee FP, Bisschops IAE, Lettinga G, Field JA.** Activated carbon as an electron acceptor and redox mediator during the anaerobic biotransformation of azo dyes. *Environ. Sci. Technol.* 2003; 37(2): 402–408.
- Van der Zee FP, Bouwman RHM, Strik DPBTB, Lettinga G, Field JA.** Application of redox mediators to accelerate the transformation of reactive azo dyes in anaerobic bioreactors. *Biotechnol. Bioeng.* 2001; 75(6): 691–701.
- Van der Zee FP, Cervantes FJ.** Impact and application of electron shuttles on the redox (bio)transformation of contaminants: A review. *Biotechnol. Adv.* 2009; 27(3): 256–277.
- Van der Zee FP, Lettinga G, Field JA.** The role of (auto)catalysis in the mechanism of an anaerobic azo reduction. *Water Sci. Technol.* 2000; 42(5–6): 301–308.
- Van der Zee FP, Villaverde S.** Combined anaerobic-aerobic treatment of azo dyes - A short review of bioreactor studies. *Water Res.* 2005; 39(8): 1425–1440.
- Vandevivere PC, Bianchi R, Verstraete W.** Treatment and reuse of wastewater from the textile wet-processing industry: Review of emerging technologies. *J. Chem. Technol. Biot.* 1998; 72(4): 289–302.
- Vlyssides AG, Loizidou M, Karlis PK, Zorpas AA, Papaioannou D.** Electrochemical oxidation of a textile dye wastewater using a Pt/Ti electrode. *J. Hazard. Mater.* 1999; B70(1–2): 41–52.
- Walker GM, Weatherley LR.** A simplified predictive model for biologically activated carbon fixed beds. *Process Biochem.* 1997; 32(4): 327–335.
- Walker GM, Weatherley LR.** Biological activated carbon treatment of industrial wastewater in stirred tank reactors. *Chem. Eng. J.* 1999b; 75(3): 201–206.
- Walker GM, Weatherley LR.** Kinetics of acid dye adsorption on GAC. *Water Res.* 1999a; 33(8): 1895–1899.
- Wang A, Qu J, Liu H, Ru J.** Mineralization of an azo dye Acid Red 14 by photoelectro-Fenton process using an activated carbon fiber cathode. *Appl. Catal. B* 2008; 84(3–4): 393–399.
- Wang A, Qu J, Ru J, Liu H, Ge J.** Mineralization of an azo dye Acid Red 14 by electro-Fenton's reagent using an activated carbon fiber cathode. *Dyes Pigments* 2005; 65(3): 227–233.
- Wang S, Zhu ZH.** Effects of acidic treatment of activated carbons on dye adsorption. *Dyes Pigments* 2007; 75(2): 306–314.
- Wang S, Zhu ZH, Coomes A, Haghseresht AF, Lu GQ.** The physical and surface chemical characteristics of activated carbons and the adsorption of methylene blue from wastewater. *J. Colloid Interf. Sci.* 2005; 284(2): 440–446.
- Wang X, Cheng X, Sun D.** Autocatalysis in Reactive Black 5 biodecolorization by *Rhodospseudomonas palustris* W1. *Appl. Microb. Biot.* 2008; 80(5): 907–915.

- Wang W, Silva CG, Faria JL.** Photocatalytic degradation of Chromotrope 2R using nanocrystalline TiO<sub>2</sub>/activated-carbon composite catalysts. *Appl. Cat. B* 2007; 70(1–4): 470–478.
- Weisburger JH.** Comments on the history and importance of aromatic and heterocyclic amines in public health. *Mutat. Res.* 2002; 506: 9–20.
- Xiong Y, Strunk PJ, Xia H, Zhu X, Karlsson HT.** Treatment of dye wastewater containing acid orange II using a cell with three-phase three-dimensional electrode. *Water Res.* 2001; 35(17): 4226–4230.
- Xu L, Zhao H, Shi S, Zhang G, Ni J.** Electrolytic treatment of C.I. Acid Orange 7 in aqueous solution using a three-dimensional electrode reactor. *Dyes Pigments* 2008; 77(1): 158–164.
- Xu Y, Lebrun RE, Gallo PJ, Blond P.** Treatment of textile dye plant effluent by nanofiltration membrane. *Sep. Sci. Technol.* 1999; 34(13): 2501–2519.
- Yang S, Wang P, Yang X, Wei G, Zhang W, Shan L.** A novel advanced oxidation process to degrade organic pollutants in wastewater: Microwave-activated persulfate oxidation. *J. Environ. Sci.* 2009; 21(9): 1175–1180.
- Yi F, Chen S.** Electrochemical treatment of alizarin red S dye wastewater using an activated carbon fiber as anode material. *J. Porous Mat.* 2008; 15(5): 565–569.
- Yi F, Chen S, Yuan C.** Effect of activated carbon fiber anode structure and electrolysis conditions on electrochemical degradation of dye wastewater. *J. Hazard. Mater.* 2008; 157(1): 79–87.
- Yin CY, Aroua MK, Daud WMAW.** Review of modifications of activated carbon for enhancing contaminant uptakes from aqueous solutions. *Sep. Purif. Technol.* 2007; 52(3): 403–415.
- Yu Y, Yu JC, Chan CY, Che YK, Zhao JC, Ding L, Ge WK, Wong PK.** Enhancement of adsorption and photocatalytic activity of TiO<sub>2</sub> by using carbon nanotubes for the treatment of azo dye. *Appl. Cat. B* 2005; 61(1–2): 1–11.
- Yuan X, Zhuo SP, Xing W, Cui HY, Dai XD, Liu XM, Yan ZF.** Aqueous dye adsorption on ordered mesoporous carbons. *J. Colloid Interf. Sci.* 2007; 310(1): 83–89.
- Zhang F, Yu J.** Decolourisation of Acid Violet 7 with complex pellets of white rot fungus and activated carbon. *Bioproc. Eng.* 2000; 23(3): 295–301.
- Zhang Y, Zheng J, Qu X, Chen H.** Effect of granular activated carbon on degradation of methyl orange when applied in combination with high-voltage pulse discharge. *J. Colloid Interf. Sci.* 2007a; 316: 523–530.
- Zhang Z, Shan Y, Wang J, Ling H, Zang S, Gao W, Zhao Z, Zhang H.** Investigation on the rapid degradation of congo red catalyzed by activated carbon powder under microwave irradiation. *J. Hazard. Mater.* 2007b; 147(1–2): 325–333.
- Zhao HZ, Sun Y, Xu LN, Ni JR.** Removal of Acid Orange 7 in simulated wastewater using a three-dimensional electrode reactor: Removal mechanisms and dye degradation pathway. *Chemosphere* 2010; 78(1): 46–51.
- Zille A, Ramalho P, Tzanov T, Millward R, Aires V, Cardoso MH, Ramalho MT, Gübitz GM, Cavaco-Paulo A.** Predicting dye biodegradation from redox potentials. *Biotechnol. Prog.* 2004; 20(5): 1588–1592.

## About the author

Gergo Mezohegyi was born in Budapest (Hungary) on 19<sup>th</sup> May, 1980. In 2003, he spent 5 months at Ghent University (Belgium) in the frame of Erasmus scholarship. In 2005 he obtained his M.Sc. degree in Food Engineering at Corvinus University of Budapest with the dissertation topic "Arsenic removal from wastewater by combination of decalcification and microfiltration". In 2007 he obtained his M.Sc. degree in Chemical and Process Engineering at Rovira i Virgili University with the dissertation topic "Novel bioreactor design for decolourisation of azo dye effluents". In October 2005 he started the Ph.D. research at the Department of Chemical Engineering of Rovira i Virgili University.



E-mail: [gergo.mezohegyi@gmail.com](mailto:gergo.mezohegyi@gmail.com)

## Publications

**Mezohegyi G, van der Zee FP, Font J, Bengoa C, Stuber F, Fortuny A, Fabregat A.**

Role of activated carbon in catalytic and non-catalytic aqueous dye removal processes: a review. *Carbon* 2010; submitted.

**Mezohegyi G, Gonçalves F, Órfão JJM, Bengoa C, Stuber F, Font J, Fortuny A, Fabregat A.** Activated carbon as catalyst in the anaerobic removal of azo colourants:

Influence of the surface chemistry. Poster. 19<sup>th</sup> *International Congress of Chemical and Process Engineering* and 7<sup>th</sup> *European Congress of Chemical Engineering*, Prague (Czech Republic), 28 Aug – 1 Sept 2010; accepted.

**Mezohegyi G, Gonçalves F, Órfão JJM, Fabregat A, Fortuny A, Font J, Bengoa C, Stuber F.** Tailored activated carbons as catalysts in biodecolourisation of textile azo dyes. *Appl. Cat. B* 2010; 94: 179–185.

**Escalona E, Bernat X, Mezohegyi G, Nabarlantz D, Stüber F, Bengoa C, Fabregat A, Font J.** Removal of commercial dyes from aqueous solution by nanofiltration. Poster. *IMeTI Workshop on "Membrane Applications in Agrofood"*, Cetraro (Italy), 18–20 October 2009.

**Mezohegyi G, Fabregat A, Font J, Bengoa C, Stuber F, Fortuny A.** Advanced bioreduction of commercially important azo dyes: modeling and correlation with electrochemical characteristics. *Ind. Eng. Chem. Res.* 2009; 48(15): 7054–7059.

**Mezohegyi G, Gonçalves F, Órfão JJM, Bengoa C, Stuber F, Font J, Fortuny A, Fabregat A.** Texture-modified activated carbons as catalysts in biodecolourisation of azo dyes. Poster. 2<sup>nd</sup> *International Congress on Green Process Engineering*, Venice (Italy), 14–17 June 2009.

- Mezohegyi G, Bengoa C, Stuber F, Font J, Fortuny A, Fabregat A.** Novel bioreactor design for decolourisation of azo dye effluents. *Chem. Eng. J.* 2008; 143(1–3): 293–298.
- Mezohegyi G, Fabregat A, Fortuny A, Font J, Bengoa C, Stuber F.** Advanced and catalytic bioreduction of azo dyes. Poster. *11<sup>th</sup> Mediterranean Congress of Chemical Engineering*, Barcelona (Spain), 21–24 October 2008.
- Mezohegyi G, Bengoa C, Stuber F, Font J, Fortuny A, Fabregat A.** Modeling of Orange II advanced biodecolourisation in upflow stirred packed-bed reactor. *10<sup>th</sup> International Chemical and Biological Engineering Conference*, Braga (Portugal), 4–6 September 2008; Book of Abstracts pp. 115–116.
- Mezohegyi G, Bengoa C, Stuber F, Font J, Fortuny A, Fabregat A.** Enhanced anaerobic treatment and modeling biodegradation of azo dyes in upflow stirred packed-bed reactor. *18<sup>th</sup> International Congress of Chemical and Process Engineering*, Prague (Czech Republic), 24–28 August 2008; Summaries (Vol.1) pp. 56–57.
- Mezohegyi G, Kolodkin A, Castro UI, Bengoa C, Stuber F, Font J, Fortuny A, Fabregat A.** Effective anaerobic decolorization of azo dye Acid Orange 7 in continuous upflow packed-bed reactor using biological activated carbon system. *Ind. Eng. Chem. Res.* 2007; 46(21): 6788–6792.
- Mezohegyi G, Bengoa C, Stuber F, Font J, Fortuny A, Fabregat A.** Innovative reactor design for anaerobic decolorization of azo dyes. *10<sup>th</sup> International Conference on Environmental Science and Technology*, Kos Island (Greece), 5–7 September 2007; Proceedings p. 128.
- Mezőhegyi G, Kolodkin A, Castro UI, Bengoa C, Stuber F, Font J, Fortuny A, Fabregat A.** Effective anaerobic decolorization of azo dye Acid Orange 7 in continuous up-flow packed bed reactor using biological activated carbon system. *First Mediterranean Congress on Chemical Engineering for the Environment*, San Servolo, Venice (Italy), 4–6 October 2006; Proceedings pp. 362-369.
- Galambos I, Mezőhegyi G, Vatai Gy.** Arsenic removal from high arsenic content wastewater. Combination of lime softening and microfiltration. Poster. *Scientific Reunion of The Special Program of The Alexander Von Humboldt Foundation Concerning The Reconstruction of The South Eastern Europe*, Timisoara (Romania), 24–25 February 2005; Proceedings pp. 169-172.
- Mezőhegyi G, Galambos I, Békássyné-Molnár E, Vatai Gy.** Membrane filtration of high arsenic content wastewater (Hungarian). Poster. *Műszaki Kémiai Napok '04*, Veszprém (Hungary), 20–22 April 2004; Proceedings p. 173.

UNIVERSITAT ROVIRA I VIRGILI  
CATALYTIC AZO DYE REDUCTION IN ADVANCED ANAEROBIC BIOREACTORS  
Gergö Mezöhegyi  
ISBN:978-693-7672-0/DL:T-1751-2010



